# Development of methods to determine pollution effects on skin and to measure the efficacy of anti-pollution formulations

Inaugural-Dissertation
to obtain the academic degree
Doctor rerum naturalium (Dr. rer. nat.)

submitted to the Department of Biology, Chemistry, Pharmacy
of Freie Universität Berlin

by
Phuong Thao Tran

2024

The following dissertation was supervised by Prof. Dr. Martina Meinke at the Center of Experimental and Applied Cutaneous Physiology at the Department for Dermatology, Venereology, and Allergology of Charité – Universitätsmedizin Berlin, Cooperate Member of Freie Universität Berlin and Humboldt-Universität zu Berlin, and Berlin Institute of Health and by Prof. Dr. Burkhard Kleuser at the Institute of Pharmacy (Pharmacology and Toxicology) of Freie Universität Berlin, from August 2020 to December 2023.


1st Reviewer: Prof. Dr. Martina Meinke

Charité Universitätsmedizin Berlin

Department of Dermatology, Venereology and Allergology

Center of Experimental and Applied Cutaneous Physiology

Charitéplatz 1

10117 Berlin

2nd Reviewer: Prof. Dr. Burkhard Kleuser

Institute of Pharmacy (Pharmacology and Toxicology)

Freie Universität Berlin

Königin-Luise-Straße 2+4

14195 Berlin


Date of Defense 1st August 2024

# Acknowledgment

First, I would like to express my gratitude to **Prof. Dr. Martina Meinke** for proposing this intriguing topic and for the collaborative discussion, which provided me with valuable insights and inspiration. Your insights and comments have greatly influenced my scientific work. I am grateful for your guidance and mentorship.

I sincerely would like to thank **Prof. Dr. Burkhard Kleuser** for the second opinion on my dissertation.

Furthermore, my gratitude goes to the working group of the Center of Experimental and Applied Physiology (CCP), especially to **Dr. Silke Lohan** and **Dr. Johannes Schleusener** for their scientific support during my experiments and helping me with scientific writing. I would like to thank **Dr. Victor Hugo Pacagnelli Infante, Marius Kröger, Daniela Zamudio Diaz, Dr. Loris Busch and Dr. Anna Lena Klein** for the collegial and helpful cooperation, support, and the pleasant lunch breaks.

In addition, I would like to express my gratitude to **Sabine Schanzer** and **Heike Richter** not only for their technical assistance, but also for the enjoyable conversations we had in our office.

I would like to express my gratitude to our collaboration partner at Gematria TestLab, **Dr. Parichat Tawornchat** and the master students **Rajae Talbi** and **Batoul Beidoun** for their invaluable assistance in this project.

Thank you, **Mrs. Traudl Vogel** and the colleagues from the “Ansbacher Apotheke” for their unwavering support since the beginning of my professional career. They have consistently recognized my potential and strengths as a pharmacist and researcher.

**Sofie Kling**, thank you for her unwavering emotional and occupational psychological support, extending all the way from Regensburg.

**Linda Döring,** thank you for providing me with an open heart and ear throughout my time in Berlin.

A big thank you goes to the members of the football club **“Gutkick Galaxy”** for their unfailing support and good cheer throughout my academic career. Despite my lack of involvement in the sport, they always made an effort to ensure that I had a good time. A special thanks go to **Malte Knudsen and Hakon Gruhn** for accompanying me on field trips to Prague, Budapest, and Poznan during my time as a doctoral student.

I would like to express my gratitude to **my Berlin party peeps**, with whom I had the pleasure of socializing during my time as a doctoral student. We shared many memorable experiences together, and I am grateful for the opportunity to get to know them. A big shout out to **Robin Marienfeld** for always making me laugh and feel seen. I am eagerly awaiting the next boat trips and prosecco brunches that will undoubtedly ensue in the future.

A special acknowledgment goes to my “ride or die” friends **Annika Eschner, Magdalena Witzel and Constanze Claus**, for the emotional support you have given me and the good times we have had. You are my safe space, and I can’t wait for our next adventures.

My biggest gratitude I will give to my life and “business” partner **Daniel Sgan Cohen** for always being there for me, for supporting me, for the patience you had when I was inpatient and for the love you have given me. I can’t wait to spend my life with you.

Finally, I would like to thank my family, for their unwavering belief in my abilities and their unconditional support throughout this journey. I would like to express my sincerest gratitude to **my mother**. I am grateful to you for my life and for the sacrifices you have made to give me the life you could not have at a young age. I am grateful for your continued support. This is for you *mẹ*.

# Statement of Authorship

I hereby certify that I have written my dissertation independently and have not used any sources or aids other than those indicated by me. I have not applied for a doctoral degree at any other university or department at any time in the past.

Berlin, 30th May 2024

_____

Phuong Thao Tran

# Table of contents

Zusammenfassung ..... VIII
Summary ..... x
Abbreviations ..... xii
**1. Introduction** ..... 1
**1.1 The skin** ..... 2
**1.1.1 Structure and function of the skin** ..... 2
**1.1.2 Established skin models for research** ..... 4
**1.2 Oxidative stress** ..... 5
**1.3 Antioxidants** ..... 7
**1.4 Source of oxidative stress** ..... 9
**1.4.1 Air pollution** ..... 9
**1.4.2 Cigarette smoke as model for air pollution** ..... 10
**1.4.3 UV irradiation** ..... 12
**1.5 Methods to expose skin to air pollution and measure the effect of pollution in skin** ..... 14
**1.5.1 Methods for cigarette smoke exposure** ..... 14
**1.5.2 Electron paramagnetic resonance (EPR) spectroscopy methods to measure the effect of cigarette smoke in skin** ..... 17
**1.5.3 Measuring autofluorescence using different Confocal spectrometers after cigarette smoke exposure in skin** ..... 20
**1.6 Evaluation of anti-pollution formulations** ..... 21
**1.7 Objectives** ..... 23
**2. Results** ..... 24
**2.1 Establishment of a method to expose and measure pollution in excised porcine skin with electron paramagnetic resonance spectroscopy** ..... 24
**2.2 Red- and Near-Infrared-Excited Autofluorescence as a Marker for Acute Oxidative Stress in Skin Exposed to Cigarette Smoke Ex Vivo and In Vivo** ..... 36
**2.3 Evidence of the protective effect of anti-pollution products against oxidative stress in skin ex vivo using EPR spectroscopy and autofluorescence measurements** ..... 56
**3. Discussion** ..... 68
**3.1 Methods to expose and measure the effect of cigarette smoke on skin** ..... 68
**3.1.1 Cigarette smoke as model for air pollution** ..... 70
**3.1.2 The impact of the parameters in the exposure chamber on the effect on skin** ..... 71
**3.2 Methods to measure the effect of cigarette smoke in skin** ..... 73
**3.2.1 Electron Paramagnetic Resonance (EPR) Spectroscopy** ..... 73

**3.2.2 Autofluorescence measurements using CRM** ..... 75
**3.2.3 Ex vivo vs in vivo** ..... 79
**3.2.4 Evaluation of methods to measure the effect of cigarette smoke in skin** 81
**3.3 Efficacy of antipollution products** ..... 83
**3.3.1 Comparison of two methods to measure the efficacy of anti-pollution products** ..... 83
**3.3.2 Antioxidants and chelators for anti-pollution products** ..... 86
**3.3.3 Guideline for formulating and testing anti-pollution products** ..... 88
**4. Conclusion and Outlook** ..... 90
**4.1 Conclusion** ..... 90
**4.2 Outlook** ..... 90
**5. List of publications** ..... 92
**6. References** ..... 93

# Zusammenfassung

Das Thema Umweltverschmutzung ist in den letzten Jahren immer relevanter für die Gesellschaft geworden. Die Menge an Schadstoffen in der Luft nimmt weltweit kontinuierlich zu und verursacht erhebliche gesundheitliche Probleme. Auch für die Haut haben diese Schadstoffe eine hohe Bedeutung. Darüber hinaus müssen wir uns auch mit anderen Aspekten der Umweltverschmutzung auseinandersetzen. Schadstoffe wie Zigarettenrauch können vorzeitige Hautalterung, Schädigungen der Hautbarriere, Pigmentstörungen und Zellschäden durch freie Radikale verursachen. Diese können die Symptome von Patienten mit bereits bestehenden Hautkrankheiten wie atopischer Dermatitis und Akne verschlimmern oder sogar neue Krankheiten auslösen. Obwohl nicht vollständig geklärt ist, wie schädlich Zigarettenrauchexposition für die Haut ist und wie man die Haut effektiv davor schützen kann, wurden in den letzten Jahren Hautpflegeprodukte mit einer "Antipollution-Wirkung" entwickelt. Bisher gibt es keine etablierten Methoden, um aussagekräftige und einfache Ergebnisse zu erzielen, die den Einfluss von Umweltverschmutzung auf der Haut messen können. Es ist wichtig, den Gefährdungsgrad von Zigarettenrauch auf die Haut oder die Schutzwirkung applizierter Substanzen eindeutig zu bestimmen.

Um eine eindeutige Bestimmung des Gefährdungsgrades zu gewährleisten, sollte eine reproduzierbare Zigarettenrauchexposition durchgeführt werden. Zu diesem Zweck wurden zwei Expositionskammern gebaut, die die Haut ex vivo und in vivo mit Zigarettenrauch exponieren. Die Konzentration in der Kammer wurde anfangs mit einem kommerziellen Partikelmessgerät ermittelt, welches Konzentrationen von 0,001 bis maximal 400 mg/m³ erfassen konnte. Der Rauch einer Zigarette überschritt den maximalen Messwert in der Kammer. Aus diesem Grund wurde eine Methode entwickelt, um die Partikelkonzentration mit der Nikotinkonzentration zu korrelieren, welcher die Haut in der Kammer ausgesetzt war. Nikotin diente hierbei als Surrogatparameter für den Zigarettenrauch im Allgemeinen. Ein reproduzierbares Berauchungsregime wurde eingerichtet, um später den Effekt der Hautexposition zu messen. Um den Nikotingehalt auf der Haut zu quantifizieren, wurde neben jeder Hautprobe ein Filterpapier platziert. Dieses wurde anschließend extrahiert und bei einer Wellenlänge von 262 nm mit einem UV-Vis Spektrometer gemessen. Ferner wurde eine Kalibrierkurve mit dem Reinstoff Nikotin erstellt. Es konnte eine signifikante positive Korrelation zwischen der gemessenen Nikotinkonzentration und der Partikelkonzentration in der Kammer nachgewiesen werden.

Nachdem eine reproduzierbare Methode für die Exposition gegenüber Zigarettenrauch etabliert wurde, wurden zwei neue Methoden entwickelt, um den Effekt von Zigarettenrauch auf der Haut zu messen.

Vorherige Untersuchungen haben gezeigt, dass die Entstehung von freien Radikalen zu oxidativem Stress führt und der hauptsächliche Mechanismus für Schäden der Haut durch Luftverschmutzung ist.

Es wurde nachgewiesen, dass Zigarettenrauch allein in der Lage ist, freie Radikale in der Haut zu induzieren. Es besteht eine Dosisabhängigkeit zwischen der gemessenen Nikotinkonzentration und der Radikalproduktion in der Haut. Die Kombination von UVA-Bestrahlung und Zigarettenrauch führte zu einer vermehrten Radikalbildung durch synergistische Effekte.

Zusätzlich konnte der durch induzierten oxidativen Stress in der exzidierten Schweinehaut verursachte Effekt anhand der erhöhten Autofluoreszenz durch das konfokale Ramanmikroskop (CRM) gemessen werden. Die CRM-Methode konnte erfolgreich auf in vivo übertragen werden. Es wurde gezeigt, dass die gemessene Autofluoreszenz bei Probanden nach Exposition gegenüber Zigarettenrauch höher war als vor der Exposition. Die Methode ist jedoch auf die Hauttypen I-III beschränkt, da ein hoher Melaningehalt in der Haut die Messungen stören kann. Die genauen Prozesse, die zu dieser erhöhten Autofluoreszenz führen, konnten noch nicht ermittelt werden. Jedoch wurde bestätigt, dass oxidativer Stress für den Anstieg in Autofluoreszenz verantwortlich ist und nicht die Bestandteile des Zigarettenrauchs.

Beide Methoden wurden angewendet, um die Effektivität bezüglich der Antipollutionwirkung von einzelnen Formulierungen mit Antioxidantien und Chelatbildnern zu überprüfen. Die Formulierung mit Epigallocatechin-3-gallate (EGCG) hat dabei am besten abgeschnitten. Dieser Wirkstoff ist ein Hauptbestandteil von grünem Tee (Camellia Sinensis). Beide Methoden sind vergleichbar; jedoch gibt es bei der EPR-Methode Einschränkungen. Bei dieser Testmethode darf das Testprodukt einerseits nicht mit der Spinsonde reagieren. Andererseits wird die Effektivität von Antioxidantien in den Formulierungen optimal gemessen. Dagegen beruhen Chelatbildner auf einem anderen Wirkprinzip, das von der EPR-Methode nicht optimal erfasst wurde. Die CRM-Methode erfasst alle Wirkstoffgruppen optimal und benötigt keine zusätzliche Markersubstanzen zur Messung der Wirkung von Zigarettenrauch und für die Exposition des Rauches ohne Creme konnte die In-Vivo-Tauglichkeit nachgewiesen werden. Es ist auch keine zusätzliche UVA-Bestrahlung erforderlich, weshalb aus bisheriger Sicht die CRM-Methode die bessere Methode zur Messung der Wirksamkeit von Anti-Pollution-Produkten ist.

# Summary

The significant relevance of air pollution increased in our society in recent years due to its adverse health effects on animals and humans. This is caused by the increasing amount of pollutants worldwide. These pollutants also have an effect on the skin as it comes into contact every day. It is important to address all the possible aspects of danger to prevent such damage. In addition, pollutants such as cigarette smoke can lead to premature skin ageing, damage to the skin barrier, pigmentation disorders, and cell damage which is caused by free radicals. These factors can worsen symptoms for patients with existing skin conditions, like atopic dermatitis and acne. Air pollution can also cause new conditions to develop. The extent of damage on the skin caused by cigarette smoke is not yet clear, and it remains uncertain how to protect the skin from it. As a result, skincare products claiming an "anti-pollution effect" have been released to the markets in recent years. Currently, there are no proper methods to produce meaningful results for measuring the effect of pollution on the skin. It is important to assess the level of risk cigarette smoke poses to the skin or the effectiveness of applied substances in providing protection.

For risk management, an unambiguous determination was necessary and hence it was deemed essential to establish cigarette smoke exposure method. For this purpose, two specially designed exposure chambers were constructed to expose ex vivo and in vivo skin tissue to cigarettes smoke. The concentration of smoke in the chamber was determined initially by a commercial particle measuring device, which was capable of measuring particles ranging from concentration 0.001 to a maximum of 400 mg/m³. It was found that the smoke from one cigarette exceeded the quantifiable levels measured with the particle measuring device in the chamber. A method was created to establish a correlation between the particle concentration and the nicotine concentration within the chamber that could come into contact with the skin. Nicotine acted as a surrogate parameter for cigarette smoke in this work. A consistent smoking regime was established for subsequent measurement of the impact of skin exposure. To quantify the nicotine content on the skin, a filter paper was positioned next to each skin sample. The sample was extracted with ethanol and the absorbance of nicotine was measured at a wavelength of 262 nm, using a UV-Vis spectrometer. A calibration curve was generated with pure substance nicotine. The results reveal a statistically significant positive correlation between the measured nicotine concentration and the particle concentration in the chamber.

Once a reproducible method for exposing the skin to cigarette smoke had been established, two new techniques have been devised for measuring the impact of cigarette smoke on the skin.

Prior investigations have demonstrated that the generation of free radicals leads to oxidative stress and is the main mechanism of skin damage caused by air pollution. Free radicals can be measured via electron spin resonance (EPR) spectroscopy. The study evaluated the impact of cigarette smoke on excised porcine skin with different spin probes.

Prior research has proven that cigarette smoke can induce free radicals in the skin. There is a dose dependency between the measured nicotine concentration and the radical production in the skin. The combination of UVA and cigarette smoke leads to an increase in radical formation due to synergistic effects.

Furthermore, the impact resulting from induced oxidative stress in the excised porcine skin was gauged via heightened autofluorescence utilizing the confocal Raman microscope (CRM). The autofluorescence technique was effectively transferred to in vivo studies. Results revealed that the measured autofluorescence was higher in test subject post-exposure to cigarette smoke than pre-exposure. Notwithstanding, the method is restricted to skin types I-III as high levels of melanin in the skin can disturb the measurements. The specific mechanisms underlying the observed increase in autofluorescence have yet to be determined. Nevertheless, it has been verified that oxidative stress, rather than cigarette smoke components, is accountable for the increase in autofluorescence.

Both methods were used to evaluate the efficacy of different formulations containing of antioxidants and chelating agents. Notably, the formulation incorporating epigallocatechin-3-gallate (EGCG), a key ingredient found in green tea (Camellia Sinensis), exhibited the optimal performance in both methods. While both methods seem similar, the EPR method is somewhat limited. Specifically, for this test procedure, it is important that the tested agent does not react with the spin probe. The efficacy of antioxidants in the formulations should be optimally measured. For instance, chelating agents are based on a distinct active principle that cannot be optimally measured through the EPR method. In contrast, the CRM method can efficiently measure all active ingredient groups without the need for additional markers. It is also a promising method to apply in vivo. No additional UVA irradiation is necessary either, making the CRM method the superior approach for measuring the effectiveness of anti-pollution products.

# Abbreviations

| | |
|---|---|
| % | Percentage |
| °C | Degree Celsius |
| 8-OHdG | 8-Hydroxy-2′-deoxyguanosine |
| AF | Autofluorescence |
| AGE | Advanced glycation end products |
| AhR | Aryl hydrocarbon receptor |
| B[a]P | Benz[a]pyrene |
| CI | Canadian Intense Regime |
| CRM | Confocal Raman Microspectroscopy |
| CS | Cigarette smoke |
| CSE | Cigarette smoke extract |
| DNA | deoxyribonucleic acid |
| DCFH-DA | Dichloro-dihydro-fluorescein diacetate assay |
| DPPH | 1,1-diphenyl-2-picrylhydrazyl |
| EGCG | Epigallocatechin-3-gallate |
| EGR | Early growth response protein |
| EPR | Electron Spin Resonance Spectroscopy |
| ETS | Environmental Tobacco Smoke |
| GSH | glutathione |
| HaCaT | Human Keratinocyte Cell Line |
| IL | Interleukin |
| ITA | Individual Typology Angle |
| ISO | International Organization for Standardization |
| MAPK | mitogen-activated protein kinase |
| MDA | malondialdehyde |

| | |
|---|---|
| MED | minimal erythema dose |
| MMP | Matrix metalloproteinase |
| NADPH | Nicotinamide Adenine Dinucleotide Phosphate Hydrogen |
| NIR | Near infrared region |
| PAH | Polycyclic Aromatic Hydrocarbon |
| PCA | 3-(carboxy)-2,2,5,5-tetramethyl-1-pyrrolidinyloxy |
| PM | particulate matter |
| ROS | reactive oxygen species |
| RPF | radical protection factor |
| RNS | reactive nitrogen species |
| SC | stratum corneum |
| SOD | superoxide dismutase |
| TEMPO | (2,2,6,6-tetramethylpiperidine-1-oxyl) |
| TNF | tumor necrosis factor |
| UV | ultraviolet |
| VIS | visible |

# 1. Introduction

Air pollution is a growing problem worldwide. The World Health Organization (WHO) reports that 7.3 billion people worldwide are exposed to unhealthy PM 2.5 concentrations. Figure 1 illustrates the percentage of the population exposed to PM 2.5 at over 5 µg/m³. The WHO guidelines state that annual average concentrations should not exceed 5 µg/m³ as it could induce and exacerbate health problems [4, 5].

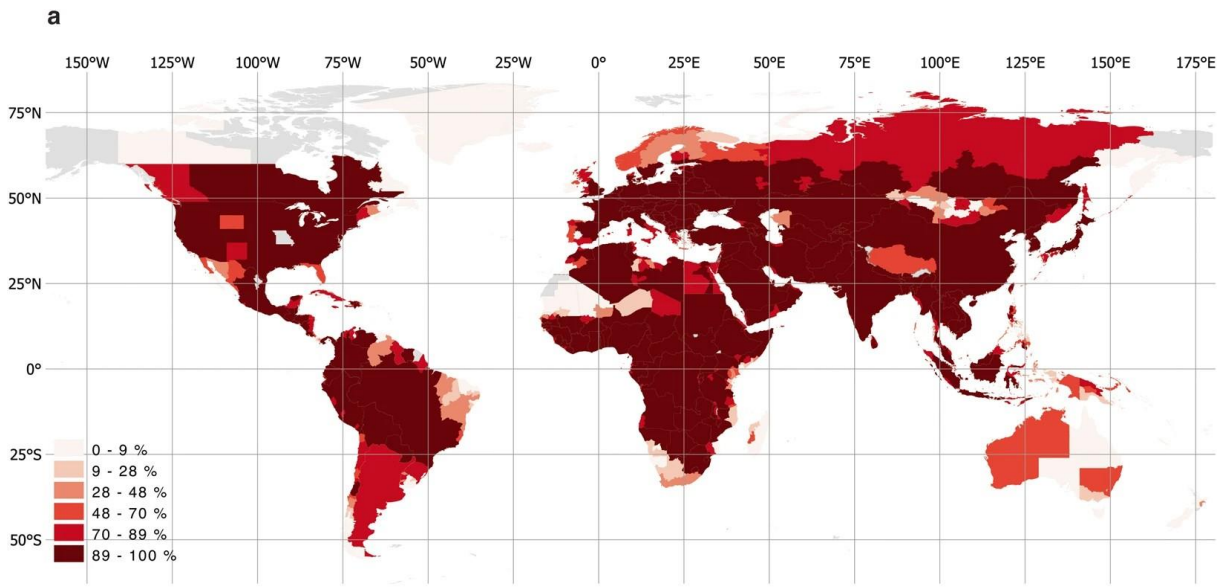


**Figure 1 The percentage of the population exposed to PM 2.5 at an average of 5 µg/m³,** as referenced in [4].

The skin, our first defense, protects the body against external surroundings. With its important functions, the skin protects the body from external influences such as solar radiation, chemo- and xenobiotics, and biological compounds, e.g. microorganisms [6, 7].

Cigarette smoke with more than 4000 compounds is not only dangerous to our lungs but also to our skin. The effects of air pollution and especially of cigarette smoke on the skin are not well studied yet. Most methods are either invasive or time-consuming. In addition, there are not many methods to reproducibly expose skin to air pollution. Therefore, to date, there are only a few meaningful methods available to determine the efficacy of anti-pollution products that purpose to protect the skin [8].

To assess the effect of cigarette smoke on oxidative stress generation in the skin, an exposure chamber was designed to allow reproducible smoke exposure to ex vivo and in vivo skin. Different measurement methods could be established to study a) the effect of cigarette smoke on the skin and b) the efficacy of anti-pollution products to protect against oxidative stress in the skin [3, 9, 10].

## 1.1 The skin

### 1.1.1 Structure and function of the skin

The skin makes up about 16 % of an adult's total body weight and is on average 2 $m^2$ in area. The main function of the skin is to protect against biological, chemical, and physical influences from the environment. It consists of three layers: The epidermis, the dermis, and the subcutis. There are also appendages such as nails, hair, sebaceous and sweat glands. Furthermore, the skin has sensory and contact functions: Heat, pain, pressure, and tactile stimuli can be perceived via the sensory receptors [6].

The epidermis consists of four layers:

Keratinocytes adhere to the basement membrane in the stratum basale. One layer of basal cells is formed. These cells in the epidermis are mitotically active. The newly generated cells ascend via the stratum granulosum and stratum spinosum during differentiation processes. The epidermis' outermost layer, the stratum granulosum, includes live cells. They are made up of flattened cells that are in charge of continuing to synthesize and alter keratinization-related proteins. The cells abruptly differentiate into horny cornified layer cells, as they get closer to the cornified layer, the stratum corneum (SC). The SC protects the skin from the outside, prevents the body from drying out and keeps chemicals and xenobiotics out. The pH level of the SC depends on the localization and is between 4.1 and 5.8 to maintain a healthy skin microbiome [11-13]. The stratum corneum's corneocytes shield the underlying epidermis mechanically. As they are encircled by an ongoing extracellular lipid matrix, the cells are low in lipid content and high in protein. A lipid matrix is holding the corneocytes together and thus forms a defense system against environmental stressors, such as ambient particulate matter (PM), pathogens, and allergens. Technically, the corneocytes are dead because they lost their nuclei during terminal differentiation. The SC acts as a barrier to stop the loss of water and the entry of contaminants and germs [12, 14, 15].

In depth, you can see that epidermis is made of multilayered and keratinized squamous epithelium. 80-90% of the epidermis consists of keratinocytes. The rest are Merkel cells, melanocytes, Langerhans cells, and lymphocytes. In the epidermis, the cells undergo a differentiation process and migrate from the basal layer to the surface of the skin [16]. In the keratinization phase, the cells pass through a synthesis and then a degradative phase. In the synthesis phase, the cells build up a cytoplasmic supply of keratin which is a fibrous intermediate filament that is the cell’s cytoskeleton. At the degradative phase, the cellular organelles are gone and the corneocytes are formed, which is the terminal differentiation.

The epidermis itself does not have its own vascular system and must be supplied from the dermis by diffusion [12]. Figure 2 shows the structure of the skin in detail.

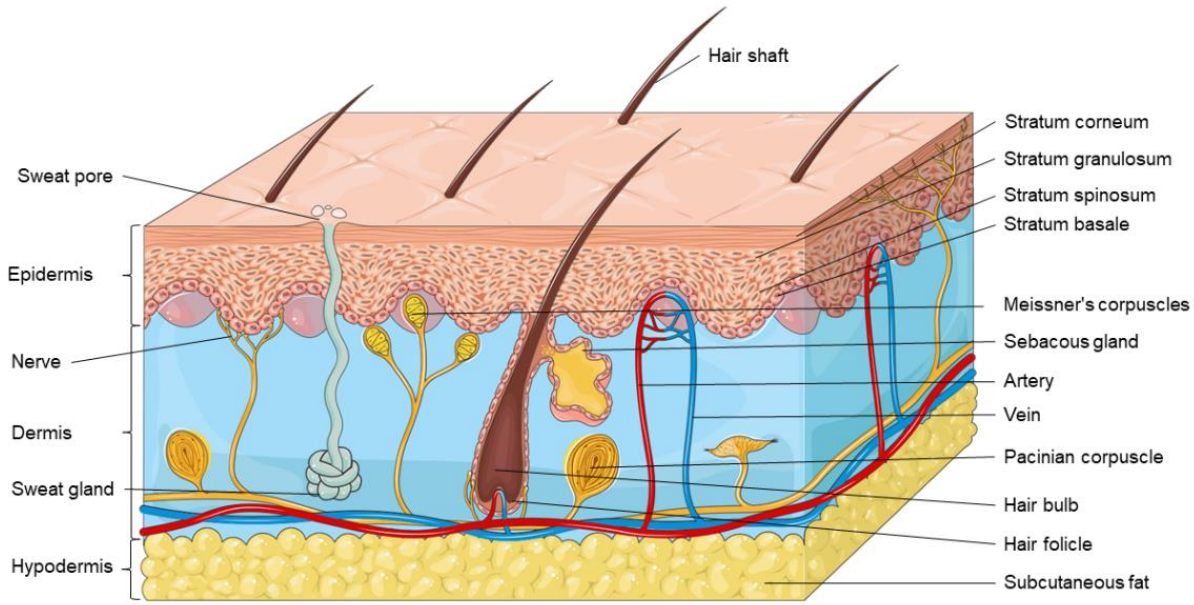


**Figure 2 Skin structure**. The Figure was partly generated using Servier Medical Art, provided by Servier, licensed under a Creative Commons Attribution 3.0 unported license. Figure modified by adding text and markings.

Underneath the epidermis is the dermis that provides mechanical protection for the body. This part of the skin contains an elastic, dense and tear-resistant fibrous network, ideal for mechanical protection. Two layers of the dermis are important: the papillary dermis and the reticular dermis. The papillary dermis is thin and contains collagen fibers that are loosely arranged. The fibroblasts are primarily situated here and are responsible for the production of fiber-and sheet-forming collagen, elastin and proteoglycans. In addition, fibroblasts produce the extracellular matrix, which maintains the connective tissue's flexibility and stability. The extracellular matrix gets decomposed by proteolytic enzymes called matrix metalloproteinases (MMPs) by replacing it with new matrix components and remodeling it [7, 12, 17].

In the reticular dermis, the fibers are coarse, have a better structure and their cell density is low, while those in the papillary dermis are fine and their cell density is higher. Fine collagen bundles can be seen in this papillary part of the dermis, where the nerve fibers and the blood vessels interact with one another. In addition, you can find components of the immune system like mast cells, macrophages and lymphocytes together with a linear network of lymphatic vessels and the blood vascular system [12, 18]. The dermis aids in heat regulation, binds water, protects the body from mechanical harm, and possesses receptors for sensory inputs. In order to preserve the characteristics of both tissues, it

interacts with the epidermis [7, 12, 19]. Subcutaneous fat is located beneath the dermis. This functions as a cushion, absorbs and distributes blunt force trauma. In addition, subcutaneous fat holds a metabolic function as well [12].

The body has different ways to protect itself, including different molecules and cells that are present in the skin. One way how the body protect itself from radiation and xenobiotics is the synthesis of melanin. This can act as a response to different stimuli such as UV radiation and air pollution [20]. Melanocytes produce the black pigment melanin. They are located in the basal layer of the epidermis and the hair follicle. Melanin synthesis occurs in response to physiological and pathological stimuli such as UV radiation and air pollution. Melanin is transferred from melanosomes to neighboring keratinocytes where it can absorb light of all wavelengths and act as radical scavenger. Thus, melanin pigmentation protects the skin and deeper structures from the consequences of UV radiation [21].

Another important group that the body uses for protection are Langerhans cells and lymphocytes, which are bone marrow-derived MHC class II antigen-tolerant leukocytes. They make up the outermost layer of the immune system because they stimulate resting T helper lymphocytes, which initiate primary T cell-dependent immune responses. In addition, they are also important in contact sensitization which initiates allergic responses [22].

Another cell type found in the epidermis is Merkel cells, which form fibroelastic tissue with high tensile strength and elasticity. They are important for the mechanical stability of the skin and important for the perception in hairy skin [23].

### 1.1.2 Established skin models for research

The preferred method for skin research is in vivo studies, which involve direct testing on humans and can mimic real-life conditions resulting in more reliable results [24, 25]. If in vivo studies are not ethically possible, alternative skin models have been established for research purposes. The initial step is typically in vitro testing, which uses cell models. These measurements are designed to replicate in vivo conditions in a laboratory setting, providing a controlled environment. In vitro measurements offer the advantage of reproducible measurement conditions for individual samples. Additionally, initial conclusions about the mechanism of action can be drawn [24-26].

However, it is important to note that there are limitations, such as overestimation, as the permeation of exogenous agent may differ due to the thinner stratum corneum or missing hair follicles in cell models. Furthermore, it should be noted that the skin’s metabolism, immune system, and microbiota are not accounted for [24].

Another available skin model is excised skin tissue, which still maintains an intact barrier under controllable conditions. However, it is important to acknowledge that the quality of the excised skin tissue depends on the donor [24].

Despite this limitation, excised skin can be a useful alternative for preliminary scientific investigations and establishing measurements. Excised human skin is often used in research due to its biological similarity to human skin in vivo. It is typically obtained through plastic surgery and has been shown in studies to have comparable tissue viability, barrier function, and extracellular matrix composition [27, 28].

Another commonly used skin model is porcine skin. Slaughterhouse waste is readily available and cheaper than human skin. Both human and porcine skin require ethical approval, but obtaining slaughterhouse waste is easier. In Germany, ethical approval by the veterinarian's office is needed for slaughterhouse waste. Various studies are carried out with excised porcine skin, like transdermal drug testing, UV radiation-exposed skin damages, wound healing, and toxicity studies [29]. Porcine skin is anatomically and physiologically similar to human skin. The morphology as the cellular composition and location of most cells of the immune system or cells responsible for melanin synthesis (melanocytes) are comparable in both skin models. In addition, the thickness of the epidermal and dermal layer is equivalent in both porcine and human skin [30, 31]. In Darvin et. al's work parameters like skin hydration, corneocytes size, and shape, nucleus size, cytoplasmic volume, and intercellular area were all found to be similar to human skin using confocal laser scanning microscopy and multiphoton tomography. However, the thickness of the adipose tissue and the lipids in the stratum corneum are less densely packed compared to human skin [32]. The work of Choe et al. reported that the barrier function of in vivo human skin is higher than that of excised porcine skin [33]. It is also important to remember that pigs can produce their vitamin C [34]. Nevertheless, porcine skin is a good substitute for skin research, even if it is not 100 % identical [31, 35].

## 1.2 Oxidative stress

Oxidative stress is characterized by an imbalance between poor activity of antioxidant systems and elevated amounts of mainly reactive oxygen species (ROS). In addition, oxidative stress can also be induced by reactive sulphur species, reactive carbon species and reactive nitrogen species (RNS). RNS are formed from nitrogen, whose radicals can become nitric oxide or peroxynitrite [36]. Increased oxidative stress has the ability to harm skin tissues by damaging cellular structure [37]. ROS are important representatives of free radicals. Free Radicals are atoms or molecules that have at least one unpaired electron. These free radicals can react with other radicals, with themselves, or with another

molecule and have a short half-life [36]. In the skin, ROS can be induced by UV radiation and other environmental factors like air pollution [38]. Depending on their lifestyle choices and mental health, it can also lead to an imbalance inside the body. In particular ROS are formed from molecular oxygen. Examples include superoxide anion radical, hydroxyl radical, singlet oxygen, and hydrogen peroxide [39].

In vivo, free radicals are continuously created and are a normal byproduct of cellular metabolism. ROS are naturally occurring by-products produced by a variety of enzymatic processes in many cellular compartments, including the mitochondria and peroxisomes. In the cell, they can perform signaling activities and be produced by enzymes like NADPH oxidase. In summary, various physiological activities include the electron transport chain in mitochondria, enzymatic events, and immunological responses [36, 40].

The only enzyme that can neutralize superoxide anion radicals is superoxide dismutase (SOD). It facilitates the radical's conversion to hydrogen peroxide. Copper, zinc, manganese, and iron all help SOD. It degrades superoxide radicals to produce oxygen and hydrogen peroxide. These enzymes are found in almost all aerobic cells as well as extracellular lipids. Catalase is responsible for converting hydrogen peroxide into water and oxygen. As a result, it completes the detoxification process that SOD began [36, 41, 42].

Hydrogen peroxide can be a stable ROS, since it is no longer a radical. However, it can become hydroxyl radicals when there are transition metals present [43]. For enzymes like NADPH oxidase, xanthine oxidase, lipoxygenases, and cytochrome P450 to operate, transition metals are necessary. Hydroxyl radicals are very reactive because of the Fenton process that produces them with the help of these transition metals. Therefore, Hydroxyl radicals are frequently generated in vivo from hydrogen peroxide. Hydrogen peroxide must thus be broken down before the hydroxyl radicals generated can cause harm. This is done by antioxidants, e.g. the enzymes catalase, glutathione (GSH) peroxidase, and GSH itself. These oxidation products can react with lipids, proteins, and DNA and can be detected in blood, plasma, urine, and tissues [44, 45].

Malondialdehyde (MDA) is a known marker in samples as it is a major product of lipid peroxidation. 8-Hydroxy-2′-deoxyguanosine (8-OHdG) is a marker of DNA oxidation. These biomarkers are found in body fluids or tissue that can signify the presence of oxidative stress in the system [46, 47].

Other known markers of oxidative stress are advanced glycation end products. Advanced glycation end products (AGEs) are harmful metabolic by-products associated with oxidative stress and resistance to insulin-mediated glucose uptake. They cause oxidative

damage to proteins, lipids, and nucleotides [48]. To analyze the concentration of all these markers, skin samples have to be taken.

## 1.3 Antioxidants

Antioxidants are essential for maintaining redox homeostasis and preventing oxidative stress. They disrupt the chain reaction of free radicals by donating their electrons. They stop these chain events by eliminating free radical intermediates and suppressing other oxidation processes. Antioxidants typically contain reducing agents such as thiols or polyphenols [36, 41, 49].

Antioxidants can be classified as endogenous enzymatic and non-enzymatic antioxidants. There is an exogenous antioxidant system in addition to the endogenous antioxidant system. It is difficult to maintain redox equilibrium without an external supply of exogenous antioxidants. The skin, in particular, needs e.g., the vitamins C and E, which must be obtained from external sources because the body is unable to produce them. These vitamins are essential not just for the body's antioxidant system, but also for the manufacture of numerous critical molecules that regulate neurotransmission and collagen metabolism [41, 50].

The majority of ROS are eliminated by vitamin C, also known as ascorbic acid. This occurs since ascorbate oxidizes to monodehydroascorbate and subsequently to dehydroascorbate. It performs a variety of tasks to maintain the typical physiological condition. Prolyl hydroxylase is an enzyme that hydroxylates prolyl residues in procollagen and elastin in the skin. It requires cofactors to function. Vitamin C's tyrosinase inhibitory action also makes it a valuable depigmentation agent. By promoting epidermal differentiation, it assists in the development of the skin barrier. Unfortunately, vitamin C does not penetrate the skin well, and its therapeutic usefulness is diminished by its instability in aqueous preparations. Consequently, vitamin C must have a pH value below 3.5, which is also problematic for the majority of cosmetic products. [49, 51, 52].

Another representative of antioxidants is vitamin E, also known as alpha tocopherol. The hydroxyl group in the chromonol ring donates a hydrogen atom, enabling vitamin E, to partially lower free radicals. It modulates cellular responses under physiological settings by upregulating synthetase mRNA, which in turn increases the synthesis of glutathione (GSH) [53]. In skin, Vitamin E can suppress UVB-induced edema, erythema, and lipid peroxidation [41, 54].

Non-enzymatic antioxidants of note also include plant polyphenols, carotenoids, and glutathione. Glutathione can be found in every cell of our body, which enhances the activity of all other antioxidants [42].

Another group worth mentioning are carotenoids. They are created spontaneously by bacteria, fungus, algae, and plants. Carotenoids can be used as a mirror of someone's lifestyle as carotenoid levels could serve as antioxidant level markers [55]. Prominent representatives are ß-carotene and astaxanthin. They have the ability to quench singlet oxygen. Astaxanthin can protect pre-loaded fibroblasts and therefore less photo-oxidative changes can be measured in cell culture [52].

Epigallocatechin-3-gallate (EGCG) derived from green tea (Camellia sinensis) are important polyphenols. They have the ability to decrease matrix metalloproteinases (MMP)-1,-8, and-13 in a dose-dependent manner, prevent disruption of the epidermal barrier, and raise the lowest erythema dose to UV light. [52, 56]. MMPs are important regulators of cell-cell and cell-extracellular matrix interactions. They affect cellular differentiation, proliferation, and modifying matrix structure, growth factor availability, and the operation of cell surface signaling systems [57].

Endogenous and exogenous antioxidant systems collaborate to establish and maintain redox equilibrium. This synergy is used, for example, in GSH that aids in the regeneration of vitamin E, which protects the body against lipid peroxidation [41].

As consumers become more health conscious, there is a growing demand for antioxidant supplementation to support the body's antioxidant system. However, data on the beneficial effects of antioxidants after oral intake are mixed. Depending on the substance, increased intake of antioxidants can have a pro-oxidant effect and cause more harm than good. For example, the risk of lung cancer and cardiovascular events increases after supplementation with beta-carotene alone. Therefore, it makes sense to apply antioxidants topically so that they act locally by protecting the skin. This also ensures that the correct dose is delivered to the site of action. It is important to ensure that the active ingredient is applied in the correct formulation so that it is active and in sufficient concentration [58, 59]. Many antioxidants are very unstable due to their chemical composition. For example, vitamin C formulations must have the correct pH of 3.5. Also, the formulation ideally should be anhydrous to avoid instabilities. It is also important to ensure that it can cross the epidermal barrier to be active at the site of action [59].

Depending on the lipophilic environment in human skin, the antioxidant system varies in the different layers of the skin. Non-enzymatic, water- and fat-soluble antioxidants such as

vitamin C, vitamin E, GSH, squalene, and coenzyme Q10 are found in the SC. There is a concentration gradient of these antioxidants from the outside to the inside existent [60].

For example, lipid-soluble antioxidants such as vitamin E and enzymes such as catalase, superoxide dismutase, and GSH peroxidase are present in the epidermis. Keratinocytes are embedded in a lipophilic matrix depending on their stage of development. In addition to other antioxidant enzymes, the dermis contains hydrophilic non-enzymatic antioxidants, including GSH and vitamin C [60].

Another important antioxidant inside the basal layer of the epidermis is melanin. Melanocytes produce melanin, which is released into these cells. Because of the constant release, melanocytes have little pigmentation. Keratinocytes and fibroblasts also contain melanin, which can scavenge hydroxyl radicals with the help of its metabolites. Melanin is therefore an important antioxidant against UV-induced oxidative stress [61].

Not only antioxidants are produced inside the epidermis. Important to remember is that small amounts of the superoxide anion radical are created in the skin to start epidermal keratinocyte differentiation and/or fibroblast proliferation [15]. Redox imbalance in skin due to UV irradiation can increase NADPH oxidase activity. This can accelerate the aging process and the development of cancer [62].

## 1.4 Source of oxidative stress

### 1.4.1 Air pollution

Air pollution is increasing worldwide. It consists of substances in the atmosphere that can harm flora and fauna and is an accelerator of climate change as well. Increasing industrial expansion, which leads to more emissions, and the burning of fossil fuels and cigarette smoke are among the main sources of air pollution [63, 64].

Air pollution includes particulate matter (PM), volatile organic compounds (VOCs), various gases such as $CO_2$, CO, $SO_2$, $NO_x$, PAHs, and heavy metals. Polycyclic aromatic hydrocarbons such as benzo[a]pyrene (B[a]P), for example are carcinogens. They can bind covalently to DNA when metabolized in vivo to more reactive intermediates. These can initiate the development of cancer [65-67]. Air pollution pose a threat not only to the lungs of animals and humans, causing lung disease but also to the skin, which comes into contact with pollution on a daily basis [68, 69]. This can lead to various effects: loss of skin elasticity, deep wrinkles, pigmented spots, disruption of the skin barrier, and impaired wound healing. Chronic exposure can also cause inflammation leading to atopic dermatitis, psoriasis, and skin cancer [67, 70, 71].

### 1.4.2 Cigarette smoke as model for air pollution

Cigarette smoke is a good model for air pollution because the composition is similar to emissions from industry and burning fossil fuels. Common compounds are PAHs, volatile compounds, and various gases [72-75].

It contains more than 4000 known chemical compounds [8]. The delivery of these compounds can be altered by modifying cigarette components such as tobacco leaf type, tobacco curing process, or cigarette filters [76]. The flavor and scent of tobacco leaves are influenced by their size, color, and vein size variations. Mixtures of several tobacco varieties are used to make cigarettes. It is critical to describe the ingredients in cigarettes and how they affect the toxicity of cigarette smoke in order to better understand the health implications of tobacco smoke [77].

The choice of cigarette brand affects the toxicity and carcinogenicity of cigarette smoke. Ingredients vary from brand to brand and from blend to blend. In a study, cigarettes from different Chinese brands were tested with Research cigarettes for free radical production and nicotine content. A lower radical production of Chinese cigarettes compared to the Research cigarettes suggested that Chinese cigarettes have a lower potential of oxidative stress induction [78].

Research cigarettes are often used in cigarette smoke studies. It is important that the cigarettes selected do not vary within a batch. Recently, 1R6F cigarettes from the University of Kentucky have been used, which are the successors to the well-studied 3R4F cigarettes. In previous studies, the 3R4F cigarettes were compared with conventional cigarettes available on the market in terms of mainstream smoke. Both cigarettes (3R4F and 1R6F) are comparable in terms of smoke composition and in vitro toxicity [79, 80].

Cigarette smoke contains tar and particulate matter as organic compounds that are condensable at room temperature. Nicotine, carbon monoxide, and nitrogen oxide are also major components of cigarette smoke. The smoke stream can be divided into two parts: mainstream and sidestream smoke. Mainstream smoke is that part which is inhaled by the smoker into the lungs. The sidestream smoke is the combination of the stream of the burnt cigarette and the exhaled air from the smoker. Sidestream smoke is also a major part of environmental tobacco smoke (ETS). This smoke has a high content of particulate matter and condensed vapors. The exchange between gas and particulate phase in ETS during continuous aging leads to chemical changes due to oxidation mechanisms [81, 82].

Tobacco consumption in Germany has been at a high level for years [82]. No other legal drug increases overall mortality like tobacco. Chronic exposure to cigarette smoke causes

many diseases, mainly affecting the internal organs [64]. When we think of the effects of cigarette smoke on the body, the lungs are always mentioned first. The effects on the lungs of cigarette smoke have been sufficiently and extensively studied. However, the effect of such pollution on skin, which is exposed to these harmful substances on a daily basis, has not been sufficiently studied. Epidemiological studies on air pollution exposure tend to be preferred but it takes longer to retrieve results [83, 84].

The effects of cigarette smoke on premature skin aging have been well studied. Comparatively, cigarette smoke has a similar effect on the skin to that of UVA radiation through the formation of free radicals [85, 86]. The effect of UV radiation on the skin will be discussed in the next chapter.

Cigarette smoke contains thousands of chemical substances, e.g. carbon monoxide, polycyclic aromatic hydrocarbons, ROS, and RNS. ROS can cause oxidative stress or initiate a cascade of oxidative events that can also lead to the depletion of antioxidants (see chapter 1.2.1) [81, 87, 88].

Cigarette smoke can be divided into gas and particulate phase. Therefore, there are different radicals in every phase initiated when a cigarette burns. In general, there are $10^{14}$ carbon- and oxygen-centered radicals per puff. Gas phase radicals have a short lifetime, thus measuring them directly is very difficult [85, 89]

In contrast, tar radicals do not have a short lifetime, thus capturing them directly with the EPR is doable. The cigarette tar radicals are semiquinone radicals that can produce superoxide by reducing oxygen. These hydrogen peroxide and hydroxyl radicals can initiate a cascade leading to more oxidative stress [85, 86, 90]

Pryor et al. described several mechanisms involving: the activation of procarcinogen through oxidation, scavenge radical scavenger, and antioxidants that are meant to protect cells from tumor formation, causing more inflammation that can lead to tumor development and higher radical activity in protumor states by increased levels of lipid or DNA oxidation products [85].

In skin, cigarette smoke can lead to the increase of transepidermal water loss, the degradation of collagen and elastic fibers caused by upregulation of matrix metalloproteinases MMP-1 and 3, and the degeneration of connective tissue in general [91]. PAHs such as Benz[a]pyrene can oxidize to electrophilic derivate that can bind to DNA with radicals [85, 92]. Figure 3 shows an overview of the effects of cigarette smoke on skin.

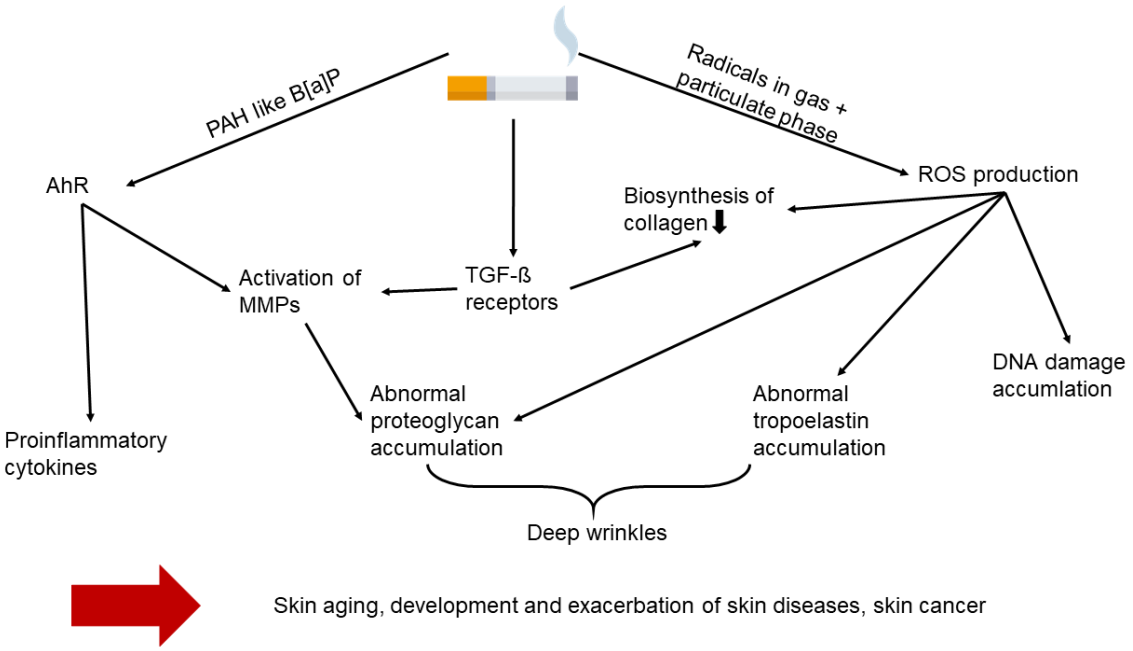


**Figure 3 Effects of cigarette smoke on skin on a molecular basis.** Modified from [1, 2].

The electromagnetic radiation emitted by the sun has a wavelength range of several hundred nanometers. A very small fraction of this radiation is able to reach the Earth's surface through the ozone layer in the atmosphere. These are the ultraviolet rays (UVR 280-400 nm), the visible light (VL 400-760 nm), and the infrared light (IR 760 nm-1 mm). Of the ultraviolet spectrum, only UVB (280-315 nm) and UVA (315 nm-400 nm) reach the earth's surface [93-95]. UVC rays (100-280 nm) are absorbed by the ozone layer and can only be measured at higher altitudes. However, in photo dermatology, UV radiation is divided into three distinct wavelength-based regions: The three main categories of UV radiation are UVA (320-400 nm), UVB (290-320 nm), and UVC (200-290 nm) [96, 97].

UV rays are important for Vitamin D synthesis and can cause i.a. acute pigmentation, erythema (sunburn) and hyperplasia. Chronically, it leads to photoaging and photocarcinogenesis [94, 98-100].

Approximately 90-95 % of the solar radiation reaching that reach the earth are UVA rays, and the remaining 5-10% are UVB rays. The intensity of UVB radiation can vary with latitude and altitude [100, 101]. Depending on the wavelength, ultraviolet rays can penetrate deeper into the skin [102]. For UVB rays, they can penetrate from the superficial layer down to the stratum basale of the epidermis. In comparison, UVA rays can penetrate deeper into the skin tissue until the dermis, as shown in Figure 4 [39].

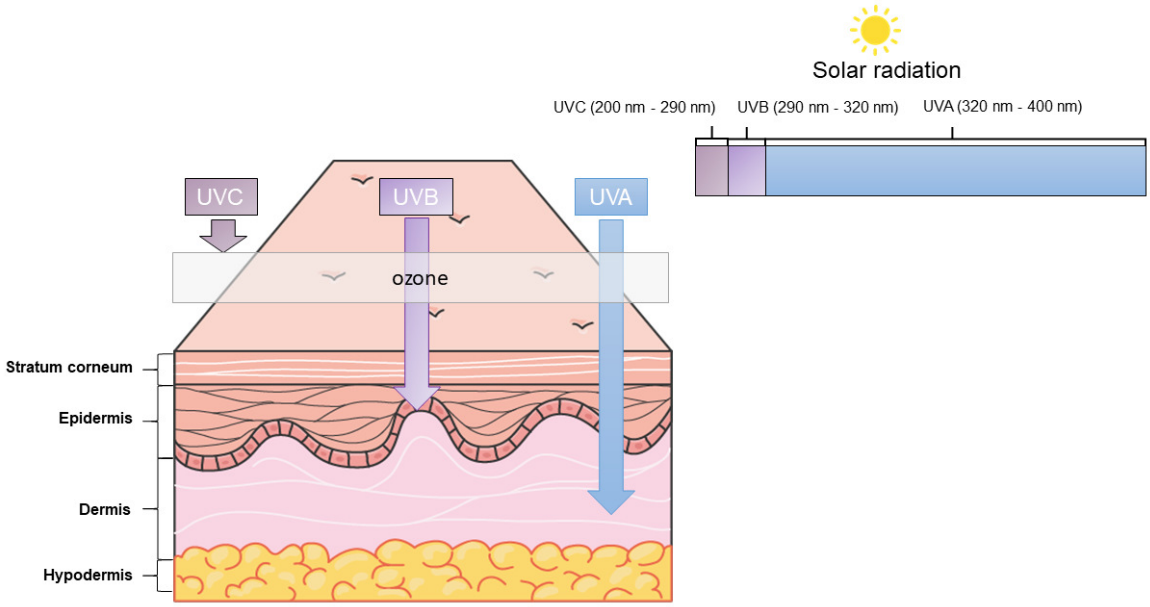


**Figure 4 The solar ultraviolet radiation spectrum and its penetration depth into human skin.** according to [39, 100, 101]. The Figure was partly generated using Servier Medical Art, provided by Servier, licensed under a Creative Commons Attribution 3.0 unported license. Figure modified by adding text and markings.

UVB rays can be absorbed directly by DNA or melanin because they are chromophores. Here, UVB rays can still cause the generation of harmful reactive oxygen and nitrogen species (ROS and RNS). A defense mechanism of the skin is delayed tanning due to melanin synthesis when it is exposed to UVB radiation to reduce sunburn. The protective effect of the melanin against UV-induced damage is limited. Studies have suggested that UVB irradiation can induce the expression and activity of MMPs. These enzymes contribute to the breakdown of extracellular matrix components, which can lead to photoaging and cancer formation [57, 103].

UVA radiation, on the other hand, penetrates deeper and is subject to a different pathomechanism. It is a photosensibilization reaction, in which UVA exposure leads to the development of oxidative stress through the formation of free radicals in the skin [39, 104, 105]. There are two types of reaction: either reactive oxygen species (ROS) are formed by electron transfer or highly reactive singlet oxygen ($^1O_2$) is formed from molecular oxygen by direct energy transfer [104, 106]. This can further promote inflammation or the development of cancer [39, 99]. When UVA rays encounter polycyclic aromatic hydrocarbons, oxidative stress in the skin can be increased. The effect of PAHs was described in chapter 1.4.1 Air pollution. The synergistic effects of UVA radiation and PAHs can lead to increased genetic damage and acceleration of photoaging and carcinogenic processes [107, 108]. This has been demonstrated by Saladi et al. who found increased levels of 8-hydroxy-29-deoxyguanosine (8-OHdG), a marker of oxidative DNA damage, in

the skin of mice [109]. Permeation rates of PAHs under UV radiation into the skin also change significantly causing more damage [110].

## 1.5 Methods to expose skin to air pollution and measure the effect of pollution in skin

### 1.5.1 Methods for cigarette smoke exposure

So far, only a few methods are available to expose skin to air pollution, especially, cigarette smoke, in a reproducible manner, being important to be evaluated. However, some steps should be followed.

The first step is to postulate a hypothesis. This will enable you to apply the right method in a targeted way. In vitro experiments and cell culture experiments are often used as a basis which can later be transferred to ex vivo and then finally to in vivo models, which are more complex.

The next step would be to select the pollutant and the exposure method. In this case, cigarette smoke is often used. It is important to note that cigarettes include tobacco leaves, which are still a natural product. Therefore, the content can still vary. The type of cigarette and the additives also have a variation effect. These can vary in terms of nicotine, tar, carbon monoxide, heavy metals, etc. [111, 112]. The next question that needs to be addressed is how the exposure should be performed [24].

Exposure chambers are the method of choice. They can vary in size from an average radius of 3 cm to a volume in the square meter range. The number of puffs per minute play also a part in this. There are two different standards for the frequency of exposure: International Organization of Standardization (ISO) and Canadian Intense (CI) standards. According to ISO, to smoke a cigarette with a machine, there is a 2s puff for every 60s and for CI it is 2s for every 30s [78, 113]. Depending on the size of the chamber, the concentration in the chamber can vary. The number of cigarettes burned can also have an effect.

So far, the effect of cigarette smoke on skin has been investigated but was rarely analyzed in combination with the actual concentration that the sample is exposed to. This is important because the dosage has an effect on the response of the sample to cigarette smoke. To date, only a few studies have used cigarette smoke as a model for air pollution on skin. Most pollution studies have used particulate matter in particle sizes smaller than PM2.5 or diesel exhaust particles (DEP) [20, 114]. These pollutants are easier to dose and standardize in experiments. Consequently, they are more popular in studies because they are easier to handle.

One popular method to expose skin to cigarette smoke is using cigarette smoke extract (CSE). In a closed system cigarettes are burnt and then the smoke is transferred to a culture medium or a buffer solution. In most cases, one cigarette is captured per 25 mL of medium [24]. This extract is 100 % from cigarette smoke and is further diluted depending on the experiment. Depending on the solvent, different aqueous or organic components of the cigarette smoke and its deposits may be dissolved. For example, PAHs may be more soluble in organic solvents [115]. CSE is then added to cell cultures to measure the effect on the cells. It is important to note that with CSE, not all the constituents of cigarette smoke end up in the extract. For example, the concentration of highly volatile components such as aldehydes varies and PAH's solubility depends on the used solvent. In addition, the concentration of short-lived reactive species may vary depending on the age of the extract [85, 86]. Most importantly, the extract does not reflect the real conditions of exposure to cigarette smoke [24].

Studies have investigated the effect of CSE in vitro and in vivo. The results of the studies indicate that CSE activates the AhR pathway in human fibroblasts and keratinocytes, resulting in the production of MMP-1. This may further stimulate extrinsic skin aging [115]. Another study showed that CSE induces Egr-1 expression in human keratinocytes via MAPK, leading to increased TNF-α expression. This may lead to the inflammation that is involved in the onset and progression of psoriasis, for example [116]. Cigarette smoke has also been shown to promote premature skin aging in an in vivo study. In this study, CSE was applied to live hairless mice three times a week for six months. It was shown that the content of collagen bundles decreased. This may promote premature skin aging [117].

Other studies apply another method to study the effect of cigarette smoke in the skin. This second method uses smoke chambers [118, 119]. These are chambers connected to a vacuum pump or fan [73, 74]. The samples are placed into these chambers and the cigarette smoke is introduced. Fans are used to increase the distribution of smoke in the chamber. Based on the puff frequency and the number of cigarettes, the intensity and concentration in the chamber can be determined. The main advantage is that not only the particulate phase but also the gas phase enters the chamber and is exposed to the sample. In addition, not only mainstream smoke but also sidestream smoke can be used [24].

In an ex vivo study, living human skin explants (HSE) were exposed to two cigarettes in a smoking chamber (Pollubox ®) for two hours. Cigarette smoke exposure was shown to cause oxidation of skin lipids. The parameters TEWL and pH were also affected by cigarette smoke [38]. Increased lipid peroxidation after exposure to cigarette smoke was also found in an in vivo study. In this study, 3 cm diameter exposure chambers were

attached to the back of subjects and the skin was exposed to cigarette smoke for 30 minutes [120].

### 1.5.2 Effects of pollution on skin

There are different ways of measuring the effects of air pollution on the skin depending on the nature of the pollutants. Each pollutant acts different on the skin, therefore it is difficult to choose a method that will cover and measure all the effects in a realistic manner. Therefore, it is important to look at each method in detail and individually and to be aware of its limitations.

Different methods are available depending on the skin model chosen to study. Regarding the effect of pollution, the focus was on skin aging, and the path mechanism studied after exposure, e.g. oxidative stress and inflammation [24].

For in vivo studies, several epidemiological studies were carried out that retrospectively described the skin aging effects of pollution on the skin. For example, wrinkles and the development of pigment spots were used to compare the magnitude of different exposure concentrations [84, 121].

Measuring lipid oxidation on the skin of human forearms after smoke exposure has been another method for in vivo studies. Measuring the skin pigmentation and melanin pigmentation associated with gene expression after pollution exposure is another recent method [20].

At the molecular level, there has been a move towards in vitro and ex vivo methods. A popular qualitative tool has been the measurement of oxidative stress after pollution exposure using the DCFH-DA assay, which is an immunohistochemistry method [74, 122], or the determination of inflammatory markers such as interleukins [119, 123].

In this work, the methods of Electron Spin Resonance Spectroscopy (EPR) and confocal Raman microspectroscopy (CRM) were used. EPR can be used to measure radical production after stress induction in the skin, while CRM can measure the increase in oxidative stress-induced autofluorescence. The following chapters will introduce these two methods.

### 1.5.2 Electron paramagnetic resonance (EPR) spectroscopy methods to measure the effect of cigarette smoke in skin

Electron spin resonance (EPR) spectroscopy is a method that allows quantitative and qualitative analysis of free radicals in the skin. This method is non-invasive and can be used in vivo, ex vivo, and in vitro. Paramagnetic substances can absorb resonant microwaves in an external magnetic field. Therefore, the EPR can measure unpaired electrons in paramagnetic substances. They have an intrinsic angular momentum due to the spin of the unpaired electrons which is defined by the spin quantum number ($m_s$) [124, 125].

This momentum generates a magnetic moment that interacts with the external magnetic field of the EPR spectrometer. In the presence of a strong external magnetic field, the electrons can split into different energy levels, which is known as the Zeeman Effect. Unpaired electrons can orient themselves in two directions. If the attraction is towards the magnetic field, it is called the “parallel” ground state. The spin quantum number ($m_s$) is then + ½. If there is a repulsion directed in the opposite direction, it is called the “anti-parallel” ground state. Here, the spin quantum number is $m_s$ – ½ [125, 126].

Zeeman splitting leads to an energy gap between the two states. This energy gap describes the difference between the potential energies of the two ground states and is proportional to the strength of the external magnetic field (Figure 5a) [124, 125, 127].

The EPR method works as follows: The sample is placed in the resonator and a homogeneous magnetic field is applied. Microwaves are emitted at a constant frequency and the magnetic field strength is adapted until resonance is achieved. Only under resonance conditions does the magnetic field strength correspond to the energy difference that occurs when the microwave radiation is absorbed [125].

The different frequencies used in EPR determine the sensitivity and depth of penetration of the measurement into the sample. For in vivo measurements, the L-band at 1 GHz is widely used. Here the microwave radiation reaches a depth of 5 - 10 mm in water-rich samples. The X-band at 9 GHz reaches a penetration depth of 0.5 - 1 mm in aqueous samples, which is ideal for ex vivo and in vitro measurements. The microwave radiation is absorbed by the water and polar lipids [128].

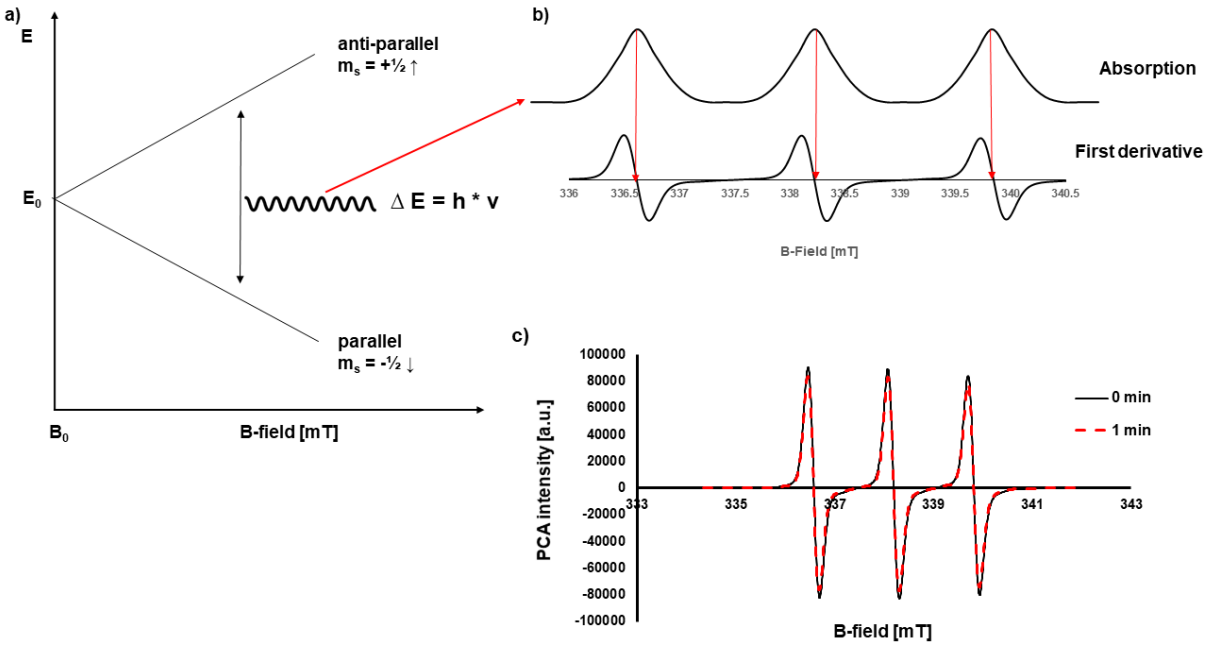


**Figure 5 a) Zeeman splitting of an electron's energy levels in an increasing strength B-field**. The spin is at $m_s$ = 1/2, shown in two different energy levels. When the energy level of the microwaves resonates with the difference of both energy levels, it will lead to absorption. **b) EPR absorption spectrum of PCA and its first derivation**. The first derivative of the absorption spectrum is the actual EPR spectrum. The important information is on the details of the spectral lines. The spin marker consists of a nitroxide radical with hydrophilic properties. **d) EPR spectrum of PCA after 0 and 1 minute.** A decrease in spectrum intensity can be evaluated after 1 minute of irradiation (red) of excised porcine skin treated with PCA compared to a non-irradiated sample (0 minute, black). According to [125, 129-132]

### 1.5.2.1 Spin probes

Free radicals have a very short half-life, which can range from one nanosecond to ten seconds [36]. In order to detect and measure them, the radicals need to be labelled. Organic molecules are used as markers for EPR measurements to stabilize the radicals in the investigated system. These adducts have a longer half-life than the pure radicals and are therefore easier to detect. Most spin probes used for EPR measurements are nitroxides, which have a free, unpaired electron in the outer shell (Figure 6a) [133-135]. This allows them to give an active signal in the EPR spectrometer. When the spin probe encounters a free radical, the spin probe reacts with the free radical and therefore becomes EPR-inactive (Figure 5c). As a result, the intensity of the EPR signal decreases as the amount of radicals in the spin probe increases [132]. This indicates of how many radicals are formed as a result of an external stressor, e.g. UV irradiation. The choice of solvent plays an important role in the interaction between electrons, nuclear spins and the signal of the spin probe, e.g. PCA ((3-(Carboxyl)-2,2,5,5-tetramethyl-1-Pyrrolidinyloxy) (Figure 6a). For example, a higher ethanol concentration has an effect on where the PCA gets distributed in the microenvironment of the SC [136].

The unpaired electron of PCA is next to the nitrogen atom of the nitroxide structure (Figure 6a). The nucleus of the nitrogen has its own magnetic momentum, which generates a local magnetic field. Thus, the magnetic field of the $^{14}N$ atom can be oriented in three different ways inside the external magnetic field $B_0$, since the nuclear spin has an exact value of 1 [137]. This can be seen in the EPR spectra. The first derivative is the absorption spectrum. The double integral of the spectrum provides an effective means of determining signal intensity (Figure 5b).

Another spin probe is TEMPO (2,2,6,6-tetramethylpiperidine-1-oxyl) (Figure 6b), which can indicate the antioxidative status of a microenvironment. TEMPO is amphiphilic due to its uncharged piperidine nitroxide radical and therefore can be used to study membrane lipids [138].

Another stable radical is 1,1-diphenyl-2-picrylhydrazyl (DPPH) the assay of which is used for radical scavenging assessment (Figure 6c). DPPH can be used to assess antioxidant activity of various compounds. The original concentration of DPPH is reduced, which is indicated by a change in color of the solution from purple to yellow. To assess the antioxidant capacity of different ingredients and formulations, the measurement of the radical protection factor (RPF) can be used. The RPF is the amount of reduced DPPH when it was put in a solution with the testing compound. The difference between the DPPH solution and the control DPPH intensity was normalized to 1 mg input. This gives a unit of RPF in $10^{14}$ radicals/mg [139, 140].

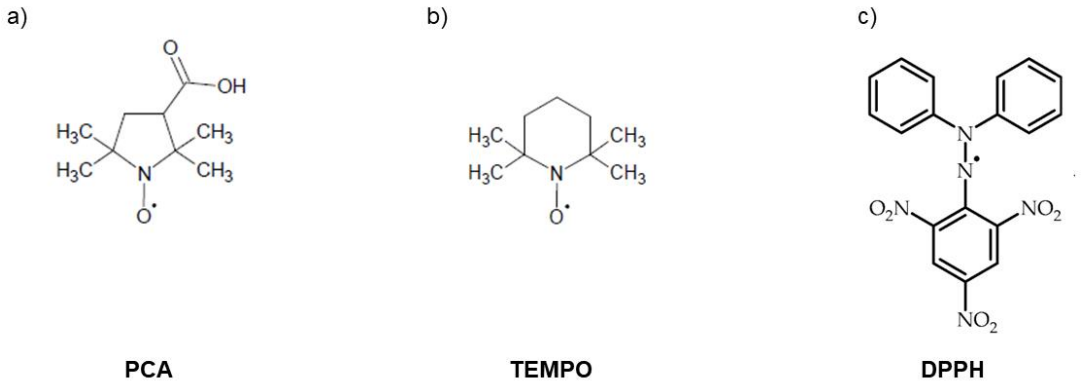


**Figure 6 EPR spin probes and their stable radicals.** a) Chemical structure of PCA b) TEMPO c) DPPH. According to [130, 141, 142]

### 1.5.3 Measuring autofluorescence using different Confocal spectrometers after cigarette smoke exposure in skin

Raman spectroscopy constitutes a distinctive vibrational spectroscopic method. It operates by discovering interactions produced by shining monochromatic light onto a sample. The light induces molecular vibrations that can be utilized to determine the traits of the sample [143].

When monochromatic light is directed at a sample, the photons can be absorbed, causing the sample to enter an electronically excited state. However, as it lacks the necessary energy to remain in this state, it returns to the ground state and releases a photon with less energy and a longer wavelength [143]. Autofluorescence needs to be distinguished from the Raman effect since both result in longer-wavelength photon emission. However, the detector of the Raman micro spectroscope fails to differentiate between the two effects, compromising the accuracy of Raman spectra. Fluorescence spectra exhibit wider bands and do not relay data about molecular vibrations [144].

In this work, the confocal Raman spectrometer was used to measure autofluorescence, which is conventionally considered an unwanted side effect. Fluorescence can be subordinated to luminescence, where susceptible molecules (fluorophores) emit light from electronically excited states created by absorption of light (Figure 7).

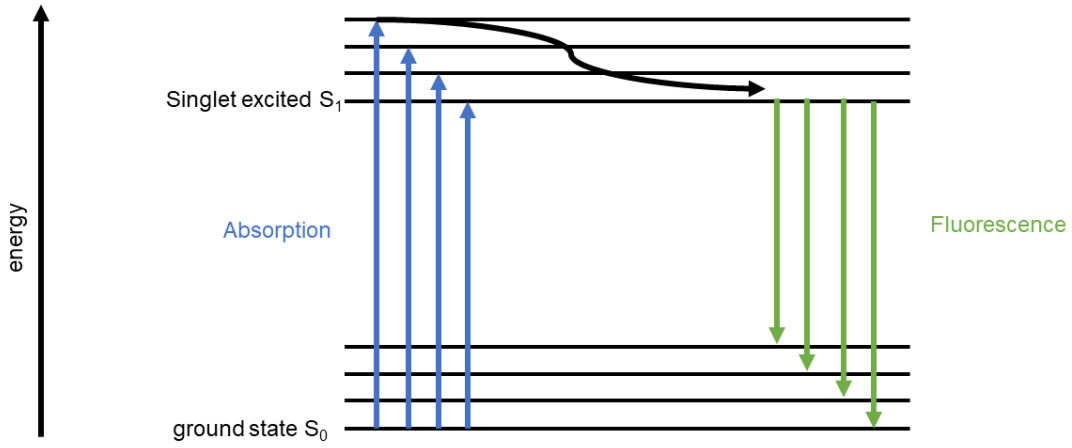


**Figure 7 Jablonski energy diagram of electronic energy levels of fluorophore molecules**. Excitation by a light source is shown in upward arrows. The emission of photons is shown in downward arrows. The relaxation to the S1- state after photon absorption are shown as wiggly arrow. According to [145, 146]

Fluorophores such as mitochondria and lysosomes can be found in biological tissues [147]. Autofluorescence in biological tissue is strongest when excited with short wavelengths, such as those in the UV range. The intensity of autofluorescence decreases

as the excitation wavelength increases, for example, with red and near-infrared light. Additionally, the intensity of autofluorescence decreases significantly as the depth of the skin increases [148].

Confocal laser scanning microscopy (CLSM) is an optical imaging technique that generates fluorescence in the visible spectrum region with a continuous-wave laser. It can also be used to assess autofluorescence. The fluorophore molecule can enter the excited state within this range. CLSM produces horizontal images and in-depth scanning, unlike CRM, which allows only for in-depth analysis [148].

## 1.6 Evaluation of anti-pollution formulations

It is essential to conduct appropriate tests to evaluate the efficacy of anti-pollution skin care products. It is crucial to consider the importance of reliability, reproducibility, and conditions that are as close to real-world settings as possible when designing a study.

For such products, there are requirements. Many products are supposed to reduce the particle load by exfoliating the skin. They should restore and reinforce the skin barrier, stop air pollution from depositing on the skin and from penetrating it, and ideally shield the skin from UV rays, which can amplify the effects of air pollution [25, 149].

Regular skin cleansing with cleansers, which removes particles and pollutants from the skin, is one type of skin protection. This ought to stop air pollutants from penetrating the skin. The use of film formers is also an option [25].

The use of ceramides, natural fat building blocks that protect our skin from moisture loss and environmental influences, can also improve the skin barrier [150].

Another option is the use of antioxidants in skin care products. Antioxidants and metal-chelating compounds can be used to mitigate the effects of oxidative stress in skin [151-153].

According to Chapter 1.1.2, the efficacy of products may be studied in vitro, ex vivo, and in vivo depending on the region of production and distribution. In terms of efficacy, products can be studied for their preventive, short-term, or long-term protection under real and controlled conditions. Examples of the study of immediate and long-term protection by anti-pollution products have already been demonstrated using spectrometric and chromatographic methods [24]. In these studies, cotton swab samples were taken from the forearms of the test persons before and after air pollution exposure and examined for the composition of the skin lipids. If an increased concentration of lipid peroxidation markers could be measured, such as squalene monohydroperoxides or malondialdehydes

(MDA), the effect of the development of oxidative stress could be demonstrated. The reduction of oxidative stress would then provide information about the effectiveness of the anti-pollution products. In these studies, Bielfeldt et al. already examined two antioxidants in a base cream formulation for their effectiveness ex and in vivo [73].

Another example of in vitro studies is the work of Áscová et al. In this study, two carotenoids were tested against synthetic antioxidants in four in vitro and ex vivo models regarding their protective properties in relation to oxidative stress. The researchers applied stressors directly to the excised porcine skin and employed a range of techniques to evaluate the antioxidant activity of the substances. In the ex vivo method, they used hydrogen peroxide to represent the production of endogenous ROS in the human body and cigarette smoke as an air pollution model [122].

However, there is still a lack of studies investigating the efficacy of anti-pollution products under real-life conditions: most of the studies did not measure the exact concentration of the pollutants, which is an important factor in assessing the effectiveness of individual products. In addition, additional in vivo studies using non-invasive techniques, which allows to study the skin alteration directly, are still missing.

## 1.7 Objectives

The aim of this work is to assess the effectiveness of anti-pollution creams ex vivo and validating them in vivo.

To accomplish this, a carefully controlled environment was created to expose the skin to air pollution. Two exposure chambers were constructed that were suitable for both ex vivo and in vivo studies. Cigarette smoke was utilized as a model pollutant, as the chemical compounds are comparable to air pollutants. The degree of exposure was determined by measuring the nicotine concentration and correlating it to the actual particle concentration inside the chamber. Moreover, the nicotine concentration was directly measured on the exposed skin enabling the establishment of a correlation between the level of exposure and the impact of pollution.

After the construction of a reproducible and realistic exposure chamber, two measurement methods were developed ex vivo and in vivo to measure the effect in the skin after exposure to pollution.

The first ex vivo method established was the EPR method, which is suitable for quantifying radicals in the skin. The EPR technique is a suitable method to measure radicals in the skin. Different spin markers were used to quantify the radical production in the skin. The study investigated the effects of cigarette smoke, both alone and in combination with UVA irradiation. However, due to practical limitations in vivo measurements were not possible.

The second ex vivo method used the autofluorescence of the skin following exposure to cigarette smoke. To measure autofluorescence, a Confocal Raman Microscope (CRM) was used as a sensitive photospectrometer. The study of autofluorescence can be useful in examining the effects of oxidative stress resulting from exposure to cigarette smoke.

This measurement method was applied to in vivo research to assess the impact of pollution on healthy skin in a clinical setting. The ex vivo results were compared with the in vivo data to validate the findings.

To evaluate the effectiveness of anti-pollution creams, five different formulations were tested using ex vivo methods. Regrettably, due to limiting factors, in vivo testing could not be conducted.

# 2. Results

## 2.1 Establishment of a method to expose and measure pollution in excised porcine skin with electron paramagnetic resonance spectroscopy

Authors: Phuong Thao Tran, Batoul Beidoun, Silke B. Lohan, Rajae Talbi, Burkhard Kleuser, Marietta Seifert, Katinka Jung, Grit Sandig, Martina C. Meinke

Journal: Journal of Ecotoxicology and Environmental Safety, 247 (2022), 114258

Available online: https://doi.org/10.1016/j.ecoenv.2022.114258



Amount performed by Phuong Thao Tran:

Design of experiments: 90%

Practical, experimental part: 80%

Data analysis: 95%

Interpretation of results: 100%

Writing: 95%

Ecotoxicology and Environmental Safety 247 (2022) 114258

Contents lists available at ScienceDirect

Ecotoxicology and Environmental Safety

journal homepage: www.elsevier.com/locate/ecoenv

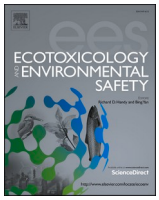

# Establishment of a method to expose and measure pollution in excised porcine skin with electron paramagnetic resonance spectroscopy

Phuong Thao Tran [a,b], Batoul Beidoun [a,d], Silke B. Lohan [a], Rajae Talbi [a,d], Burkhard Kleuser [b], Marietta Seifert [c], Katinka Jung [c], Grit Sandig [c], Martina C. Meinke [a,*]

[a] Center of Experimental and Applied Cutaneous Physiology, Department of Dermatology, Venerology and Allergology, Charité – Universitätsmedizin Berlin, Corporate Member of Freie Universität Berlin and Humboldt-Universität zu Berlin, Charitéplatz 1, 10117 Berlin, Germany
[b] Institute of Pharmacy, Department of Pharmacology, Freie Universität Berlin, Königin-Luise-Str. 2+4, 14195, Berlin, Germany
[c] Gematria Test Lab GmbH, 13187 Berlin, Germany
[d] Berliner Hochschule für Technik Berlin, Luxemburger Straße 10 in, 13353 Berlin, Germany

ARTICLE INFO

Edited by Professor Bing Yan

*Keywords:*
Pollutant
Cigarette smoke
Electron paramagnetic resonance spectroscopy
Exposure chamber

ABSTRACT

Health problems associated with the amount of air pollutants are increasing worldwide. Pollution damages not only the lungs; it also has an impact on skin health and is co-responsible for the development of skin diseases.

Anti-pollution products are on the rise in the cosmetic market but so far, there is no established method to directly assess the impact of pollution on the skin and to test the efficacy of anti-pollution products.

To address this problem, two different chambers were developed for the reproducible exposure to realistic air pollutant concentrations. One chamber for the exclusive use of excised skin and hair samples, the second chamber for *ex vivo* and *in vivo* measurements. Measurements of nicotine next to the investigated skin area allow conclusions to be drawn on the particle concentration to which the skin is exposed. Electron paramagnetic resonance spectroscopy, which enables the detection of free radicals in different systems, was applied to assess the hazard potential of pollution in the skin. A direct proof of the formation of free radicals in the skin by the model pollutant cigarette smoke could be demonstrated. An additional application of UV irradiation even increased the formation of free radicals in the skin seven-fold (sum parameter). Depending on the question of interest, the use of different spin probes allows various assessments of the radical formation in skin: the amount of radicals but also the antioxidant status of the microenvironment can be estimated.

Using two exposure chambers, the direct formation of oxidative stress by cigarette smoke on *ex vivo* skin, with and without additional UV exposure, could be reproducibly examined. This measurement method is promising for the assessment of anti-pollution products and could allow a direct causal connection between pollutant, effect on the skin and the protective function of skin care products.

## 1. Introduction

The increase of air pollutants worldwide causes major health problems. According to WHO (World Health Organization), it leads to more than 7 million deaths each year (Organization, 2021). Pollution not only affects the mucous membrane in the lungs, it can also damage our skin barrier and is linked to the development of skin diseases (Mannucci and Franchini, 2017). Main components of air pollution are particulate matter, hydrocarbons, carbon monoxide, carbon dioxide, nitrogen monoxide, nitrogen dioxide, and sulphur trioxide (Ferrara et al., 2021; Kampa and Castanas, 2008). The main cause of advancing air pollution is the worldwide industrialization. The increased use of machines, the growing mobility of people by cars and airplanes, and the rising energy demand are leading to an increase in air pollution, which, in addition to climate change, also affects global health (7 million deaths, 2014).

Causal relationships between oxidative stress-associated phenotypes and air pollution are given. Epidemiological and mechanistic studies could demonstrate that air pollution promotes premature skin aging: a positive correlation between exposure to air pollution and external signs of skin aging and skin hyperpigmentation has been demonstrated and a 20% concentration-dependent increase in pigment spots due to air pollution could been shown (Vierkotter et al., 2010). Furthermore, air

* Correspondence to: Charitéplatz 1, 10117 Berlin, Germany.
*E-mail address:* Martina.meinke@charite.de (M.C. Meinke).

https://doi.org/10.1016/j.ecoenv.2022.114258
Received 27 July 2022; Received in revised form 26 October 2022; Accepted 29 October 2022
Available online 4 November 2022

pollutants can lead to aggravation of already existing symptoms through oxidizing chain reactions, e.g., in atopic dermatitis (Kim et al., 2015).

In general, oxidative stress is manifested by an increased concentration of free radicals (reactive oxygen species, ROS) in the body, resulting in an imbalance in the redox homeostasis (Baek and Lee, 2016). It has been proven that ROS are involved in the development of many diseases such as cardiovascular disease (Rosoff et al., 2020) and cancer (Sobus and Warren, 2014), as well as in the aging of the organism (Liguori et al., 2018). The increasing rate of ROS can lead to extended oxidative destruction of single cell components and tissues (Bacic et al., 2016).

Endogenous as well as exogenous antioxidants, which have to be taken up by nutrition, are responsible for maintaining the balance between oxidants and antioxidants (Wolf, 1998). Antioxidants are the best choice to counteract elevated levels of ROS. In recent years, the cosmetic industry has been launching anti-pollution care products on the market whose effectiveness has not yet been sufficiently proven. In order to prove the effectiveness of anti-pollution products, a suitable and reproducible measurement method is to be established, which will be able to directly detect the effects of air pollutants and demonstrate the effect of anti-pollution products on excised skin (*ex vivo*) or *in vivo* after exposure to pollution.

Since cigarette smoke contributes to air pollution, it serves as a good experimental representative, because of its ubiquitously presence and a similar PM 2.5 concentration like diesel exhaust (Invernizzi et al., 2004), which is a major outdoor pollutant. Cigarette smoke is an aerosol which contains over $10^{15}$-$10^{17}$ particles per puff. Polycyclic aromatic hydrocarbons, nitrosamines, and other organic noxious substances represent the main components (Kopa and Pawliczak, 2018) and up to 4000 different chemical compounds are released during cigarette consumption or burning (Bourgeois et al., 2016).

Cigarette smoke can be divided into a particle phase and a gas phase. The gas phase contains free radicals and oxidants that are in a steady state, meaning that they are continuously formed and destroyed. Over time, the concentration of free radicals increases. The particle phase contains at least 3500 toxic chemical compounds and is mostly responsible for the ROS production which promotes the development of carcinogenic and mutagenic effects in humans (Pfeifer et al., 2002). In the particle phase the tar in cigarettes is smaller than 2.5 μm in size and can therefore penetrate easily into the deeper airways up to the alveoli promoting damage of cell components (Bernhard et al., 2007). To date, however, the effects of such cigarette smoke particles on the skin have not been further characterized and no precise PM values have been published for skin exposed to extensive pollution so far.

The electron paramagnetic resonance (EPR) spectroscopy enables the direct measurement of paramagnetic substances, i.e., free radicals by the use of spin probes or spin traps (Pryor et al., 1983; Yamaguchi et al., 1992; Marchand et al., 2017). In this study, the spin probes PCA (3-(carboxyl)− 2,2,5,5-tetramethyl-1-pyrrolidinyloxy) and TEMPO (2,2,6,6-tetramethylpiperidine-1-oxyl) were used. PCA enables the detection of free radicals due to external stress sources, e.g., irradiation because this spin probe shows only a slow or no penetration rate into cells (Swartz et al., 1986) so that metabolic radicals have only little influence on the measured radical concentration. The nitroxide TEMPO is a typical spin probe for the investigation of the antioxidant status. Its amphiphilic character allows the uptake into cells enabling the spin probe to interact directly with metabolically produced radicals and antioxidants (Elpelt et al., 2020).

Numerous studies on the formation of radicals in tobacco smoke using EPR technology have already been published (Pryor et al., 1983; Yamaguchi et al., 1992). First investigations are being conducted to investigate the effect of cigarette smoke on the metabolism and skin by EPR spectroscopy (Bielfeldt et al., 2021). Bielfeldt et al (Bielfeldt et al., 2021). were able to demonstrate radical formation by cigarette smoke in combination with additional irradiation on skin.

Gao et al (Gao et al., 2002). have shown the effect of the gaseous phase of cigarette smoke in rat mitochondria membrane.

Interestingly, the effect of cigarette smoke alone and the absolute quantification of smoke-induced radicals on skin has not been previously studied by EPR.

In addition to air pollution, the skin is exposed to numerous exogenous factors, including UV radiation. Cigarette smoke as well as UV radiation belong to exposomal factors that can lead to skin aging as summarized by Krutmann et al (Krutmann et al., 2021). In general, UVA and UVB radiation are sources of radical production in the skin, leading to skin aging, inflammation, and cancer (Tarbuk et al., 2016). UVA mainly induces radicals, while UVB primary causes DNA damage (Meinke et al., 2021). Thus, sunlight or UVA represents an additional parameter to enhance a stress response in skin (Herrling et al., 2006).

In this study, two exposure chambers have been developed for the targeted exposure of skin to realistic pollution concentrations. Therefore, cigarette smoke was chosen as a model pollutant. It can be easily applied and is readily accessible for investigations. Nicotine measurements were implemented to determine the concentration of the particular matter of the smoke. The amount of cigarette smoke exposure was controlled by the number of cigarettes and a targeted smoke release, regulated by the experimental setup. EPR spectroscopy was applied using the spin probes PCA and TEMPO. The radical-inducing effect of the particle phase as such, and the combination with the exogenous factor UV irradiation on skin were investigated.

## 2. Materials and methods

### 2.1. Materials

#### 2.1.1. Exposure chambers

To enable a reproducible, uniform and realistic smoking of the skin, two exposure chambers have been developed, into which excised skin, hair as well as a complete forearm of a volunteer can be inserted (Fig. 1).

These two chambers, which were designed in cooperation with the in-house Center for Scientific Workshops of the Charité - Universitätsmedizin Berlin, have a cylindrical shape with different ventilation openings for an even distribution of the pollutant. They are compact chambers made of polyacryl, whose opening is provided with a removable lid for insertion of skin samples, a forearm of a volunteer or hair. For the big chamber (Fig. 1a), a silicon ring was integrated into the removable lid to ensure an airtight seal of the chamber, despite an inserted forearm. It provides a volume of 3800 $cm^3$ , with a length of 34 cm and a cross section of 113.1 $cm^2$. The smaller chamber (Fig. 1b) has a volume of 520 $cm^3$ and is placed upright. The height of both chambers (horizontal position for the big chamber and vertical position for the small chamber) are comparable with 12 cm. The big chamber also has a baffle plate and a fan for even distribution of the pollutant. The small chamber was not equipped with a baffle plate or fan in order not to interfere with hair analysis.

#### 2.1.2. Research cigarettes

For the exposure experiments, the research cigarettes 1R6F (ISTD = internal standard, https://www.coresta.org/university-kentucky-reference-cigarette) were applied (ISO standard, ingredients per cigarette: tar: 8.6 mg; nicotine: 0.72 mg; carbon monoxide: 10.1 mg) (Sakai et al., 2020).

#### 2.1.3. Irradiation unit

UV irradiation was used as an additional stressor for a distinct measurement of free radicals induced by smoke exposure vs. untreated skin. For the MS 5000 EPR system, a UVA-LED irradiation unit with a wavelength of 365 ± 5 nm (Freiberg Instruments GmbH, Freiberg, Germany) and a UVA irradiance of 18 mW/$cm^2$ for 7 min was used. For the *in situ* irradiation, an irradiation time was selected which corresponds to about 1/3 minimal erythema dose for UVA (MED, 9 J/$cm^2$) (Diffey and Farr, 1989). The intensity of the UVA-LED light source was

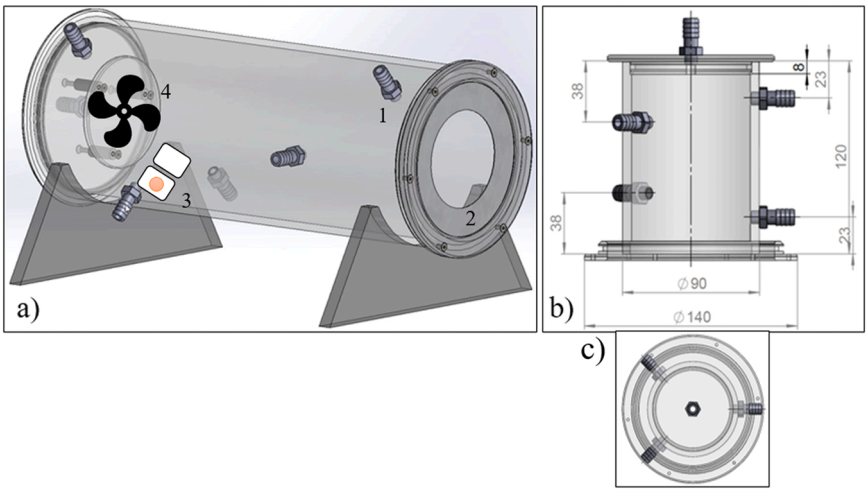


**Fig. 1.** Two smoking chambers manufactured by the center for scientific workshops (Charité - Universitätsmedizin Berlin, Germany). a): big smoking chamber for *ex* and *in vivo* studies; 1: vents, 2: silicon ring, 3 two filter papers placed next to each other, skin sample on one filter, second filter for nicotine extraction, 4: baffle plate with fan for smoke distribution b): small chamber for *ex vivo* studies only (skin and hair).c) small chamber view from above.

measured with an 843-R Power Meter (Newport Corporation, CA, USA). Thereby, the distance was chosen according to the irradiated skin sample within the resonator of the EPR device.

For the investigation using the MS 300 EPR spectrometer, a Hönle SOL 2 sun simulator H2 (Dr. Hönle AG, Gilching, Germany (range 280–1400 nm) was used. The irradiances as integrated value over the spectral ranges were E (UVB=280–320 nm) = 1.5 mW/cm$^2$ and E (UVA = 320–400 nm) = 18.8 mW/cm$^2$, corresponding to a MED of 1.2 after 5 min of irradiation. The intensity of the light source was measured with a UV-Meter μC Basic (Dr. Hönle AG, Gilching, Germany).

## 2.2. Methods

### 2.2.1. Particle measurements

With an aerosol monitor (DustTrak™ Aerosol Monitor, Model 8530EP, Driesen + Kern GmbH, Bad Bramstedt, Germany); the particle concentration of cigarette smoke could be measured up to a maximum concentration of 400 mg/m$^3$ whereby all particles with a diameter up to 10 μm were recorded. With only one cigarette the maximum measurable particle concentration is reached, but this range does not reflect real environmental conditions. In order to be able to detect particle concentrations above 400 mg/m$^3$ , an additional measuring method for recording the nicotine concentration in the exposure chambers was established (see 2.2.2). A correlation between the particle concentration and nicotine concentration was used to draw conclusions about the final aerosol concentration inside each exposure chamber.

### 2.2.2. Determination of nicotine concentration

Nicotine is a major component in cigarette smoke (Hammond et al., 1987), why it is often used as a surrogate parameter. In this approach, the nicotine absorption spectrum was applied to measure the increase of particle concentration in the exposure chambers. A positive correlation between the concentration of nicotine and the number of particles should be given.

In Fig. 2, the general set up of the particle measurement method for the big chamber is shown. From the chamber, the smoke is either directed via the measuring gas washing bottle or, if the taps are closed, sucked directly into the washing bottle by the pump. The bypass valves are required to regulate the pump flow. The total amount of the cigarette extract was collected in the measuring washing bottle and nicotine was finally quantified by UV–VIS spectroscopy (Perkin Elmer, Inc., Waltham, MA, USA). Here, the second maximum of the nicotine UV absorption λ 260 nm curve was used.

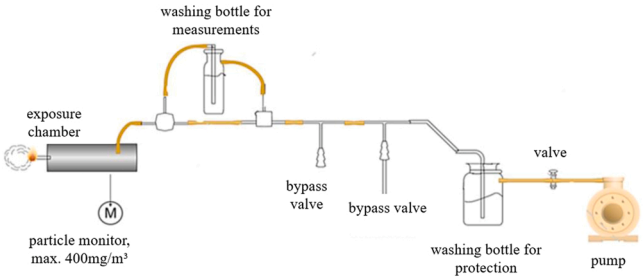


**Fig. 2.** Setup of the particle and nicotine measurement with the big exposure chamber. The particle monitor, which can measure particles sizes < 10 μm up to 400 mg/m$^3$ , is attached to the exposure chamber. The smoke of a cigarette passes the chamber and exposes the sample in the chamber. Then the smoke passes the washing bottle for measurements (=extraction) and the washing bottle for protection until it reaches the pump. Different valves allow the control of the pump power for regulating the smoke amount in the big chamber.

The cigarette smoke introduced into the exposure chamber was transferred into a washing bottle containing water (Fig. 2, washing bottle for measurement). The absorption of nicotine of this aqueous solution was also determined by the UV–VIS spectrometer Perkin Elmer Lambda 650 S (Perkin Elmer, Inc., Waltham, MA, USA). In addition, the absorption of pure nicotine in the aqueous (260 nm) (Clayton et al., 2013) and ethanolic solution (262 nm) (Swain et al., 1949) was measured and calibration curves were created.

The nicotine measurement results from the measuring washing bottle allow conclusions to be drawn about the average concentration in the air, but they do not reflect the exposure on the skin. Therefore, an additional filter was placed next to the skin sample. After each smoking exposure, the filter was extracted in 10 ml either ethanol or distilled water for 30 min and the UV absorption of nicotine was analyzed by the UV–VIS-spectrometer. Thus, the smoke exposure on the skin can be reflected independent of the size of the chamber and the smoking regime.

In this way, the smoke exposure of the skin could be quantified with a relative standard derivation of 2.6%.

### 2.2.3. Electron paramagnetic resonance spectroscopy

*2.2.3.1. EPR devices.* Two different EPR devices were applied for the quantification of the radicals in the skin samples.

On the one hand, the X-band EPR system MiniScope MS 5000

(Magnettech, Freiberg Instruments GmbH, Freiberg, Germany) was used, on the other hand the MiniScope MS 300 (Magnettech GmbH Berlin, Germany) was applied. A special feature of the MS 5000 is that irradiation can take place *in situ* what allows the direct determination of the absolute amount of induced radicals in the skin.

For better overview, both devices and their settings are shown in Table S1.

*2.2.3.2. Sample preparation and EPR measurements.* Porcine ears were obtained from a local butcher and were used within 48 h after slaughtering, which is a time range ensuring metabolic response, as shown for radical formation due to infrared irradiation (Darvin et al., 2010) and enzymatic response e.g. catalase activity (Haag et al., 2010). The Veterinary Office Dahme-Spreewald approved the experiments in accordance with Section 3, Article 17, paragraph 1, of Regulation (EC) No 1069/2009 of the European Parliament and Council dated October 21, 2009, laying down health rules for animal products not intended for human consumption by-products. After receiving the porcine ears, these were washed with cold water and the hair was carefully removed by shaving. They were kept at 4 °C until use.

For the measurements with the MS 5000, 300 μm thick slices of split skin were cut by using a dermatome (type GA 140, Aesculap-Werke AG, Melsungen, Germany). The split skin was kept refrigerated in moist towels until use, max. 6 h after dermatomization. An 8 mm (ø) punch biopsy from split skin was placed into a tissue culture plate (24 Well, Falcon, NC, USA) on one filter disc (Filter Disks for Finn Chambers 8 mm, Smart Practice, Denmark) moistened with 15 μl PBS. Then an additional filter disc soaked with 38.4 μl 1.5 mM PCA (Sigma-Aldrich, Steinheim, Germany) was applied on top of the skin biopsy. After an incubation time of 5 min the skin was measured with the EPR spectrometer (untreated) or was exposed to cigarette smoke (treated) using the big exposure chamber. The time interval between the spin probe incubation and the EPR measurement had always been maintained, regardless of whether the skin was untreated or treated. For the EPR measurements, a skin sample of 4 mm (ø) was punched out from the center of the incubated biopsy. The skin sample was then placed into a tissue cell (Magnettech Freiberg Instruments GmbH, Freiberg, Germany) which was placed in the EPR resonator for measurement.

EPR measurements were performed at 32 °C with the help of a temperature control unit (BTC01, Magnettech, Berlin, Germany) and measured in a single scan operation mode with 14 spectra over a time of 400 s. The magnetic parameters for the measurement were already established in Lohan et al (Lohan et al., 2021a). and are shown in Table S1.

The preparation method for the MS 300 was different: Fresh porcine ear skin was prepared by removal of the subcutaneous fat. 1 cm by 1 cm skin samples were placed on filter that were incubated with 30 μl of PBS in a weighing pan. For the EPR investigations, two spin probes were used: PCA and TEMPO (Merck KGaA, Darmstadt, Germany). A spin probe solution was diluted in 50% ethanol/water to a concentration of 1 mM PCA (10 mM TEMPO). 5 μl of the PCA or TEMPO solution was applied directly onto the skin surface, evenly distributed and allowed to penetrate for 10 min prior to cigarette smoke exposure.

After the smoking-procedure (treated or untreated), a 4 mm (ø) punch biopsy was taken, placed into a tissue flat cell (Magnettech Berlin, Germany) and the PCA signal was determined using EPR spectroscopy (magnetic parameters are listed in Table S1) after 6 different UV irradiation time points (t = 0, 30 s, 1 min, 2 min, 3 min, 5 min, Hönle SOL2 sun simulator). For a better overview, the different sample preparation techniques are shown in Table S2.

*2.2.4. Cigarettes exposure*

The number of cigarettes was adapted to the size of the exposure chamber. Five cigarettes with cut off filters were used simultaneously for the big exposure chamber, the skin sample was actively exposed to smoke for 5 min, pumping time was one minute, and the following four minutes the smoke had time to settle on the skin.

For the small exposure chamber, one cigarette was applied. Cigarette smoke has been applied for 5 min by interval smoke exposure (2 s on/ 30 s off).

### 2.3. Data analysis and statistics

The data are presented as mean + /- standard error of the mean (SEM). Per ear, double measurements were carried out. An IBM Statistical Package for the Social Sciences (SPSS) Statistics version 27 (IBM Corporation, Armonk, USA) was applied for the statistical analysis. The significance of the radical production in excised porcine skin over the entire measurement period was evaluated by generalized estimating equation (GEE). A p-value of less than 0.05 was considered as statistically significant.

Calculations of the quantification of the spin concentration with the MS 5000 were based on the method of Lohan et al (Lohan et al., 2021b).

Relative radical production was calculated by evaluating the peak to peak intensity of the spin probe.

## 3. Results

### 3.1. Determination of particle and nicotine concentration on excised skin samples

Reproducible exposure of the skin to cigarette smoke was the prerequisite for reliable radical measurement in skin. As the concentration of the particle-measuring device is limited to 400 $mg/m^3$, another method has to be established which allows the reproducible detection of higher exposure concentrations. Therefore, the particle concentration and the nicotine concentration in the washing bottle were determined in parallel and correlated with each other after the smoke exposure in the chambers. The particulate matter concentration correlates significantly ($p < 0.001$) with the nicotine concentration measured in the washing bottle (Fig. 3a).

The particle concentration measured with the particle-measuring device fluctuates; the relative standard deviation is around 12%, which is comparable with the total standard deviation of the absorption values from the photometric determination of the cigarette extract from the washing bottle (Table S3).

Taking this correlation into account, a rough estimation of the PM concentration would be possible at higher PM concentration where radical formation could be observed if we assume that this relationship can be extrapolated. The disadvantage of this procedure is that the amount of smoke passing through the chamber does not necessarily correlate with the amount of exposed smoke on the skin. This depends on the pumping power and the residence time of the individual smoke regimes and the homogenous distribution within the chamber.

The deposition of nicotine on a filter near the skin samples exposed inside chambers could provide a measurement of the portion of the smoke that reaches the skin. The variation of the different methods to estimate the particle or nicotine concentration in the chamber is shown in Table S3. The nicotine deposit on the filter was determined with the lowest SD of 2.6% in comparison to the extract from the washing bottle (SD %: 12) and the particle concentration from the particle measuring device (SD %: 12) and most accurately represents the amount of smoke on the skin.

For all further measurements, the smoke exposure on the skin samples was determined using the “filter assisted method“.

To be able to transfer the PM concentration from the nicotine

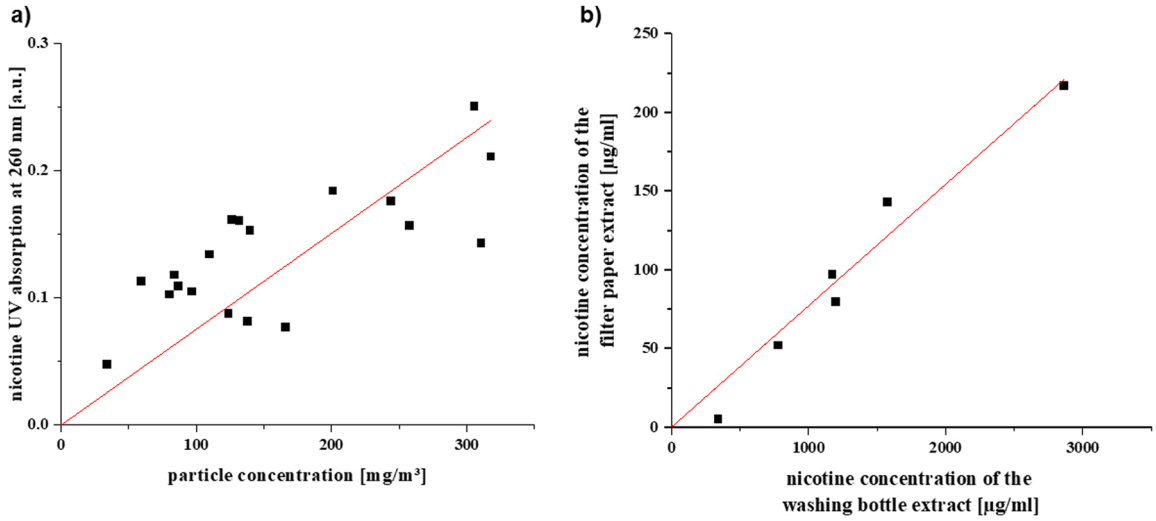


**Fig. 3.** Calibration curves of nicotine absorption and concentration in the washing bottle in correlation to a) particle monitor and b) filter paper extract, a) nicotine absorption at 260 nm of the extract of the washing bottle as a function of the particle concentration measured by a particle monitor in the big chamber. The mean particle concentration in the chamber was measured within seven minutes, $R^2 = 0.551$; * **$p \leq 0.001$, b) nicotine concentration in washing bottle extract and filter paper extract after smoke exposure of five minutes. Nicotine concentration was calculated from the nicotine absorption at their second maximum λ 260 nm for washing bottle extract and λ 262 nm for filter paper extract. $R^2 = 0.955$, * *$p \leq 0.01$.

concentration on the filter, both nicotine absorptions in the extract of the washing bottle and the extraction of the filter paper were investigated. Fig. 3b shows a significant ($p \leq 0.01$) linear correlation of both nicotine concentrations. This correlation provides the possibility to estimate the PM for each measurement and possibly to normalize the data to the quantity applied.

### 3.2. Ex vivo measurements with various X-Band EPR spectrometers

#### 3.2.1. Comparison of smoked and non-smoked skin

The effect of cigarette smoke without additional stressor application on excised porcine skin is shown in Fig. 4. The formation of free radicals was investigated with the spin probes PCA and TEMPO. The MS 5000 EPR spectrometer is a further development of the MS 300 EPR spectrometer and enables the direct quantification of radicals as shown in Fig. 4. For the measurements with the MS 300, the relative radical production is presented.

Fig. 4a shows the absolute cumulative radical production of cigarette smoke-exposed and non-exposed excised porcine skin. In smoke-exposed porcine ears, significantly more radicals were produced ($p \leq 0.001$) than in non-smoked porcine ears. Compared to the metabolic activity in non-exposed skin, the absolute radical production in smoke-exposed skin is almost twice as much ($1.06 \pm 0.31 \times 10^{13}$ to $2.85 \pm 0.36 \times 10^{13}$ radicals/mm$^3$). Nicotine concentration on the skin was $319 \pm 17$ µg/cm$^2$, which corresponds to a PM concentration of 96,771 mg/m$^3$ in the big chamber.

Fig. 4b shows the relative cumulative radical production of cigarette smoke-exposed and non-exposed excised porcine skin with TEMPO. A significance between these two groups is given ($p \leq 0.05$). Nicotine concentration on the skin was $72.4 \pm 6.6$ µg/cm$^2$.

#### 3.2.2. Comparison of the effect of smoke and UV on skin

To enhance the effect of cigarette smoke on the skin, irradiation was additionally applied as an external stress factor. Cigarette smoke, UV

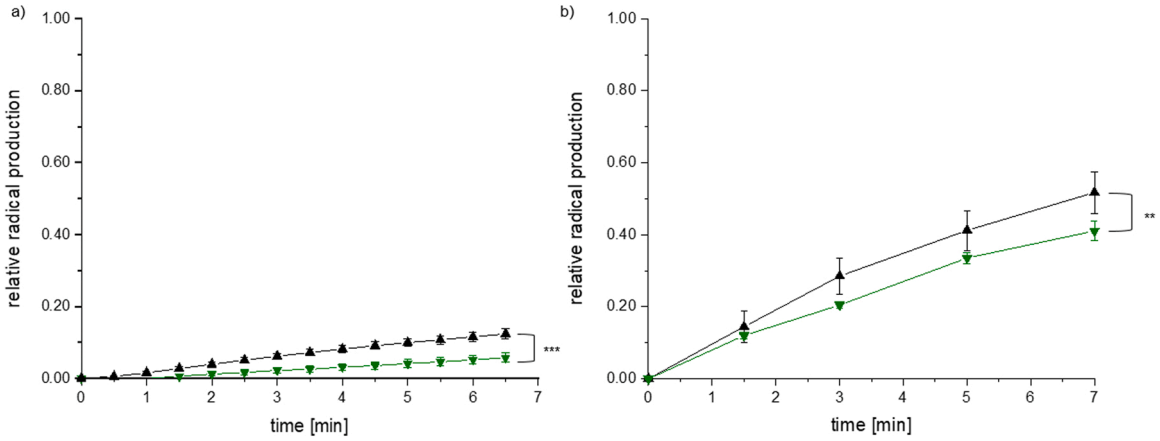


**Fig. 4.** Cumulative radical production after exposure of cigarette smoke only, using the spin probes PCA and TEMPO.a) Absolute cumulative radical production in porcine skin caused by 5 min cigarette smoke exposure of five cigarettes (black triangles) within the big exposure chamber compared to its metabolic activity (green triangles). The skin samples were incubated for 10 min with 38.4 µl of an 1.5 mM PCA solution at 32 °C and were measured with setup A; Mean ± SEM (n = 7), * ** $p \leq 0.001$.b) Relative cumulative radical production in porcine skin caused by 5 min exposure to smoke of one cigarette (black triangles) within the small exposure chamber compared to its metabolic activity (green triangles). The skin samples were incubated with 5 µl/cm$^2$ 10 mM TEMPO solution for 10 min and were measured with setup B; Mean ± SEM (n = 3), * *$p \leq 0.01$.

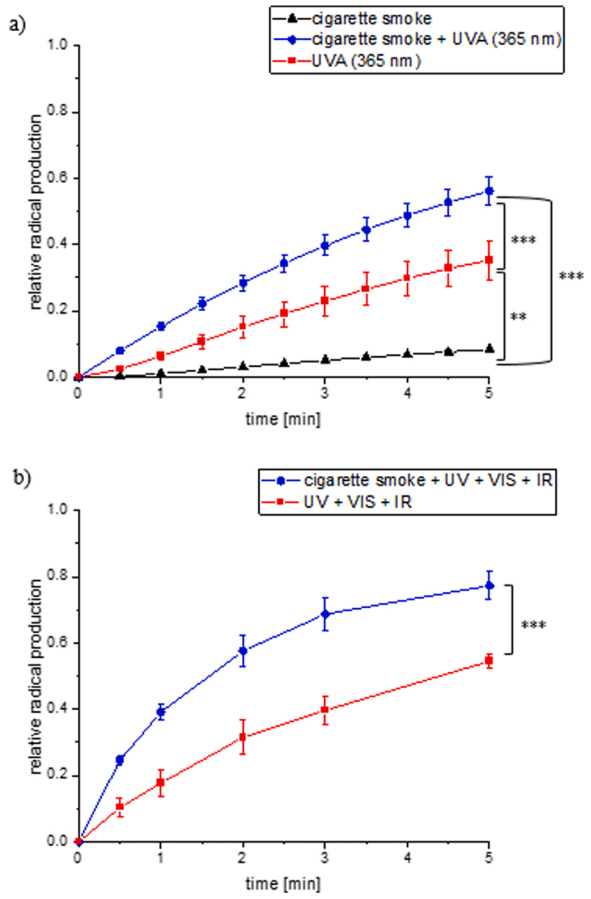


**Fig. 5.** Relative cumulative radical formation induced by irradiation and smoke alone and in combination. a) Comparison of the relative radical production in ex vivo porcine skin after exposure to smoke of five cigarettes for 5 min (black triangle) within the big exposure chamber, and in-situ UVA irradiation (365 nm) at 18 mW/cm$^2$ (red square) and combination of both (blue circle). The skin samples were incubated with 38.4 µl 1.5 mM PCA for 10 min at 32 °C and were measured with the MS 5000; Mean ± SEM.(n = 5); * *p ≤ 0.01; * **p ≤ 0.001.b) Comparison of the relative radical production in ex vivo porcine skin after smoke exposure by one cigarette for 5 min within the small exposure chamber and sun simulator irradiation (blue circle) irradiation alone (red square). The skin samples were incubated with 5 µl/cm$^2$ 1 mM PCA for 10 min and were measured with the MS 300; Mean ± SEM (n = 4); * **p ≤ 0.001.

irradiation and the combination of both stress factors were examined on excised skin with regard to the formation of radicals via EPR (Fig. 5).

Cigarette smoke and UVA irradiation alone, but also the combination of both exogenous stress factors lead to a significant ($p \leq 0.01$, $p \leq 0.001$) radical production (Fig. 5a). In a direct comparison, smoke alone generated $1.28 \pm 0.33 \times 10^{13}$ radicals/mm$^3$ in the skin. Compared to UVA irradiation of 5 min ($2.7 \pm 0.5 \times 10^{13}$ radicals/mm$^3$), cigarette smoke induced round about half as many radicals in the skin. The combination of cigarette smoke and UVA irradiation is three times higher ($6.8 \pm 1.1 \times 10^{13}$ radicals/mm$^3$) compared to 5 min cigarette smoke alone and increased by 20% compared to UV irradiation alone. The induction of free radicals in the skin by smoke alone was achieved by an average nicotine amount of 308 ± 27 µg/cm$^2$ after 5 min. In the experiments using the combination with UVA irradiation, an average nicotine amount of 297 ± 25 µg/cm$^2$ was detected.

With the MS 300, the radical production was measured not only by irradiation but also in combination with cigarette smoke. The UV-induced radical formation in the porcine skin due to cigarette smoke has increased by 40% with a high significance ($p \leq 0.001$) (Fig. 5b). Nicotine concentration on the skin was 62.7 ± 3.5 µg/cm$^2$ after 5 min

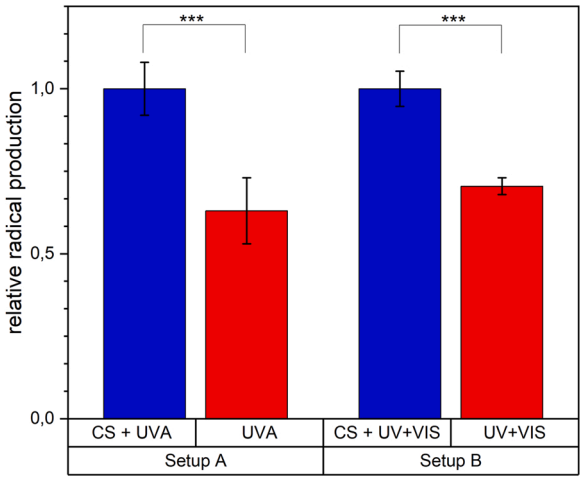


**Fig. 6.** Comparison of the relative radical production of two EPR methods run by two different EPR devices. Setup A: Five cigarettes in 5 min within the big exposure chamber, UVA 365 nm; 18 mW/cm$^2$, Mean ± SEM (n = 5), Setup B: One cigarette in 5 min within the small exposure chamber, Sun light simulator, UVB 280–320 nm; 1.5 mW/cm$^2$ and UVA 320–400 nm; 18.8 mW/cm$^2$, Mean ± SEM (n = 4). With the addition of cigarette smoke (CS), there is an increase in radical production in both systems. Between both devices and methods, the differences between the groups are comparable. Within the experiment, both devices reveal significant differences between irradiated skin on the one hand and smoked and irradiated skin on the other.

exposure which was 4 times lower than in the big exposure chamber.

In Fig. 6 the relative radical production of the two applied setups are compared. Both setups were individually optimized to maximal radical production per applied smoke or smoke plus irradiation. UV and VIS range was used for the MS 300, and UVA *in-situ*-irradiation was applied for the MS 5000. Not only the preparation of the samples varied in both setups, also the dose of exposure in both chambers was different. Interestingly, both EPR methods show a comparable development of free radicals in skin. Cigarette smoke in combination with irradiation led to an increased radical production for both measurement methods: 29% for the MS 300 with simulated sun light (setup B) and 37% for the MS 5000 using UVA light (setup A). For the setup B, an average of 68 µg/cm$^2$ nicotine was detected on the filter next to the exposed skin, for the MS 5000 the average was 296 ± 24.5 µg/cm$^2$ nicotine, when cigarette smoke and irradiation were combined.

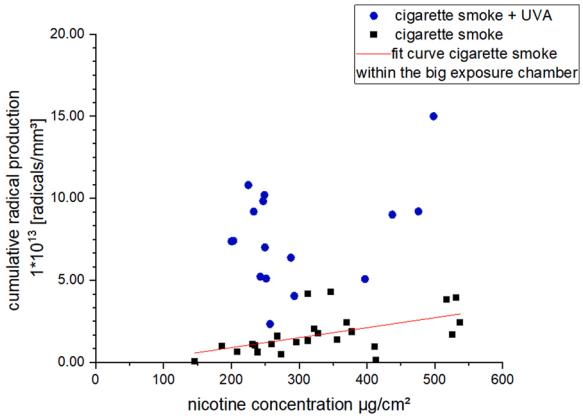


**Fig. 7.** Correlation of nicotine concentration [µg/cm$^2$] on porcine skin and cumulative radical production [radicals/mm$^3$ ] in excised porcine skin after 5 min measurement time/ irradiation time. The black squares represent the radical production due to cigarette smoke. The blue dots due to the combination of CS and UVA. A possible correlation is shown with cigarette smoke alone ($R^2$ =0.2983, p * ≤ 0.05),in combination with UVA irradiation ($R^2$= 0.1391).

In Fig. 7 the correlation between the nicotine concentration on skin and the induced radical production is given. A positive trend of correlation between nicotine concentration and cumulative radical formation can be shown ($R^2 = 0.2983$, $p \leq 0.05$). If one combines cigarette smoke with UVA irradiation, no significant correlation ($R^2 = 0.1391$) is given.

## 4. Discussion

### 4.1. Controlled smoke exposure

In this study, newly constructed exposure chambers were established, which can expose skin samples to cigarette smoke (Fig. 1). It could be demonstrated that smoke, which settles down on the excised skin samples, induces free radicals, which can be directly measured by EPR spectroscopy (Fig. 4). With the help of a particle-measuring device, values up to 400 mg/m$^3$ could be measured in the big chamber. However, one cigarette already exceeded this value by far. Using a calibration curve, values above 400 mg/m$^3$ could be determined by taking nicotine absorption values from the extracts from the washing bottle (Fig. 3a). In order to record the exact exposure of smoke on the skin, a filter paper was placed next to it and was evaluated for nicotine concentration. A correlation between the nicotine absorption between the washing bottle extract and the extraction of the filter was given (Fig. 3b) and allows also an estimation of the particle concentration.

There are already some pollution chambers on the market, but the pollution load has not been evaluated in sufficient detail, neither has a realistic smoke exposure been considered. There are two smoking regimes standardized by ISO and CI (Hammond et al., 2007), one with a 60 s puff interval and 2 s duration and one with a 30 s puff interval and 2 s duration. The CI regime, which was applied with the small chamber, as well as the ISO regime could not be converted to the big smoking chamber because the number of radicals produced by these regimes was not enough to be detectable in the big volume of the chamber in *ex vivo* skin by EPR measurements (data not shown).

However, pure smoking-exposure on the skin was not measured in the past in general. In this research project, a method was developed that enables the precise determination of nicotine as a marker for smoke exposure on skin after application. Many factors need to be considered here which has a major impact on the smoke exposure: The size of the exposure chamber, the number and brand of cigarettes and the smoking regime (Goel et al., 2018). Goel et al (Goel et al., 2018). have found out that the frequency, as well as the length of puffing during smoking, has a significant impact on the radicals produced in the gas and particulate phase. The two standard methods, ISO and CI, refer to small chambers developed in the past. The transfer of these smoke regimes to bigger chambers (as in this research approach) is difficult due to the difference in volume. To ensure a reproducible amount of smoke in an exposure chamber, a certain concentration must be achieved. Smoke concentrations below 140 mg/cm$^2$in the chamber lead to no or hardly measurable radical production (Fig. 7). From previous studies, it was shown that the majority of the stable ROS produced originated from the particulate phase of cigarette smoke (Baum et al., 2003).

With the filter method next to the skin sample, the amount of exposed smoke on the skin can be determined with high precision, regardless of the size of the exposure chamber and smoking regime used. Thus, the amount of smoke reaching the skin might not be perfectly reproducible but can be monitored with high concision.

### 4.2. Spin probes for investigating smoke effects

To determine the effect of cigarette smoke on excised porcine skin, the radical production was investigated using two different EPR devices. Both devices were able to measure the radical production caused by smoke exposure in skin. Furthermore, different spin probes were applied. TEMPO can be easily taken up by cells and can be oxidized and reduced (Fuchs et al., 1997); both reactions lead to a decrease in the EPR signal. In contrast to PCA, the reaction of TEMPO with antioxidants is more pronounced so that the antioxidant status of a microenvironment can be assessed (Elpelt et al., 2020). Nevertheless, significant differences between with and without smoking regime could be measured with setup B (Table S2) using the spin probe TEMPO (Fig. 4b). TEMPO was more sensitive compared to PCA, which did not show altered EPR signals if the skin samples were exposed to one cigarette (data not shown). In future, cream formulations are to be tested which could include antioxidants, thus TEMPO might not be a suitable candidate because it can react with the antioxidants of the creams so that radical measurements are no longer possible (depletion of the spin probe).

PCA is widely used to probe short-lived radicals in samples. It is also EPR-active, like TEMPO, and becomes inactive upon reaction with radicals. Based on the PCA decay, the number of produced radicals can be calculated for quantification (Herrling, 2003). Due to its signal intensity and high stability, this spin probe was used for both EPR systems with different concentrations depending on the detection rate (Table S2).

Depending on the EPR system's sensitivity and smoke regime, radical production due to smoke exposure alone and combined with irradiation could be detected (Fig. 4). With a concentration of 1.5 mM for the big chamber and 1 mM PCA for the small chamber, a significant difference between smoked and non-smoked skin alone (big chamber) ($p \leq 0.001$) and with additional irradiation (small exposure chamber, $p \leq 0.05$) could be measured. The induction of radicals due to UV+VIS+IR irradiation is higher than UVA alone (Fig. 5).

### 4.3. Effects of smoke alone and combined with light

In Fig. 6, the comparison of the two setups has shown that similar results can be achieved. The combination of irradiation and smoke led to an increase of radical production in excised porcine skin.

In various literature, the synergistic effect of cigarette smoke and UVA irradiation is described. The combination of these exogenous stress factors led to a measurable increase in radical formation in the skin (Fig. 5), but the nicotine concentration per cm$^2$ did not change much (Fig. 7). The radical inducing effect of UVA seems to promote radical production more strongly in a shorter time vs. cigarette smoke alone (Ibuki et al., 2002). UVA penetrates the full epidermis and reaches the dermis and can decrease the skin's protective immune response (Herrling, 2003). Not only UVA alone, also in combination with an environmental pollutant, e.g. cigarette smoke, ROS are generated. One of them is polycyclic aromatic hydrocarbons incl. benz[*a*]pyrene (BaP) that are photosensitizers, which undergo more reactions under UVA irradiation. Saladi et al (Saladi et al., 2003). investigated the DNA damage due to the combination of BaP and UVA in murine skin. BaP alone could form DNA adducts that can lead to carcinogenesis; but this process can be accelerated by UVA light. In the review of Burke and Wei (Burke and Wei, 2009), more investigations of the combination of UVA and pollutants are listed. For example, there is a higher risk for dysplastic and malignant lip lesions when exposed to sunlight and cigarette smoke (King et al., 1995). The induction of tumors by UVA or BaP alone requires a high dose, whereas a lower intensity is required when both are combined (Wang et al., 2005). This is also shown for the EPR data (Fig. 5). The combination of UVA and cigarette smoke led to a 1.75 times higher radical production as by the sum of both, thus reinforcing effects occur.

### 4.4. Influence of setups

In addition, it could be shown that a significant difference between smoked and non-smoked skin was only determined when the measured nicotine concentration on the area reached a threshold at 140 μg/cm$^2$ within the big chamber (Fig. 7). Therefore, this effect could not be shown with PCA in the small chamber, as the nicotine concentration was too low, here one cigarette only in combination with irradiation was

enough to induce measurable radical formation in skin. At this smoke concentration, only TEMPO was sensitive enough to show relative low but still significant differences.

Nicotine has no direct influence on radical production in the skin, but an influence on other signaling cascades in the skin that can induce oxidative stress (Valacchi et al., 2012). However, the nicotine concentration can give conclusions about the concentration of other radical-inducing substances. To measure a significant impact of cigarette smoke in skin, a higher concentration of ROS was needed, which could be achieved by using 5 cigarettes (big chamber)/1 cigarette (small chamber). This means a threshold must be exceeded to induce further radicals in excised porcine skin (140 mg/cm$^2$). In the small chamber, the nicotine concentration was much below this radical generating threshold. Nevertheless, radical formation induced by cigarette smoke in lower concentrations can be detected when the skin is additionally irradiated (Fig. 5).

The nicotine concentration of five cigarettes in the big chamber corresponds to the amount of nicotine intake of more than 8 h in a disco/pub in Europe within five minutes (Lopez et al., 2008). Therefore, this setup was adapted to mimic cigarette smoke long time exposure of real-life situations.

Experiments with one cigarette alone in the big exposition chamber showed no significant differences in radical production between unexposed and exposed skin in contrast to the small exposure chamber (data not shown). The smoking regime had to be adapted first.

With cigarette smoke alone, a tendency of correlation between the nicotine concentration and the radical formation in excised skin is given. In contrast, no correlation between nicotine concentration and radical production was found with the combination of cigarette smoke and UVA irradiation (Fig. 7). After burning cigarettes, the skin was covered in a layer of tobacco (Ortiz and Grando, 2012). This can result in the skin's protection from UVA. It was discussed that nicotine from tobacco could protect the skin from the inflammatory reaction caused by UV radiation and hence reducing the risk of melanoma (Sondermeijer et al., 2020).

A stronger decrease of the spin probe PCA could be detected in individual cases depending on the applied nicotine concentration. The amount of exposure could be quantified in our work in contrast to various similar studies regarding cigarette smoke exposure on skin.

In the next step, the irradiation intensity was adjusted. In the beginning, the irradiation was 100 mW/cm$^2$ and was gradually reduced to 18 mW/cm$^2$. This equals less than one-third MED-UVA. It could be seen that the amplitude drop of the spin probe at a high irradiation intensity was too big to detect a significant difference. Therefore, the intensity and spin probe concentration were adapted until a sufficient decrease in PCA was shown.

### 4.5. General discussion

In general, the detection of metabolic radicals is difficult due to their low concentration and short lifetime (Buettner and Jurkiewicz, 1993). Various detection methods are available in this regard: from the determination of the total ROS concentration in tissues/cell culture to the specific detection of oxidation products of various cell components, e.g., DNA (comet assay). These detection methods are primarily based on the detection of fluorogenic compounds using fluorescence spectroscopy (Zhang et al., 2009). It has already been established that the radicals generated in cigarette smoke could be measured with methods like the DCFH-DA (2′,7′-dichlorofluorescin-diacetate) assay (Hergesell et al., 2022).

DCFH-DA assays indicate the presence of ROS by the oxidation of non-fluorescent molecules into a fluorescent one. Due to many reaction steps and the complex system that is needed, it can lead to misleading results (Bonini et al., 2006; Ahlberg et al., 2016). In comparison, the EPR spectroscopy is an alternative non-invasive method for the detection of radical formation in tissue (*in vivo* , *ex vivo*) and cell cultures (Meinke et al., 2012; Mišík and Riesz, 1999). It can identify and quantify free radicals in samples directly and needs no intermediate reaction steps (Peijnenburg et al., 2020). The use of so-called spin probes allows statements about the formation of radicals (e.g., PCA) or the endogenous redox state (e.g., TEMPO) (Elpelt et al., 2020). Furthermore, EPR could also be used to identify the formed radicals using spin traps as shown for dose dependent irradiation (Lohan et al., 2021b).

Furthermore, in terms of radical production, similar patterns have been observed when comparing human skin (*in vivo*) with excised skin. The expression of the absolute radical quantity in excised skin is lower due to the non-continuous oxygen supply, but the relative ratios between *ex vivo* and *in vivo* skin are comparable (Meinke et al., 2015; Lohan et al., 2016).

## 5. Conclusion

In this study, an innovative EPR method has been established which allows the direct measurement of smoke-induced radicals alone and in combination with UV irradiation in two different smoke exposition chambers.

The smoke exposition can be reproducibly determined. Cigarette smoke alone could induce radicals, when the smoke exposure threshold of 140 μg/cm$^2$was exceeded. The amount of radicals is correlated to the amount of smoke. Below this threshold, there was a very good detection of smoke induced radicals using PCA by additional UV irradiation and a low but significant using TEMPO. PCA was chosen as detection molecule of choice because of its more stable chemical nature. The combination of cigarette smoke and UVA induced the highest number of radicals in the skin due to synergistic effects. Cigarette smoke was able to increase the UV-induced radicals in porcine skin again by up to 20% but independent from the amount of smoke applied to the skin. These results add to the knowledge that the combination of both is most harmful. This new method is intended to be used to assess the effectiveness of anti-pollution products in the future.

## CRediT authorship contribution statement

**Phuong Thao Tran:** Investigation, Data analysis, Methodology, Validation Writing – original draft; **Batoul Beidoun**: Investigation, Data analysis; **Silke B. Lohan**: Project administration, Conceptualization, Methodology Writing – review & editing; **Rajae Talbi**: Investigation, Data analysis; **Burkhard Kleuser**: Investigation, Supervision, Writing – review & editing; **Marietta Seifert:** Writing – review & editing; **Katinka Jung**: Funding acquisition, Project administration, Writing – review & editing; **Grit Sandig**: Project administration, Conceptualization, Investigation, Data analysis, Validation Methodology, Writing – review & editing; **Martina C. Meinke**: Funding acquisition, Project administration, Conceptualization: Writing – review & editing.

## Declaration of Competing Interest

The authors declare that they have no known competing financial interests or personal relationships that could have appeared to influence the work reported in this paper.

## Data Availability

Data will be made available on request.

## Acknowledgements

The work was funded by European Regional Development Fund within the program "Pro FIT – Programm (grant ID:10168708) zur Förderung von Forschung, Innovationen und Technologien".

## Appendix A. Supporting information

Supplementary data associated with this article can be found in the online version at doi:10.1016/j.ecoenv.2022.114258.

## References


7 million deaths annually linked to air pollution. Cent Eur J Public Health, 2014. 22(1): p. 53, 59.

Ahlberg, S., et al., 2016. Comparison of different methods to study effects of silver nanoparticles on the pro- and antioxidant status of human keratinocytes and fibroblasts. Methods 109, 55–63.

Bacic, G., Pavicevic, A., Peyrot, F., 2016. In vivo evaluation of different alterations of redox status by studying pharmacokinetics of nitroxides using magnetic resonance techniques. Redox Biol. 8, 226–242.

Baek, J., Lee, M.G., 2016. Oxidative stress and antioxidant strategies in dermatology. Redox Rep. 21 (4), 164–169.

Baum, S.L., et al., 2003. Electron spin resonance and spin trap investigation of free radicals in cigarette smoke: development of a quantification procedure. Anal. Chim. Acta 481 (1), 1–13.

Bernhard, D., et al., 2007. Cigarette smoke–an aging accelerator? Exp. Gerontol. 42 (3), 160–165.

Bielfeldt, S., et al., 2021. Anti-pollution effects of two antioxidants and a chelator—Ex vivo electron spin resonance and in vivo cigarette smoke model assessments in human skin. Ski. Res. Technol.

Bonini, M.G., et al., 2006. The oxidation of 2′,7′-dichlorofluorescin to reactive oxygen species: a self-fulfilling prophesy? Free Radic. Biol. Med 40 (6), 968–975.

Bourgeois, J.S., et al., 2016. The bioavailability of soluble cigarette smoke extract is reduced through interactions with cells and affects the cellular response to CSE exposure. PLoS One 11 (9), e0163182.

Buettner, G.R., Jurkiewicz, B.A., 1993. Ascorbate free radical as a marker of oxidative stress: An EPR study. Free Radic. Biol. Med. 14 (1), 49–55.

Burke, K., Wei, H., 2009. Synergistic damage by UVA radiation and pollutants. Toxicol. Ind. Health 25 (4–5), 219–224.

Clayton, P.M., et al., 2013. Spectroscopic studies on nicotine and nornicotine in the UV region. Chirality 25 (5), 288–293.

Darvin, M.E., et al., 2010. Formation of free radicals in human skin during irradiation with infrared light. J. Investig. Dermatol. 130 (2), 629–631.

Diffey, B.L., Farr, P.M., 1989. The normal range in diagnostic phototesting. Br. J. Dermatol. 120 (4), 517–524.

Elpelt, A., et al., 2020. Investigation of TEMPO partitioning in different skin models as measured by EPR spectroscopy - Insight into the stratum corneum. J. Magn. Reson. 310, 106637.

Ferrara, F., et al., 2021. Inflammasome activation in pollution-induced skin conditions. Plast. Reconstr. Surg. 147 (1S-2), 15S–24S.

Fuchs, J., et al., 1997. Electron paramagnetic resonance studies on nitroxide radical 2,2,5,5-tetramethyl-4-piperidin-1-oxyl (TEMPO) redox reactions in Human skin. Free Radic. Biol. Med. 22 (6), 967–976.

Gao, J., et al., 2002. EPR study of the toxicological effects of gas-phase cigarette smoke and the protective effects of grape seed extract on the mitochondrial membrane. Appl. Magn. Reson. 22 (4), 497.

Goel, R., et al., 2018. Influence of smoking puff parameters and tobacco varieties on free Radicals yields in cigarette mainstream smoke. Chem. Res. Toxicol. 31 (5), 325–331.

Haag, S.F., et al., 2010. Comparative study of carotenoids, catalase and radical formation in human and animal skin. Ski. Pharmacol. Physiol. 23 (6), 306–312.

Hammond, D., et al., 2007. Revising the machine smoking regime for cigarette emissions: implications for tobacco control policy. Tob. Control 16 (1), 8.

Hammond, S.K., et al., 1987. Collection and analysis of nicotine as a marker for environmental tobacco smoke. Atmos. Environ. 1967 21 (2), 457–462.

Hergesell, K., et al., 2022. Common cosmetic compounds can reduce air pollution-induced oxidative stress and pro-inflammatory response in the skin. Ski. Pharm. Physiol.

Herrling, T., 2003. UV-induced free radicals in the skin detected by ESR spectroscopy and imaging using nitroxides. Free Radic. Biol. Med. 35 (1), 59–67.

Herrling, T., Jung, K., Fuchs, J., 2006. Measurements of UV-generated free radicals/reactive oxygen species (ROS) in skin. Spectrochim. Acta Part A Mol. Biomol. Spectrosc. 63 (4), 840–845.

Ibuki, Y., et al., 2002. Coexposure to benzo[a]pyrene plus ultraviolet A induces 8-oxo-7,8-dihydro-2′-deoxyguanosine formation in human skin fibroblasts: preventive effects of anti-oxidant agents. Environ. Toxicol. Pharmacol. 12 (1), 37–42.

Invernizzi, G., et al., 2004. Particulate matter from tobacco versus diesel car exhaust: an educational perspective. Tob. Control 13 (3), 219–221.

Kampa, M., Castanas, E., 2008. Human health effects of air pollution. Environ. Pollut. 151 (2), 362–367.

Kim, E.-H., et al., 2015. Indoor air pollution aggravates symptoms of atopic dermatitis in children. PloS One 10 (3) p. e0119501-e0119501.

King, G.N., et al., 1995. Increased prevalence of dysplastic and malignant lip lesions in renal-transplant recipients. New Engl. J. Med. 332 (16), 1052–1057.

Kopa, P.N., Pawliczak, R., 2018. Effect of smoking on gene expression profile - overall mechanism, impact on respiratory system function, and reference to electronic cigarettes. Toxicol. Mech. Methods 28 (6), 397–409.

Krutmann, J., et al., 2021. Environmentally-induced (extrinsic) skin aging: exposomal factors and underlying mechanisms. J. Invest. Dermatol.

Liguori, I., et al., 2018. Oxidative stress, aging, and diseases. Clin. Inter. Aging 13, 757–772.

Lohan, S.B., et al., 2016. Free radicals induced by sunlight in different spectral regions - in vivo versus ex vivo study. Exp. Dermatol. 25 (5), 380–385.

Lohan, S.B., et al., 2021a. EPR Spectroscopy as a Method for ROS Quantification in the Skin. In: Espada, J. (Ed.), Reactive Oxygen Species: Methods and Protocols. Springer US, New York, NY, pp. 137–148.

Lohan, S.B., et al., 2021b. Switching from healthy to unhealthy oxidative stress – does the radical type can be used as an indicator? Free Radic. Biol. Med. 162, 401–411.

Lopez, M.J., et al., 2008. Secondhand smoke exposure in hospitality venues in Europe. Environ. Health Perspect. 116 (11), 1469–1472.

Mannucci, P.M., Franchini, M., 2017. Health effects of ambient air pollution in developing countries. Int J. Environ. Res Public Health 14 (9).

Marchand, V., et al., 2017. Use of a cocktail of spin traps for fingerprinting large range of free radicals in biological systems. PLoS One 12 (3), e0172998.

Meinke, M.C., et al., 2012. In vivo photoprotective and anti-inflammatory effect of hyperforin is associated with high antioxidant activity in vitro and ex vivo. Eur. J. Pharm. Biopharm. 81 (2), 346–350.

Meinke, M.C., et al., 2015. Evaluation of carotenoids and reactive oxygen species in human skin after UV irradiation: a critical comparison between in vivo and ex vivo investigations. Exp. Dermatol. 24 (3), 194–197.

Meinke, M.C., Busch, L., Lohan, S.B., 2021. Wavelength, dose, skin type and skin model related radical formation in skin. Biophys. Rev. 13 (6), 1091–1100.

Mišík, Vr, Riesz, P., 1999. EPR characterization of free radical intermediates formed during ultrasound exposure of cell culture media. Free Radic. Biol. Med. 26 (7), 936–943.

Organization, W.H. Ambient (outdoor) air pollution. 2021 16.03.2022]; Available from: ⟨https://www.who.int/news-room/fact-sheets/detail/ambient-(outdoor)-air-quality-and-health⟩.

Ortiz, A., Grando, S.A., 2012. Smoking and the skin. Int J. Dermatol. 51 (3), 250–262.

Peijnenburg, W., et al., 2020. A method to assess the relevance of nanomaterial dissolution during reactivity testing. Materials 13 (10).

Pfeifer, G.P., et al., 2002. Tobacco smoke carcinogens, DNA damage and p53 mutations in smoking-associated cancers. Oncogene 21 (48), 7435–7451.

Pryor, W.A., Prier, D.G., Church, D.F., 1983. Electron-spin resonance study of mainstream and sidestream cigarette smoke: nature of the free radicals in gas-phase smoke and in cigarette tar. Environ. Health Perspect. 47, 345–355.

Rosoff, D.B., et al., 2020. Evaluating the relationship between alcohol consumption, tobacco use, and cardiovascular disease: a multivariable Mendelian randomization study. PLoS Med. 17 (12), e1003410.

Sakai, Y., et al., 2020. Inter-laboratory reproducibility and interchangeability of 3R4F and 1R6F reference cigarettes in mainstream smoke chemical analysis and in vitro toxicity assays. Contrib. Tob. Nicotine Res. 29 (3), 119–135.

Saladi, R., et al., 2003. The combination of benzo[a]pyrene and ultraviolet a causes an in vivo time-related accumulation of DNA damage in mouse skin ¶. Photochem. Photobiol. 77 (4), 413–419.

Sobus, S.L., Warren, G.W., 2014. The biologic effects of cigarette smoke on cancer cells. Cancer 120 (23), 3617–3626.

Sondermeijer, L., et al., 2020. Cigarette smoking and the risk of cutaneous melanoma: a case-control study. Dermatology 236 (3), 228–236.

Swain, M.L., Eisner, A., et al., 1949. Ultraviolet absorption spectra of nicotine, nornicotine and some of their derivatives. J. Am. Chem. Soc. 71 (4), 1341–1345.

Swartz, H.M., Sentjurc, M., Morse, P.D., 1986. Cellular metabolism of water-soluble nitroxides: effect on rate of reduction of cell/nitroxide ratio, oxygen concentrations and permeability of nitroxides. Biochim. Biophys. Acta BBA Mol. Cell Res. 888 (1), 82–90.

Tarbuk, A., Grancarić, A.M., Šitum, M., 2016. Skin cancer and UV protection. Autex Res. J. 16 (1), 19–28.

Valacchi, G., et al., 2012. Cutaneous responses to environmental stressors. Ann. N.Y. Acad. Sci. 1271, 75–81.

Vierkotter, A., et al., 2010. Airborne particle exposure and extrinsic skin aging. J. Investig. Dermatol. 130 (12), 2719–2726.

Wang, Y., et al., 2005. Combined subcarcinogenic benzo[a]pyrene and UVA synergistically caused high tumor incidence and mutations in H-ras gene, but not p53, in SKH-1 hairless mouse skin. Int J. Cancer 116 (2), 193–199.

Wolf, R., 1998. Smoking and the skin, radically speaking. Clin. Dermatol. 16 (5), 633–639.

Yamaguchi, K.T., et al., 1992. Measurement of free radicals from smoke inhalation and oxygen exposure by spin trapping and ESR spectroscopy. Free Radic. Res Commun. 16 (3), 167–174.

Zhang, X., et al., 2009. The role of oxidative stress in deoxynivalenol-induced DNA damage in HepG2 cells. Toxicon 54 (4), 513–518.

***Table S1: Comparison of the applied magnetic parameters for MS 5000 and MS 300***

| EPR device | MiniScope MS 5000 | MiniScope MS 300 |
|---|---|---|
| Microwave frequency | 9.4 GHz | 9.3-9.55 GHz |
| microwave power | 10 dB (10 mW) | 20 dB |
| Modulation | 0.20 mT | 1 G |
| Modulation frequency | 100 kHz | 100 kHz |
| sweep time (measuring time) | 10 sec | 30 sec |
| coupling time | 15 sec | n.d. |
| magnetic field B0 | 337.16 mT | 336.2 mT |
| Sweep | 7.67 mT | 8.8 mT |

***Table S2: Comparison of two EPR methods run by different EPR devices***

| | Setup A | Setup B |
|---|---|---|
| EPR system | MS 5000 | MS 300 |
| EPR spin marker | 38.4 µl 1.5 mM PCA | 5µl 10 mM TEMPO / 1 mM PCA |
| Exposure chamber | big chamber | small chamber |
| sample size | 4 mm in diameter | 1x1 cm square, 4 mm in diameter |
| Incubation time | 5 min | 10 min |
| Smoke exposure | 5 min | 5 min |
| Amount of cigarettes | 5 | 1 |

***Table S3 Comparison of variation in particle or nicotine concentration measurement methods with the comparable setting for the big exposition chamber (setup A)***. *One cigarette was burned for 7 min. The experiments were carried out twice. The same cigarette exposure setting was measured for all three methods.*

| | sample a | sample b | mean | SD | SD % |
|---|---|---|---|---|---|
| particle concentration [mg/m³] | 59 | 50 | 55 | 7 | 12 |
| washing bottle extract [absorption a.u.] | 0.062 | 0.074 | 0.068 | 0.0084 | 12 |
| filter at the front extracted [absorption a.u.] | 0.027 | 0.028 | 0.028 | 0.0007 | 2.6 |

## 2.2 Red- and Near-Infrared-Excited Autofluorescence as a Marker for Acute Oxidative Stress in Skin Exposed to Cigarette Smoke Ex Vivo and In Vivo

Authors: Phuong Thao Tran, Parichat Tawornchat, Burkhard Kleuser, Silke B. Lohan, Johannes Schleusener, Martina C. Meinke, and Maxim E. Darvin

Journal: Antioxidants 2023, 12, 1011

Available online: https://doi.org/10.3390/antiox12051011



Amount performed by Phuong Thao Tran:

Design of experiments: 80%

Practical, experimental part: 50%

Data analysis: 90%

Interpretation of results: 90%

Writing: 95%

*antioxidants*

MDPI

*Article*

# Red- and Near-Infrared-Excited Autofluorescence as a Marker for Acute Oxidative Stress in Skin Exposed to Cigarette Smoke Ex Vivo and In Vivo

**Phuong Thao Tran [1,2], Parichat Tawornchat [1,3], Burkhard Kleuser [2], Silke B. Lohan [1], Johannes Schleusener [1], Martina C. Meinke [1,*] and Maxim E. Darvin [1]**

[1] Charité—Universitätsmedizin Berlin, Corporate Member of Freie Universität Berlin and Humboldt-Universität zu Berlin, Department of Dermatology, Venereology and Allergology, Center of Experimental and Applied Cutaneous Physiology, Charitéplatz 1, 10117 Berlin, Germany
[2] Institute of Pharmacy, Department of Pharmacology, Freie Universität Berlin, Königin-Luise-Str. 2+4, 14195 Berlin, Germany
[3] Center of Excellence on Petrochemical and Materials Technology, Chulalongkorn University, Bangkok 10330, Thailand
* Correspondence: martina.meinke@charite.de; Tel.: +49-30-450-518244

**Abstract:** Air pollution is increasing worldwide and skin is exposed to high levels of pollution daily, causing oxidative stress and other negative consequences. The methods used to determine oxidative stress in the skin are invasive and non-invasive label-free in vivo methods, which are severely limited. Here, a non-invasive and label-free method to determine the effect of cigarette smoke (CS) exposure on skin ex vivo (porcine) and in vivo (human) was established. The method is based on the measurement of significant CS-exposure-induced enhancement in red- and near-infrared (NIR)-excited autofluorescence (AF) intensities in the skin. To understand the origin of red- and NIR-excited skin AF, the skin was exposed to several doses of CS in a smoking chamber. UVA irradiation was used as a positive control of oxidative stress in the skin. The skin was measured with confocal Raman microspectroscopy before CS exposure, immediately after CS exposure, and after skin cleaning. CS exposure significantly increased the intensity of red- and NIR-excited skin AF in a dose-dependent manner in the epidermis, as confirmed by laser scanning microscopy AF imaging and fluorescence spectroscopy measurements. UVA irradiation enhanced the intensity of AF, but to a lower extent than CS exposure. We concluded that the increase in red- and NIR-excited AF intensities of the skin after CS exposure could clearly be related to the induction of oxidative stress in skin, where skin surface lipids are mainly oxidized.

**Keywords:** cigarette smoke; oxidative stress; Raman spectroscopy; NIR autofluorescence; red autofluorescence; skin fluorophores; metabolic imaging



**Citation:** Tran, P.T.; Tawornchat, P.; Kleuser, B.; Lohan, S.B.; Schleusener, J.; Meinke, M.C.; Darvin, M.E. Red- and Near-Infrared-Excited Autofluorescence as a Marker for Acute Oxidative Stress in Skin Exposed to Cigarette Smoke Ex Vivo and In Vivo. *Antioxidants* **2023**, *12*, 1011. https://doi.org/10.3390/antiox12051011

Academic Editors: Moo-Yeol Lee and Keshav Raj Paudel

Received: 23 March 2023
Revised: 18 April 2023
Accepted: 25 April 2023
Published: 27 April 2023



## 1. Introduction

The increase in air pollution over the years has had a major effect on human health and the quality of life. In 2022, the World Health Organization reported that exposure to air pollution (e.g., polycyclic aromatic hydrocarbons, volatile organic compounds, oxides, particulate matter, and ozone) was estimated to cause over 7 million annual premature deaths worldwide [1]. The majority of deaths are caused by ischemic heart disease, stroke, and chronic obstructive pulmonary disease; in addition, air pollution has enormous effects on human skin [2,3].

Cigarette smoke (CS) is a pollutant that consists of particulate matter, polycyclic hydrocarbons, and thousands of other components [4]. Active and passive smokers are exposed to the fumes of cigarettes on a daily basis. CS induces oxidative stress and contributes to the development of premature skin aging and several inflammatory pathologies [5,6].

Skin—especially its superficial layer, the stratum corneum—acts as the most important defense barrier against environmental contaminants. Exposure to air pollutants can induce a harmful effect on the skin by increasing the concentration of reactive oxygen species (ROS). The excess of ROS disturbs the oxidant/antioxidant balance, resulting in oxidative stress. Oxidative stress induces severe alterations of lipids, DNA, proteins, antioxidants, etc., in the skin, leading to impairment of the skin barrier function and the skin's protection ability. It can also lead to the development of premature skin aging and inflammatory or allergic conditions, such as contact dermatitis, atopic dermatitis, eczema, psoriasis, and acne, as well as skin cancer, which is the most serious result [7–9].

Currently, methods of evaluating air-pollution-induced skin damage are limited. Most of these methods are indirect and/or invasive (e.g., skin biopsies, blood sampling, tape-stripping, trans-epidermal water loss measurements, and epidemiological studies over a long time period) [10–14]. In addition, there are in vitro experiments (e.g., cytotoxicity, collagen metabolism, glutathione assays) [15–17], which might not always be representative for non-invasive in vivo skin studies [18–20].

To address the above challenges, a label-free optical method to investigate depth-dependently the effect of CS exposure on skin was applied. Red- and near-infrared (NIR)-excited autofluorescence (AF) intensities in skin were measured depth-dependently on excised porcine skin biopsies and on healthy human volunteers after dose-dependent CS exposure and UVA irradiation using a confocal Raman microscope. As control, compartments of CS alone were investigated and the skin was measured directly after exposure and after a cleaning procedure to remove particular matter and compounds on the skin surface, which could potentially influence AF intensity.

## 2. Materials and Methods

### *2.1. Preparation of Ex Vivo Porcine Skin Samples*

Porcine ears were obtained from a local butcher, cleaned with cold water, and stored at 4 °C. The ears were used within 48 h after slaughtering. Experiments were approved by the veterinary office in Dahme–Spreewald, Germany, in accordance with Section 3, Article 17, paragraph 1, of Regulation (EC) No 1069/2009 of the European Parliament and Council dated 21 October 2009, which establishes health regulations for animal byproducts that are not intended for human consumption.

To perform the experiments, the hair on the porcine ear skin was trimmed with scissors without affecting the stratum corneum. Subsequently, the trimmed skin area was cut to $\approx 1 \times 1$ cm$^2$ pieces. At least five pieces per ear were prepared for analysis.

### *2.2. Preparation for In Vivo Human Skin Study*

Ten healthy Caucasian volunteers (five male and five female) aged from 20 to 36 years (mean 27.2 $\pm$ 4.5 years) were included in the study. Nine of the ten volunteers were nonsmokers. No skin care products were used on the volunteers' inner forearms for at least 12 h before the experiments. At first, the volunteers acclimated for 10 min in the laboratory at set conditions (temperature +20 °C, relative humidity ≈40–60%). At least six positions on their inner forearms were used for measurements.

Before starting the experiment, the study design and possible risks were explained and the volunteers provided their informed written consent. This study was approved by the Ethics Committee of the Charité—Universitätsmedizin Berlin (EA1/291/21, DRKS00029235) and all procedures followed the Code of Ethics of the World Medical Association (Declaration of Helsinki).

### *2.3. Cigarettes*

Research cigarettes (1R6F, University of Kentucky, Lexington, KY, USA) (ISTD = internal standard) [21] and commercially available cigarettes (Gauloises Blonde Bleu, Tarnowo Podgórne, Poland) were used in this study. The composition of the two kinds of cigarettes are comparable. The ingredients of the research cigarettes 1R6F (mg/cig) were tar (8.6 mg);

nicotine (0.72 mg); and carbon monoxide (10.1 mg) [22]. The ingredients of Gauloises Blonde Bleu (mg/cig) are tar (10 mg); nicotine (0.8 mg); and carbon monoxide (10 mg) [23].

### *2.4. Cigarette Smoke Exposure on Skin*

The porcine skin sample was placed in an exposure chamber that was designed by the Charité for exposure to CS generated by the combustion of Gauloises or research 1R6F cigarettes. For the first ex vivo measurements, Gauloises cigarettes were used. For repetitions and in vivo experiments, the 1R6F cigarettes were used. The smoking chamber was constructed by the Centrum Wissenschaftliche Werkstaetten (CWW) der Charité—Universitaetsmedizin Berlin. This chamber was used for ex vivo and in vivo studies, as illustrated in Figure 1. In a previous study, the reproducible CS exposure was measured and validated [6]. The chamber was connected to a pump, which represents the continuous aspiration of CS. The dose of CS exposed on the skin surface was controlled by the number of cigarettes and the pump time. For CS exposure on human skin in vivo, gloves protecting the skin of both hands and arms were used; only the measurement area of $\approx 3 \times 4$ cm$^2$ was left unprotected and sealed with tapes (Figure 1b).

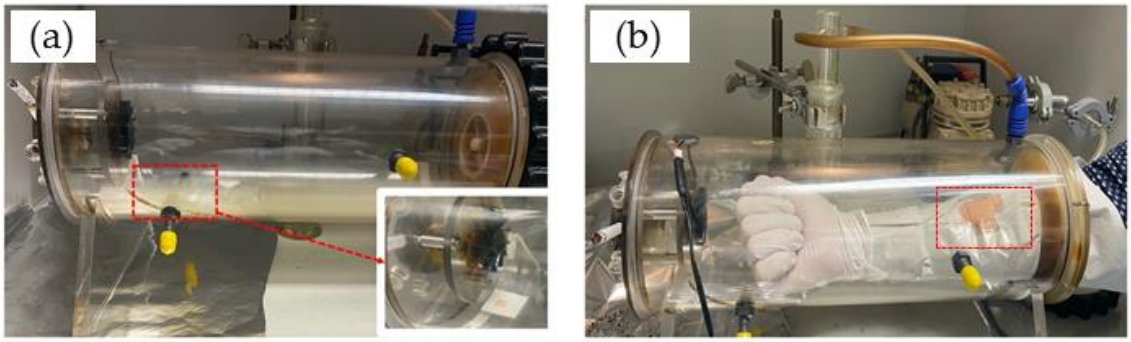


**Figure 1.** Exposure of a skin sample ex vivo (**a**) or human forearm skin in vivo (**b**) to cigarette smoke in a smoking chamber.

In the case of five cigarettes and one cigarette, the pump was turned on for 1 min after one cigarette or five cigarettes were simultaneously lighted. For $\frac{1}{2}$ and $\frac{1}{4}$ cigarettes, the pump was turned on for 30 s and 15 s, respectively, after a cigarette was lighted. After the pump was turned off, all experimental samples were incubated in the chamber for a total of 5 min. After exposure, the skin was immediately investigated using confocal Raman microspectroscopy (CRM). Then, the skin piece was cleaned using distilled water (1 mL/cm$^2$ skin) to remove any chemicals/particulate matter on the skin surface and was again investigated using CRM. Intact non-exposed skin was used as a negative control. UVA irradiation (2 minimal erythema dose (MED)) was used as positive control.

For each experiment, an absorbing filter paper ($3.5 \times 2.5$ cm$^2$) was inserted into the chamber next to the measurement area on the forearm or skin sample to investigate the nicotine concentration exposed on the skin surface. To extract the nicotine, the exposed filter paper was incubated in 10 mL of ethanol (Uvasol® Ethanol 99.9%, Merck KGaA, Darmstadt, Germany). Then, the solution was measured by a UV spectrometer (Perkin Elmer, Inc., Waltham, MA, USA) to determine the nicotine content with the aid of a standard curve prepared from nicotine standard solutions, using the maximum wavelength of nicotine in ethanol at 262 nm and pure ethanol as a blank. The method was previously described in detail by Tran et al. [6].

### *2.5. Cigarette Smoke Exposed on a Glass Slide*

An uncoated glass slide (R. Langenbrinck GmbH, Emmendingen, Germany) was put into the smoking chamber and exposed with five cigarettes. The smoking-induced particles deposited on the glass slide were further measured with CRM.

### *2.6. UVA Irradiation of Porcine Skin*

To induce oxidative stress (positive control), skin samples were irradiated using an UVA–LED lamp at 365 ± 5 nm (Freiberg Instruments GmbH, Freiberg, Germany) for 106 min, while untreated skin was used as a negative control and subjected to CRM analyses. The applied UVA dose was 52 J/cm$^2$, which equals 2 MED and is sufficient to induce oxidative stress in the skin [24].

### *2.7. Chemical Induced Oxidation of Porcine Skin*

To induce chemical oxidation in excised porcine skin, the skin samples were each incubated with 150 µL/cm$^2$ 2 mM hydrogen peroxide, according the protocol of Hergesell et al. [25], and 30% hydrogen peroxide for 30 min.

### *2.8. Red and NIR Excited Autofluorescence of Nicotine*

One drop of pure nicotine (Caesar and Loretz GmbH, Hilden, Germany) was transferred to an uncoated glass slide. The Raman spectrum was recorded using CRM.

### *2.9. Confocal Raman Microspectroscopy (CRM)*

For ex vivo and in vivo measurements, the Model 3510 skin composition analyzer (RiverD International B.V., Rotterdam, The Netherlands) was used. For the fingerprint region (FP: 400–2000 cm$^{-1}$), the excitation wavelength was 785 nm, the exposure time 5 s, and the power 20 mW. For the high wavenumber region (HWN: 2000–4000 cm$^{-1}$), the excitation wavelength was 671 nm, the exposure time was 1 s, and the power was 17 mW [26,27]. Raman spectra were recorded from the skin surface down to 40 µm at 2 µm increments. The utilized CRM was described in detail elsewhere [28]; it is widely used for the analysis of skin composition and drug penetration [29–31].

### *2.10. Confocal Laser Scanning Microscopy (LSM) and Fluorescence Microscopy*

To investigate the effect of CS exposure on the skin surface, a confocal laser scanning microscope (LSM, VivaScope® 1500, Multilaser, MAVIG, Munich, Germany) was used to capture the AF in skin. In this study, the laser diode of 785 nm was chosen. Before and after CS exposure, a laser power of 5 mW was used to compare recorded AF intensities.

For both samples, a drop of immersion oil (Crodamol STS, Croda Inc., Snaith, UK) was applied on the skin and fixated by a ring glass (adhesive window with crosshair, Lucid Vision Labs GmbH, Ilsfeld, Germany). For optimal optical contact, ultrasonic gel (Aquasonic 100, Parker laboratories Inc., Fairfield, CT, USA) was applied between the objective and the ring of the investigated sample.

To confirm the results of the LSM, tape strips of untreated and CS exposed skin were taken to measure the AF of the skin samples with fluorescence microscopy.

For the tape-stripping method, cyanoacrylate was applied on the porcine skin and covered with adhesive tapes (Tesa®, No. 5529, Beiersdorf AG, Hamburg, Germany). With a weighted rubber roller of 746 g, the area was rolled 10 times without additional pressure. After 20 min, the adhesive tapes were collected and cut into two 1 × 1 cm$^2$ pieces per porcine ear. Every piece was solved in 2 mL ethanol (Uvasol® Ethanol 99.9%, Merck KGaA, Darmstadt, Germany) that was added to the ultrasonic bath (Banderlin Sonorex Super RK 102H, Berlin, Germany) for 10 min at 35 kHz and, afterwards, centrifuged at 1.920× *g* for an additional ten minutes. The supernatant of the solution was pipetted, filled into 500 µL cuvettes, and measured by fluorescence spectroscopy (LS-55, PerkinElmer Inc., Waltham, MA, USA). The excitation wavelength was 785 nm. Absorbance was measured in the wavelength range of 820–900 nm at a rate of 100 nm per minute.

### *2.11. Data Analysis*

#### 2.11.1. Comparison of Autofluorescence Intensities

Images measured by the LSM were analyzed with the ImageJ software (Wayne Rasband, National Institute of Health, Bethesda, MD, USA, Version 1.54b). To compare the AF intensity values, the brightness was determined.

#### 2.11.2. Determination of Depth-Dependent Autofluorescence Intensity

To quantify the AF intensity, the fluorescence background in the fingerprint Raman spectra at the position 1800 $cm^{-1}$ was used due to the absence of superposition with Raman bands at this wavenumber. For the high wavenumber region, the AF intensity was determined at position 2600 $cm^{-1}$ due to the absence of superposition with Raman bands.

The mean AF intensity was determined depending on the skin depth. The investigations were performed before CS exposure, right after CS exposure, and after an additional cleaning step with distilled water following CS exposure.

### *2.12. Statistical Analysis*

The data are presented as mean ± standard error of the mean (SEM). For statistical analysis, IBM Statistical Package for the Social Sciences (SPSS) Statistics version 28 (IBM Corporation, Armonk, NY, USA) was applied. Normal distribution was tested using the Shapiro–Wilk test. To compare significant differences, the Kruskal–Wallis Test with the (Dunn–Bonferroni) post hoc test was used. The significance between the increase of AF intensity in excised porcine skin and in vivo human skin over the entire measurement was calculated with a generalized estimating equation (GEE). A $p$-value $\leq 0.05$ was considered to be statistically significant.

## 3. Results

### *3.1. Cigarette Smoke Increases NIR- and Red-Excited Autofluorescence Intensity in Ex Vivo Porcine Skin*

First, we assessed whether CS exposure would change the Raman spectra of porcine skin that was being excited in the NIR range (Figure 2a–c). As shown in Figure 2b, the NIR excited AF intensity in the representative Raman spectrum of CS-exposed porcine skin increased dramatically—about 10-fold compared to the non-exposed skin (Figure 2a). Skin surface cleaning results in an obvious reduction in AF intensity (Figure 2c). However, even after removing the CS residue on the skin surface, the AF intensity was still approximately three times higher, compared to that of the non-exposed skin serving as control (Figure 2c).

Next, we observed the increase in AF intensity excited in the red spectral range (Figure 2d–f). Compared to the non-exposed skin (Figure 2d), CS exposure resulted in an obvious increase in red-excited AF intensity (Figure 2e). Again, after the cleaning of CS-exposed skin, the AF intensity remained approximately three times higher (Figure 2f) than that in the non-exposed skin serving as control (Figure 2d).

### *3.2. Dose-Dependent Increase in NIR- and Red-Excited Autofluorescence Intensity of the Skin due to Cigarette-Smoke Exposure*

After assessing the impact of CS in general in excised porcine skin, the dose-dependent relation was investigated. Porcine skin was exposed to 1/4, 1/2, one, and five cigarettes in totals of five minutes (Figure 3). As shown in Figure 3a, the NIR-excited skin AF intensity increased with the number of burned cigarettes. Although the skin was cleaned, a dose-dependency between skin exhibiting NIR-excited AF intensity and the amount of burned cigarettes could be observed (Figure 3b). The exact amount of nicotine as a surrogate parameter for particle concentration on the skin was determined (Figure 3c) and significantly increased with the increasing number of burned cigarettes.

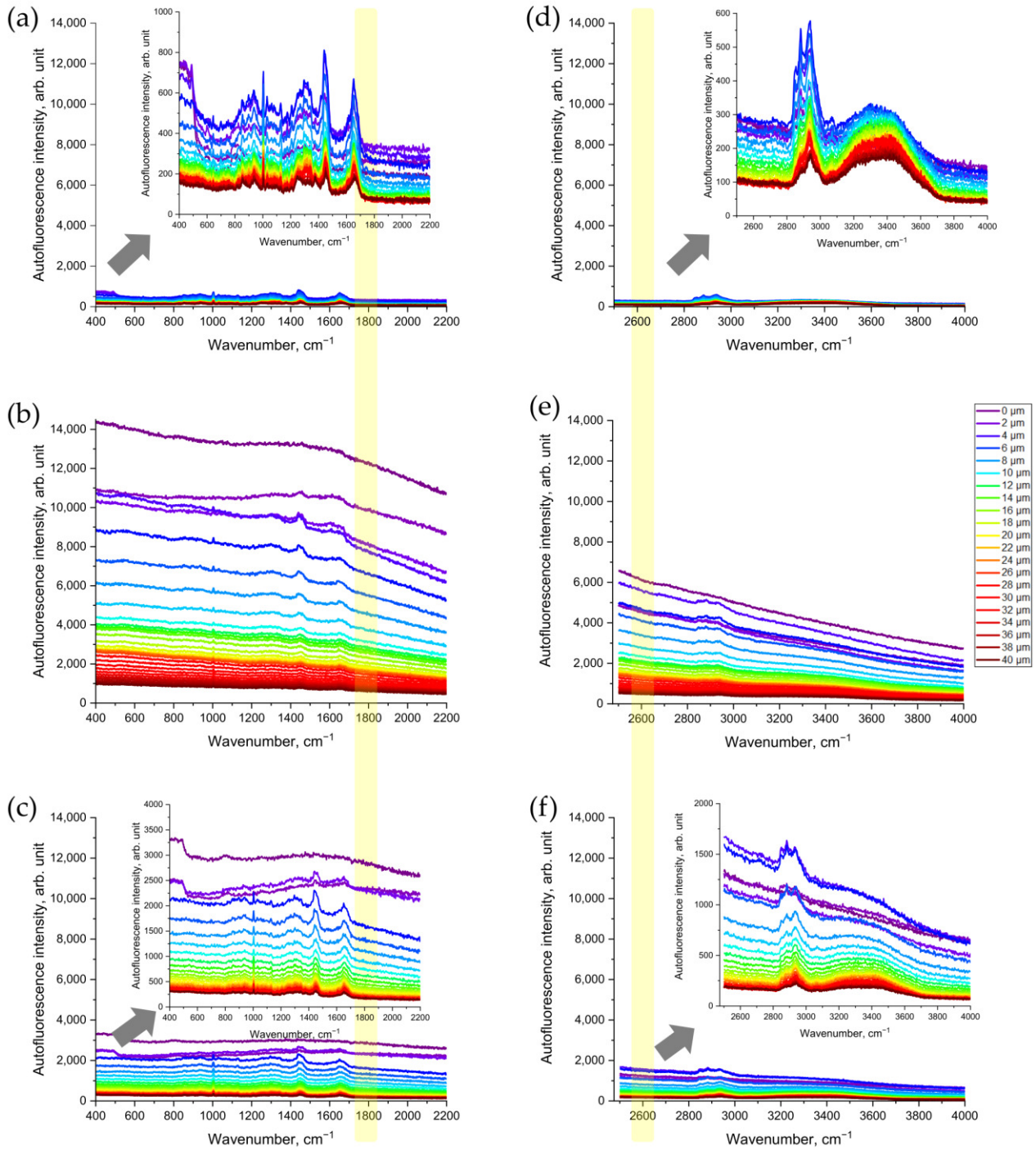


**Figure 2.** Representative Raman spectra of CS-exposed and non-exposed porcine skin at different depths (0–40 µm) excited in NIR with a wavelength of 785 nm (**a**–**c**) and in red with a wavelength of 671 nm (**d**–**f**) spectral ranges: (**a**,**d**) control skin before CS exposure; (**b**,**e**) uncleaned skin after CS exposure; (**c**,**f**) cleaned skin after CS exposure. The arrows point to the inserts in (**a**,**c**,**d**,**f**) that show the zoomed spectra, for clarity. The yellow color shows the area where the AF intensity was analyzed where no Raman bands can interfere.

NIR-excited skin AF intensity was highest before cleaning the skin surface; however, even after cleaning there was a clear difference between the CS exposed and the control group in NIR-excited skin AF intensity. After cleaning, in the superficial depth (0–5 µm), the NIR-excited skin AF intensity was 2925 ± 344 arb. units after exposure with five cigarettes and, therefore, more than 10-fold higher than that of the control group (246 ± 21 arb. units).

For one cigarette, the NIR-excited AF intensity after cleaning at the skin surface was 1331 ± 68 arb. units; for 1/2 cigarette, it was 1082 ± 91 arb. Units; and for 1/4 cigarette, it was 355 ± 21 arb. units. The values decreased with increasing skin depth, as shown in Figure 3a,b.

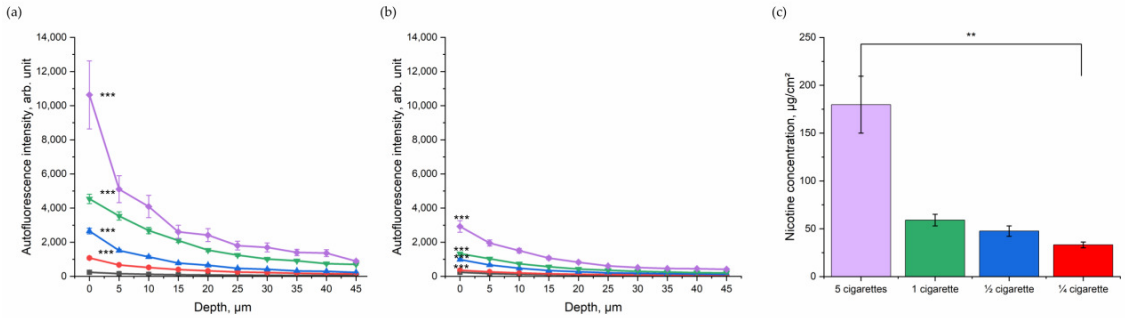


**Figure 3.** Depth profile of 785 nm NIR-excited AF intensity (mean ± SEM) of ex vivo porcine skin after dose-dependent exposure to CS (purple—five cigarettes, green—one cigarette, blue—1/2 cigarette, and red—1/4 cigarette) immediately after CS exposure (**a**) and after cleaning (**b**), compared to control non-exposed skin (black). A general estimated equation was utilized; *** $p \leq 0.001$ (CS-exposed vs. control skin). (**c**) Nicotine concentration (mean ± SEM) measured on a filter in the smoking chamber after exposure with five cigarettes in the smoking chamber (purple, 180 µg/cm$^{2)}$; 1 cigarette in the smoking chamber (green, 59 µg/cm$^2$); 1/2 cigarette in the smoking chamber (blue, 48 µg/cm$^2$); and 1/4 cigarette in the smoking chamber (red, 33 µg/cm$^2$). Kruskal–Wallis test with Dunn–Bonferroni post hoc test. ** $p \leq 0.01$.

### *3.3. Nicotine and Cigarette-Induced Residues Do Not Enhance NIR- and Red-Excited Skin Autofluorescence Intensity*

To verify that nicotine, as one of the main components of CS, is not the source of the NIR- and red-excited AF intensity of CS-exposed skin, pure nicotine was investigated with CRM. The results showed that nicotine is a Raman-active molecule, which does not generate any fluorescence signal under NIR- excitations (Figure 4a) or red excitations (Figure 4b). According to Baranska et al. [32], the peak at 1592 cm$^{-1}$ could also refer to the pyridine ring, 1042 and 1026 and 924 cm$^{-1}$ to C-C and C-N stretching vibrations of the alkaloid in the pyridine ring.

In addition, we measured the CS-exposed glass slide in order to check whether CS-related particles deposited on the skin surface are a source of NIR- and red-excited AF of CS-exposed skin. The results established that the CS-exposed glass slide did not show any significant increase in the NIR-excited (Figure 4c) and red-excited (Figure 4d) fluorescence intensity.

### *3.4. UVA Irradiation as a Positive Control of Oxidative Stress*

As a positive control of oxidative stress, the changes in NIR-excited and red-excited AF intensity were analyzed in UVA-irradiated porcine skin. The results showed that UVA irradiation of the skin led to a significant depth-dependent increase in NIR- and red-excited AF intensity (Figure 4d,e). This result demonstrates that UVA-induced oxidative stress causes an increase in NIR-excited skin's AF intensity. In comparison, at the skin surface (0 µm), the NIR-excited AF intensity in CS-exposed skin was approximately ten times higher than after UVA irradiation at 2 MED (Figure 4g). After cleaning the CS-exposed porcine skin, the AF intensity remained approximately two times higher than in UVA-irradiated skin. In the Appendix, the AF intensity of 2 UVA–MED is presented and compared with the samples of cleaned skin, for an overview. Here, the effect of 2 UVA–MED is comparable to that of one cigarette (Figure S2).

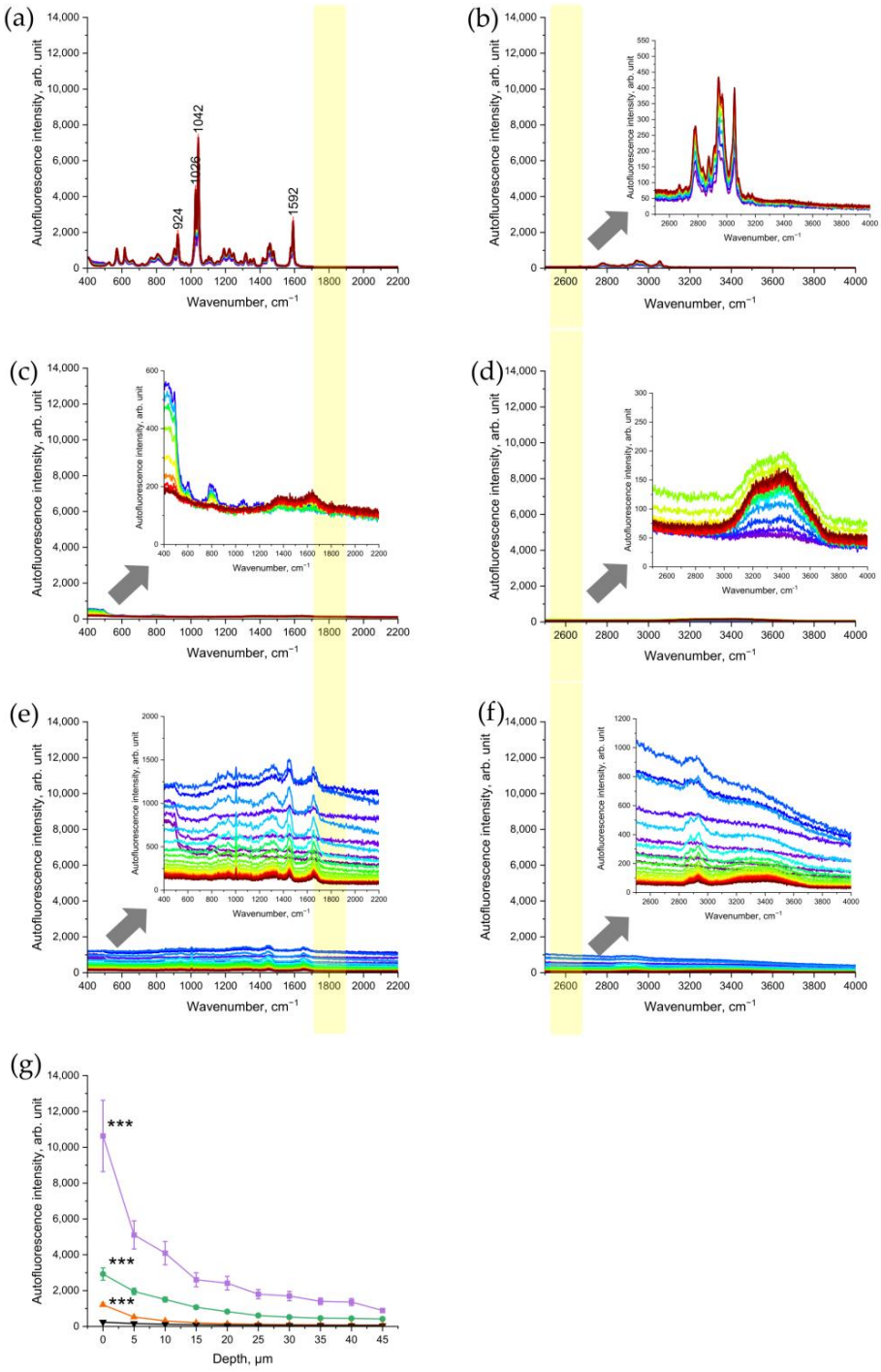


**Figure 4.** Representative Raman spectra of nicotine excited in 785 nm NIR (**a**) and in 671 nm red (**b**); spectral ranges of a glass slide after CS exposure excited in NIR (**c**) and in red (**d**); porcine skin excited in NIR (**e**) and in red (**f**) spectral ranges after exposure to UVA irradiation at 52 J/cm$^2$ for 106 min (2 MED). The arrows point to the inserts in (**b**–**f**) that show the zoomed spectra for clarity. The yellow color shows the area where the AF intensity was analyzed where no Raman bands can interfere. (**g**) Comparison of NIR-excited AF intensity in porcine skin: five cigarettes immediately after 5 min of exposure (purple squares), five cigarettes after cleaning the skin sample (green circles), 2 UVA-MED with a 365 ± 5 nm LED for 106 min at 52 J/cm$^2$ (red upward triangles), and control skin before CS exposure (black downward triangles). Graphs show mean ± SEM. GEE was applied; *** $p \leq 0.001$ (CS-exposed vs. UVA-irradiated skin vs. control).

### *3.5. Chemically-Induced Oxidative Stress*

In Figure S3, there is no significant difference in AF intensity between the control group and chemically-induced oxidative stress.

### *3.6. In Vivo Skin Measurements*

In order to evaluate the effect of CS exposure on human skin in vivo, the ex vivo method was transferred to an in vivo setting. The lower forearm of each of the ten healthy human volunteers was exposed to five cigarettes within 5 minutes in the smoking chamber (Figure 1b). The NIR-excited AF intensity was measured before and after CS exposure and after cleaning the CS residue from the skin surface.

The results are presented in Figure 5; they show that at the surface, the NIR-excited AF intensity was approximately five-fold higher in the skin of the CS-exposed group, compared to the non-exposed control area. Even after cleaning the skin after CS exposure, an approximately three-fold increase in NIR-excited AF intensity was measured in human skin in vivo. This result shows that CS exposure leads to an increase in NIR-excited AF intensity in human skin in vivo. NIR-excited Raman spectra of the human skin in vivo are shown in the Supplementary Materials (Figure S1a–c).

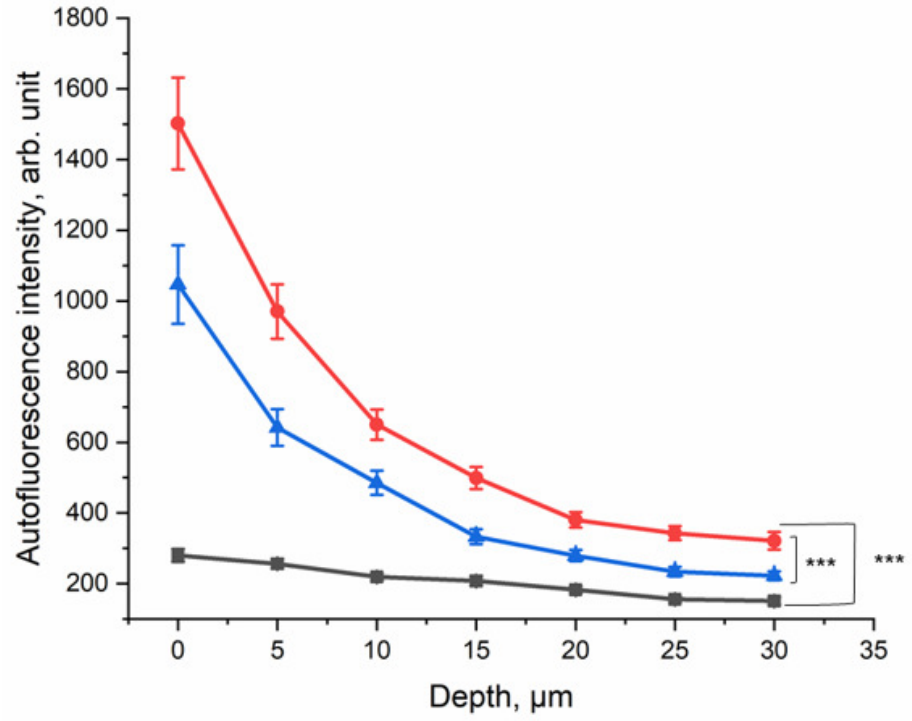


**Figure 5.** Depth profile of 785 nm NIR-excited AF intensity of CS-exposed human skin in vivo ($n$ = 10) before CS exposure (black squares), after CS exposure to five cigarettes within 5 minutes (red circles), and after cleaning CS-exposed skin (blue triangles). The average nicotine concentration on the filter paper was 45.5 ± 9.3 μg/cm$^2$. In depths of 0–30 μm, the difference between CS-exposed and non-exposed skin was significant (GEE, *** $p \leq 0.001$).

Red-excited Raman spectra of the human skin in vivo are shown in the Supplementary Materials (Figure S1d–f). A similar depth-dependent increase in the red-excited AF intensity of human skin in vivo was observed.

### *3.7. LSM Imaging Confirms an Enhancement of NIR-Excited Skin AF after Cigarette-Smoke Exposure*

To support the obtained results, the AF intensities on the skin surface before and after CS exposure were recorded, using LSM. Figure 6 illustrates selected NIR-excited AF images of porcine skin before (Figure 6a) and after CS exposure (Figure 6b), recorded

using LSM (785 nm). A strong, almost two-fold, increase in AF intensity, calculated as image brightness, could be observed in the LSM images of CS-exposed skin (4.0 arb. units), compared to that of non-exposed skin (1.9 arb. units).

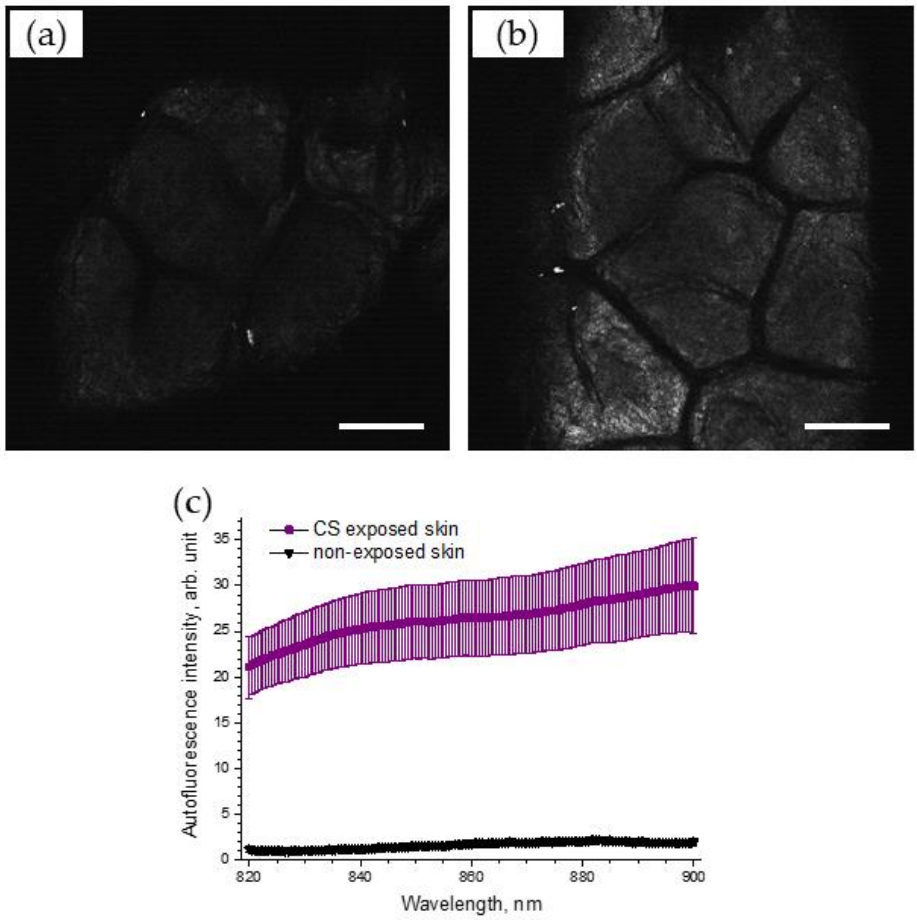


**Figure 6.** Exemplary 785 nm NIR-excited AF LSM images of the superficial stratum corneum of porcine skin before (**a**) and after (**b**) CS exposure to one cigarette within 5 min in the exposure chamber. Scale bar: 100 µm. (**c**) AF spectrum (mean ± SEM) of CS-exposed (five cigarettes within 5 min) porcine skin (purple) and non-exposed control skin (black), $n = 6$.

The spectrum of 785 nm NIR-excited porcine skin AF is shown in Figure 6c for CS-exposed and non-exposed skin. The enhanced NIR-excited AF intensity in CS-exposed skin is obvious, compared to that of non-exposed skin (the average increase was 17.4 ± 3.6 times in the spectral range of 820–900 nm).

## 4. Discussion

The increase in air pollution not only affects the health of our lungs, but also our skin. So far, insufficient non-invasive methods are available to measure the effect of pollution, especially CS exposure during a short time period. We chose CS because it is among the most toxic environmental pollutants that include particulate matter, such as polycyclic hydrocarbons [4]. The nicotine concentration in the smoking chamber with five cigarettes for 5 min is comparable to spending 8 h in a bar where smoking is allowed [33]. Therefore, to emulate the real-life CS-exposure conditions, we changed the CS exposure dose from $\frac{1}{4}$ of a cigarette to five cigarettes within 5 min in the smoking chamber.

In this study, the non-invasive and label-free CRM method was used. It is a powerful technique to determine depth profiles of skin components and barrier-function-related parameters ex vivo and in vivo. Fluorescence background is always present in the Raman spectra and has an influence on the signal-to-noise ratio [34]. Usually, it is removed to ana-

lyze the Raman bands in a proper way. A short acquisition time significantly minimizes the effect of AF photobleaching [35] and allows AF intensity measurements to be very precise.

As shown in Figure 2a, at an NIR excitation of 785 nm, non-exposed porcine skin emits only a tiny amount of AF. The same is observed at red excitation of 671 nm (Figure 2d). After CS exposure, the NIR- and red-excited AF intensities of porcine skin ex vivo (Figure 2b,e) and human skin in vivo (Figures 5 and S1) increased substantially. For NIR excitation, this was confirmed by LSM AF imaging (Figure 6a,b) and by measuring the spectrum of skin AF (Figure 6c) at the superficial depth for CS-exposed and non-exposed skin. The sensitivity of CRM for AF measurements is, however, much higher than that of the LSM imaging that was used.

In this study, our hypothesis was that CS exposure leads to an increase in NIR- and red-excited AF intensity of the skin through the induction of oxidative stress. In the NIR-excited fingerprint region and the red-excited high wavenumber region, there is no interference in the skin between AF and Raman bands at 1800 and 2600 $cm^{-1}$, respectively. Therefore, these wavenumber positions were used to further calculate the NIR- and red-excited AF intensity of the skin. Analysis of skin Raman spectra after CS exposure did not reveal the appearance of new components that could help to identify the source of oxidative-stress products. Both ex vivo and in vivo experiments showed that the increase in NIR- and red-excited skin AF intensities was observed mainly in the stratum corneum up to the depth of 25 µm with highest intensity at the surface. The effect on the deeper epidermis was in agreement with the method used by Grether-Beck et al. [20], where the melanin located in the basal layer was stimulated by diesel-exhaust-particle exposure in in vivo skin.

To confirm the hypothesis that oxidative stress leads to an increase in NIR- and red-excited AF intensities in skin, the source of AF was investigated. As a negative control, no evidence was found that nicotine or the CS residue itself led to a significant increase in NIR- and red-excited skin AF intensities (Figure 4a–d). No correlation between the NIR- and red-excited AF intensities and the CS dose represented by nicotine concentration could be found (Figure 3a,b). As a positive control, we used UVA irradiation, which is known to induce oxidative stress in excised skin through the generation of ROS [36,37]. The significant increase in NIR- and red-excited AF intensities was measured in excised porcine skin after UVA irradiation at UVA–MED (Figure 4e,f). This might indicate that oxidative stress is not only induced by UVA irradiation but also by CS exposure, which increases NIR- and red-excited AF intensities in the skin.

After cleaning the ex vivo and in vivo skin following the CS exposure, an increased NIR- and red-excited AF intensity could still be measured depth-dependently and compared to non-exposed skin with a most pronounced change in the superficial layer of stratum corneum depth (Figures 3b and 5). Skin cleaning removes the CS particulate residues located on the skin surface but, as shown in Figure 4a–d, such residues are not a source of fluorescence. Thus, we concluded that oxidized skin surface lipids are mainly responsible for the NIR- and red-excited AF intensities in the CS-exposed skin.

Skin AF was previously investigated in smokers, due to an increase in the advanced glycation end product concentration that serves as a biomarker for aging and is a contributing factor for degenerative diseases [38]. Endogenous fluorophores, such as porphyrins, that are allocated on skin [39] are known to emit AF at 785 nm [35]. As porphyrins play a key role in metabolic processes [40], oxidative stress induced by CS could increase their AF. Moreover, the oxidized lipids, proteins, and amino acids can serve as molecular sources of NIR- and red-excited AF in the skin [41]. It should be noted that in the skin, the number of fluorophores absorbing light in the red and NIR ranges is strongly limited, so that reabsorption is negligible and the depth-resolved detection of red and NIR quanta is determined very accurately [42].

Chemically-induced oxidation through hydrogen peroxide did not increase AF intensity, shown in Figure S3. Hydrogen peroxide that induces intracellular stress in skin was used as a positive control in the DCFH assays of Hergesell et al. [25]. Our method could not detect an increase in AF intensity in red and NIR spectral regions when oxidative stress

was induced by hydrogen peroxide, compared to that of CS exposure and UV irradiation. One possible explanation could be the oxidation of fluorophores due to hydrogen peroxide, as was stated for AF induced by UV radiation combined with hydrogen peroxide [43] and in a study using microspectrofluorometry to detect AF emission from human leukemic living cells under oxidative stress [44]. Thus, not all intracellular stress can be detected by the presented red- and NIR-excited AF method.

It was previously shown that CS induces oxidative stress by 4-hydroxynoenal (4-HNE), a lipid peroxidation marker and a second messenger for oxidative stress [45], and an increase in pro-inflammatory interleukins [46,47] and via ROS [6]. Different pathways can lead to the development of oxidative stress in skin. In previous studies, ROS production due to UVA irradiation and CS exposure was investigated. Tran et al. [6] concluded that UVA irradiation with less than 1/3 MED induces more ROS in the skin than the exposure to five cigarettes. In contrast, the obtained results show that the effect on the skin is more pronounced by CS exposure than by UVA irradiation of 2 UVA–MED (Figure 4f). Therefore, CS exposure could induce effects other than the formation of ROS, because it leads to stronger enhancement of NIR- and red-excited AF intensities in the skin than UVA.

In in vivo human skin, the increase in NIR- and red-excited AF intensities was shown after CS exposure; in addition, even after cleaning the forearm, the increase was significant compared to the non-exposed control. The AF intensity after CS exposure in excised porcine skin was higher than in in vivo human skin, not only because of the higher CS concentration in the chamber but also because of the higher antioxidant status and, therefore, better protection in in vivo human skin [48,49]. Skin components in darker skin types emit higher NIR- and red-excited AF due to the higher melanin content [50]. The AF of melanin in the NIR at 785 nm was investigated by Huang et al. [51] and Han et al. [52] and in NIR at 785 nm and red at 671 nm by Yakimov et al. [50]. Here, a higher melanin content was related to a higher AF in the NIR- and red-excitation regions. This result shows that this method has limitations in measuring stratum spinosum and stratum basal epidermal layers of dark skin (skin types $\geq$ IV), as melanin interferes with the NIR- and red-excited AF induced by oxidative stress. The limitations are expected to be less-pronounced in the stratum corneum and stratum granulosum layers of dark skin. Porcine epidermis contains a much lower melanin concentration than human epidermis, enabling clear investigations of NIR- and red-excited AF without the superposition with melanin-excited AF [53]. For precise measurements, additional stress should be avoided, as short-term sun exposure could lead to an increase in NIR- and red-excited AF intensities. In the present in vivo human study, melanin did not interfere with the AF signal because the volunteers had skin types I–III, meaning that their melanin content in the epidermis was sufficiently low.

Nonetheless, we provide an alternative fast method to investigate the effect of CS on skin, because it is label-free and non-invasive. In addition, the effect of CS on the skin can be seen immediately by measuring skin AF, compared to the patch test of Grether-Beck et al. [20], where the results were only visible after nine days. Here, topical application of diesel exhaust particles led to an increase in skin pigmentation, due to induction of melanogenesis.

## 5. Conclusions

The results of the present work show that skin exposure to the model pollutant cigarette smoke (CS) led to the development of dose-dependent oxidative stress in the epidermis. Oxidative stress was detected non-invasively by a significant increase in 785 nm NIR-excited and 671 nm red-excited autofluorescence (AF) of the skin ex vivo and in vivo by analysis of depth-resolved Raman spectra. The intensity of the NIR- and red-excited AF was determined at positions of 1800 and 2600 $cm^{-1}$, respectively, which did not contain Raman bands. Our findings demonstrate that the origin of AF of CS-exposed skin is not related to nicotine and other CS-induced residues in the superficial stratum corneum, but is related to induced oxidative stress, in which skin surface lipids are mainly involved. This was confirmed by the fact that cleaning CS-exposed skin resulted in a reduction

in AF intensity, compared to uncleaned CS-exposed skin, but the AF intensity was still significantly higher than that of non-exposed skin. An increase in NIR-excited skin AF was also confirmed by laser scanning microscopy AF imaging and fluorescence spectroscopy. Thus, the novel label-free, non-invasive method for assessing oxidative stress in the skin due to CS exposure, based on the measurement of increased skin AF intensity, was presented. With this method, it will be possible in the future to assess the protective effects of anti-pollution skin care products.

**Supplementary Materials:** The following supporting information can be downloaded at: https://www.mdpi.com/article/10.3390/antiox12051011/s1, Figure S1: Representative Raman spectra of CS-exposed (five cigarettes within five minutes) and non-exposed human forearm skin in vivo at different depths (0–40 µm) excited in NIR (785 nm) (a–c) and in red (d–f) spectral ranges. (a,d) Control skin before CS exposure; (b,e) uncleaned skin after CS exposure; (c,f) cleaned skin after CS exposure. The inserts in (a,c,d,f) show the zoomed spectra for clarity. Figure S2: Depth profile of 785 nm NIR-excited AF intensity (mean ± SEM) of ex vivo porcine skin after dose-dependent exposure to CS (purple—five cigarettes; green—one cigarette; blue—1/2 cigarette; and red—1/4 cigarette. Orange—2 UVA-MED) immediately after CS exposure and after cleaning the skin probes. Figure S3: Depth profile of 785 nm NIR-excited AF intensity (mean ± SEM) of ex vivo porcine skin after 30 min $H_2O_2$ incubation (red circles—2 mM $H_2O_2$; blue triangles—30% $H_2O_2$), compared to control excised porcine skin (black squares).

**Author Contributions:** Conceptualization, M.C.M. and M.E.D.; methodology, M.C.M., P.T.T., S.B.L. and M.E.D.; validation, M.C.M., M.E.D., P.T.T., J.S. and B.K.; formal analysis, P.T.T., P.T., J.S., M.E.D. and B.K.; investigation, P.T.T. and P.T.; writing—original draft preparation, P.T.T. and P.T.; writing—review and editing, M.C.M., M.E.D., J.S., S.B.L. and B.K.; visualization, P.T.T. and P.T.; supervision, M.C.M.; project administration, M.C.M. and S.B.L.; funding acquisition, M.C.M. All authors have read and agreed to the published version of the manuscript.

**Funding:** The work is funded by the European Regional Development Fund within the program "Pro FIT—Programm zur Förderung von Forschung, Innovationen und Technologien", grant ID: 10168708.

**Institutional Review Board Statement:** The study was conducted according to the guidelines of the Declaration of Helsinki and approved by the Institutional Review Board (or Ethics Committee) of Charité—Universitätsmedizin Berlin (EA1/291/21 from 16 November 2021) with public study registration number DRKS00029235.

**Informed Consent Statement:** Informed consent was obtained from all subjects involved in the study.

**Data Availability Statement:** All data are contained within the article and the Supplementary Materials.

**Acknowledgments:** We would like to thank Heike Richter for technical support.

**Conflicts of Interest:** The authors declare no conflict of interest. The authors M.E.D and P.T. are no longer affiliated with Charité-Universitätsmedizin Berlin. However, with the permission of the Center of Experimental and Applied Cutaneous Physiology, where the entire work was carried out, the author uses the Charité affiliation.

## References

1. World Health Organization. *Compendium of WHO and Other UN Guidance on Health and Environment*; World Health Organization: Geneva, Switzerland, 2022.
2. Krutmann, J.; Moyal, D.; Liu, W.; Kandahari, S.; Lee, G.-S.; Nopadon, N.; Xiang, L.F.; Seité, S. Pollution and acne: Is there a link? *Clin. Cosmet. Investig. Dermatol.* **2017**, *10*, 199. [CrossRef] [PubMed]
3. Huls, A.; Abramson, M.J.; Sugiri, D.; Fuks, K.; Kramer, U.; Krutmann, J.; Schikowski, T. Nonatopic eczema in elderly women: Effect of air pollution and genes. *J. Allergy. Clin. Immunol.* **2019**, *143*, 378–385.E9. [CrossRef]
4. Prieux, R.; Eeman, M.; Rothen-Rutishauser, B.; Valacchi, G. Mimicking cigarette smoke exposure to assess cutaneous toxicity. *Toxicol. In Vitro* **2020**, *62*, 104664. [CrossRef]
5. Farris, P.K.; Valacchi, G. Ultraviolet light protection: Is it really enough? *Antioxidants* **2022**, *11*, 1484. [CrossRef]
6. Tran, P.T.; Beidoun, B.; Lohan, S.B.; Talbi, R.; Kleuser, B.; Seifert, M.; Jung, K.; Sandig, G.; Meinke, M.C. Establishment of a method to expose and measure pollution in excised porcine skin with electron paramagnetic resonance spectroscopy. *Ecotoxicol. Environ. Saf.* **2022**, *247*, 114258. [CrossRef]
7. Puri, P.; Nandar, S.K.; Kathuria, S.; Ramesh, V. Effects of air pollution on the skin: A review. *Indian J. Dermatol. Venereol. Leprol.* **2017**, *83*, 415–423. [CrossRef] [PubMed]

8. Sen, C.K. Oxygen toxicity and antioxidants: State of the art. *Indian J. Physiol. Pharmacol.* **1995**, *39*, 177–196.
9. Darvin, M.E.; Lademann, J.; von Hagen, J.; Lohan, S.B.; Kolmar, H.; Meinke, M.C.; Jung, S. Carotenoids in Human SkinIn Vivo: Antioxidant and Photo-Protectant Role against External and Internal Stressors. *Antioxidants* **2022**, *11*, 1451. [CrossRef] [PubMed]
10. Pavlou, P.; Rallis, M.; Deliconstantinos, G.; Papaioannou, G.; Grando, S.A. In-vivo data on the influence of tobacco smoke and UV light on murine skin. *Toxicol. Ind. Health* **2009**, *25*, 231–239. [CrossRef]
11. Murray, C.S.; Woodcock, A.; Smillie, F.I.; Cain, G.; Kissen, P.; Custovic, A.; Group, N.S. Tobacco smoke exposure, wheeze, and atopy. *Pediatr. Pulmonol.* **2004**, *37*, 492–498. [CrossRef]
12. Maarouf, M.; Maarouf, C.L.; Yosipovitch, G.; Shi, V.Y. The impact of stress on epidermal barrier function: An evidence-based review. *Br. J. Dermatol.* **2019**, *181*, 1129–1137. [CrossRef] [PubMed]
13. Lin, Z.; Niu, Y.; Jiang, Y.; Chen, B.; Peng, L.; Mi, T.; Huang, N.; Li, W.; Xu, D.; Chen, R.; et al. Protective effects of dietary fish-oil supplementation on skin inflammatory and oxidative stress biomarkers induced by fine particulate air pollution: A pilot randomized, double-blind, placebo-controlled trial. *Br. J. Dermatol.* **2021**, *184*, 261–269. [CrossRef] [PubMed]
14. Li, M.; Vierkötter, A.; Schikowski, T.; Hüls, A.; Ding, A.; Matsui, M.S.; Deng, B.; Ma, C.; Ren, A.; Zhang, J. Epidemiological evidence that indoor air pollution from cooking with solid fuels accelerates skin aging in Chinese women. *J. Dermatol. Sci.* **2015**, *79*, 148–154. [CrossRef] [PubMed]
15. Knuutinen, A.; Kokkonen, N.; Risteli, J.; Vahakangas, K.; Kallioinen, M.; Salo, T.; Sorsa, T.; Oikarinen, A. Smoking affects collagen synthesis and extracellular matrix turnover in human skin. *Br. J. Dermatol.* **2002**, *146*, 588–594. [CrossRef]
16. Cervellati, F.; Muresan, X.M.; Sticozzi, C.; Gambari, R.; Montagner, G.; Forman, H.J.; Torricelli, C.; Maioli, E.; Valacchi, G. Comparative effects between electronic and cigarette smoke in human keratinocytes and epithelial lung cells. *Toxicol. In Vitro* **2014**, *28*, 999–1005. [CrossRef]
17. Gould, N.S.; Min, E.; Gauthier, S.; Martin, R.J.; Day, B.J. Lung glutathione adaptive responses to cigarette smoke exposure. *Respir. Res.* **2011**, *12*, 133. [CrossRef] [PubMed]
18. Damevska, K.; Boev, B.; Mirakovski, D.; Petrov, A.; Darlenski, R.; Simeonovski, V. How to prevent skin damage from air pollution. Part 1: Exposure assessment. *Dermatol. Ther.* **2020**, *33*, e13171. [CrossRef]
19. Yin, L.; Morita, A.; Tsuji, T. Skin aging induced by ultraviolet exposure and tobacco smoking: Evidence from epidemiological and molecular studies. *Photodermatol. Photoimmunol. Photomed.* **2001**, *17*, 178–183. [CrossRef] [PubMed]
20. Grether-Beck, S.; Felsner, I.; Brenden, H.; Marini, A.; Jaenicke, T.; Aue, N.; Welss, T.; Uthe, I.; Krutmann, J. Air pollution-induced tanning of human skin. *Br. J. Dermatol.* **2021**, *185*, 1026–1034. [CrossRef]
21. Ji, H.W.Y.; Fannin, F.F.; Bush, L.P. Stability of the Certified 1R6F Reference Cigarette. Available online: https://www.coresta.org/abstracts/stability-certified-1r6f-reference-cigarette-30768.html (accessed on 16 February 2023).
22. Jaccard, G.; Djoko, D.T.; Korneliou, A.; Stabbert, R.; Belushkin, M.; Esposito, M. Mainstream smoke constituents and in vitro toxicity comparative analysis of 3R4F and 1R6F reference cigarettes. *Toxicol. Rep.* **2019**, *6*, 222–231. [CrossRef]
23. Pauwels, C.; Klerx, W.N.M.; Pennings, J.L.A.; Boots, A.W.; van Schooten, F.J.; Opperhuizen, A.; Talhout, R. Cigarette Filter Ventilation and Smoking Protocol Influence Aldehyde Smoke Yields. *Chem. Res. Toxicol.* **2018**, *31*, 462–471. [CrossRef]
24. Lohan, S.; Ivanov, D.; Schüler, N.; Berger, B.; Zastrow, L.; Lademann, J.; Meinke, M. Switching from healthy to unhealthy oxidative stress–does the radical type can be used as an indicator? *Free Radic. Biol. Med.* **2021**, *162*, 401–411. [CrossRef] [PubMed]
25. Hergesell, K.; Valentova, K.; Velebny, V.; Vavrova, K.; Doleckova, I. Common Cosmetic Compounds Can Reduce Air Pollution-Induced Oxidative Stress and Pro-Inflammatory Response in the Skin. *Skin Pharmacol. Physiol.* **2022**, *35*, 156–165. [CrossRef] [PubMed]
26. Caspers, P.J.; Bruining, H.A.; Puppels, G.J.; Lucassen, G.W.; Carter, E.A. In Vivo Confocal Raman Microspectroscopy of the Skin: Noninvasive Determination of Molecular Concentration Profiles. *J. Investig. Dermatol.* **2001**, *116*, 434–442. [CrossRef] [PubMed]
27. Darvin, M.E.; Meinke, M.C.; Sterry, W.; Lademann, J. Optical methods for noninvasive determination of carotenoids in human and animal skin. *J. Biomed. Opt.* **2013**, *18*, 61230. [CrossRef] [PubMed]
28. Zhu, Y.; Choe, C.S.; Ahlberg, S.; Meinke, M.C.; Alexiev, U.; Lademann, J.; Darvin, M.E. Penetration of silver nanoparticles into porcine skin ex vivo using fluorescence lifetime imaging microscopy, Raman microscopy, and surface-enhanced Raman scattering microscopy. *J. Biomed. Opt.* **2015**, *20*, 051006. [CrossRef] [PubMed]
29. Yakimov, B.P.; Venets, A.V.; Schleusener, J.; Fadeev, V.V.; Lademann, J.; Shirshin, E.A.; Darvin, M.E. Blind source separation of molecular components of the human skin in vivo: Non-negative matrix factorization of Raman microspectroscopy data. *Analyst* **2021**, *146*, 3185–3196. [CrossRef]
30. Darvin, M.E.; Schleusener, J.; Lademann, J.; Choe, C.S. Current Views on Noninvasive in vivo Determination of Physiological Parameters of the Stratum Corneum Using Confocal Raman Microspectroscopy. *Ski. Pharmacol. Physiol.* **2022**, *35*, 125–136. [CrossRef]
31. Choe, C.; Schleusener, J.; Ri, J.; Choe, S.; Kim, P.; Lademann, J.; Darvin, M.E. Quantitative determination of concentration profiles of skin components and topically applied oils by tailored multivariate curve resolution-alternating least squares using in vivo confocal Raman micro-spectroscopy. *J. Biophotonics* **2022**, *16*, e202200219. [CrossRef]
32. Baranska, M.; Dobrowolski, J.C.; Kaczor, A.; Chruszcz-Lipska, K.; Gorz, K.; Rygula, A. Tobacco alkaloids analyzed by Raman spectroscopy and DFT calculations. *J. Raman Spectrosc.* **2012**, *43*, 1065–1073. [CrossRef]

33. Lopez, M.J.; Nebot, M.; Albertini, M.; Birkui, P.; Centrich, F.; Chudzikova, M.; Georgouli, M.; Gorini, G.; Moshammer, H.; Mulcahy, M.; et al. Secondhand smoke exposure in hospitality venues in Europe. *Environ. Health Perspect.* **2008**, *116*, 1469–1472. [CrossRef] [PubMed]
34. Lunter, D.; Klang, V.; Kocsis, D.; Varga-Medveczky, Z.; Berko, S.; Erdo, F. Novel aspects of Raman spectroscopy in skin research. *Exp. Dermatol.* **2022**, *31*, 1311–1329. [CrossRef]
35. Schleusener, J.; Lademann, J.; Darvin, M.E. Depth-dependent autofluorescence photobleaching using 325, 473, 633, and 785 nm of porcine ear skin ex vivo. *J. Biomed. Opt.* **2017**, *22*, 91503. [CrossRef]
36. Podda, M.; Traber, M.G.; Weber, C.; Yan, L.-J.; Packer, L. UV-Irradiation Depletes Antioxidants and Causes Oxidative Damage in a Model of Human Skin. *Free. Radic. Biol. Med.* **1998**, *24*, 55–65. [CrossRef] [PubMed]
37. Punnonen, K.; Autio, P.; Kiistala, U.; Ahotupa, M. In-vivo effects of solar-simulated ultraviolet irradiation on antioxidant enzymes and lipid peroxidation in human epidermis. *Br. J. Dermatol.* **1991**, *125*, 18–20. [CrossRef]
38. Meerwaldt, R.; Links, T.; Graaff, R.; Thorpe, S.R.; Baynes, J.W.; Hartog, J.; Gans, R.; Smit, A. Simple noninvasive measurement of skin autofluorescence. *Ann. NY Acad. Sci.* **2005**, *1043*, 290–298. [CrossRef]
39. Leite, M.G.A.; Campos, P.M. Correlations between sebaceous glands activity and porphyrins in the oily skin and hair and immediate effects of dermocosmetic formulations. *J. Cosm. Dermatol.* **2020**, *19*, 3100–3106. [CrossRef] [PubMed]
40. Maitra, D.; Bragazzi Cunha, J.; Elenbaas, J.S.; Bonkovsky, H.L.; Shavit, J.A.; Omary, M.B. Porphyrin-Induced Protein Oxidation and Aggregation as a Mechanism of Porphyria-Associated Cell Injury. *Cell. Mol. Gastroenterol. Hepatol.* **2019**, *8*, 535–548. [CrossRef]
41. Semenov, A.N.; Yakimov, B.P.; Rubekina, A.A.; Gorin, D.A.; Drachev, V.P.; Zarubin, M.P.; Velikanov, A.N.; Lademann, J.; Fadeev, V.V.; Priezzhev, A.V.; et al. The Oxidation-Induced Autofluorescence Hypothesis: Red Edge Excitation and Implications for Metabolic Imaging. *Molecules* **2020**, *25*, 1863. [CrossRef]
42. Chen, Y.; Wang, S.; Zhang, F. Near-infrared luminescence high-contrast in vivo biomedical imaging. *Nat. Rev. Bioeng.* **2023**, *1*, 60–78. [CrossRef]
43. Elleder, M.; Borovanský, J. Autofluorescence of Melanins Induced by Ultraviolet Radiation and Near Ultraviolet Light. A Histochemical and Biochemical Study. *Histochem. J.* **2001**, *33*, 273–281. [CrossRef] [PubMed]
44. Bondza-Kibangou, P.; Millot, C.; Dufer, J.; Millot, J.-M. Microspectrofluorometry of autofluorescence emission from human leukemic living cells under oxidative stress. *Biol. Cell* **2001**, *93*, 273–280. [CrossRef] [PubMed]
45. Csala, M.; Kardon, T.; Legeza, B.; Lizák, B.; Mandl, J.; Margittai, É.; Puskás, F.; Száraz, P.; Szelényi, P.; Bánhegyi, G. On the role of 4-hydroxynonenal in health and disease. *Biochim. Biophys. Acta BBA Mol. Basis Dis.* **2015**, *1852*, 826–838. [CrossRef]
46. Percoco, G.; Patatian, A.; Eudier, F.; Grisel, M.; Bader, T.; Lati, E.; Savary, G.; Picard, C.; Benech, P. Impact of cigarette smoke on physical-chemical and molecular proprieties of human skin in an ex vivo model. *Exp. Dermatol.* **2021**, *30*, 1610–1618. [CrossRef] [PubMed]
47. Sakamaki-Ching, S.; Schick, S.; Grigorean, G.; Li, J.; Talbot, P. Dermal thirdhand smoke exposure induces oxidative damage, initiates skin inflammatory markers, and adversely alters the human plasma proteome. *EBioMedicine* **2022**, *84*, 104256. [CrossRef]
48. Haag, S.; Bechtel, A.; Darvin, M.; Klein, F.; Groth, N.; Schäfer-Korting, M.; Bittl, R.; Lademann, J.; Sterry, W.; Meinke, M. Comparative study of carotenoids, catalase and radical formation in human and animal skin. *Ski. Pharmacol. Physiol.* **2010**, *23*, 306–312. [CrossRef] [PubMed]
49. Meinke, M.C.; Müller, R.; Bechtel, A.; Haag, S.F.; Darvin, M.E.; Lohan, S.B.; Ismaeel, F.; Lademann, J. Evaluation of carotenoids and reactive oxygen species in human skin after UV irradiation: A critical comparison between in vivo and ex vivo investigations. *Exp. Dermatol.* **2015**, *24*, 194–197. [CrossRef]
50. Yakimov, B.P.; Shirshin, E.A.; Schleusener, J.; Allenova, A.S.; Fadeev, V.V.; Darvin, M.E. Melanin distribution from the dermal-epidermal junction to the stratum corneum: Non-invasive in vivo assessment by fluorescence and Raman microspectroscopy. *Sci. Rep.* **2020**, *10*, 14374. [CrossRef]
51. Huang, Z.; Zeng, H.; Hamzavi, I.; Alajlan, A.; Tan, E.; McLean, D.I.; Lui, H. Cutaneous melanin exhibiting fluorescence emission under near-infrared light excitation. *J. Biomed. Opt.* **2006**, *11*, 34010. [CrossRef]
52. Han, X.; Lui, H.; McLean, D.; Zeng, H. Near-infrared autofluorescence imaging of cutaneous melanins and human skin in vivo. *J. Biomed. Opt.* **2009**, *14*, 024017. [CrossRef]
53. Darvin, M.E.; Richter, H.; Zhu, Y.J.; Meinke, M.C.; Knorr, F.; Gonchukov, S.A.; Koenig, K.; Lademann, J. Comparison of in vivo and ex vivo laser scanning microscopy and multiphoton tomography application for human and porcine skin imaging. *Quantum Electron.* **2014**, *44*, 646–651. [CrossRef]

# Supplementary materials

# Supplementary Figure S1

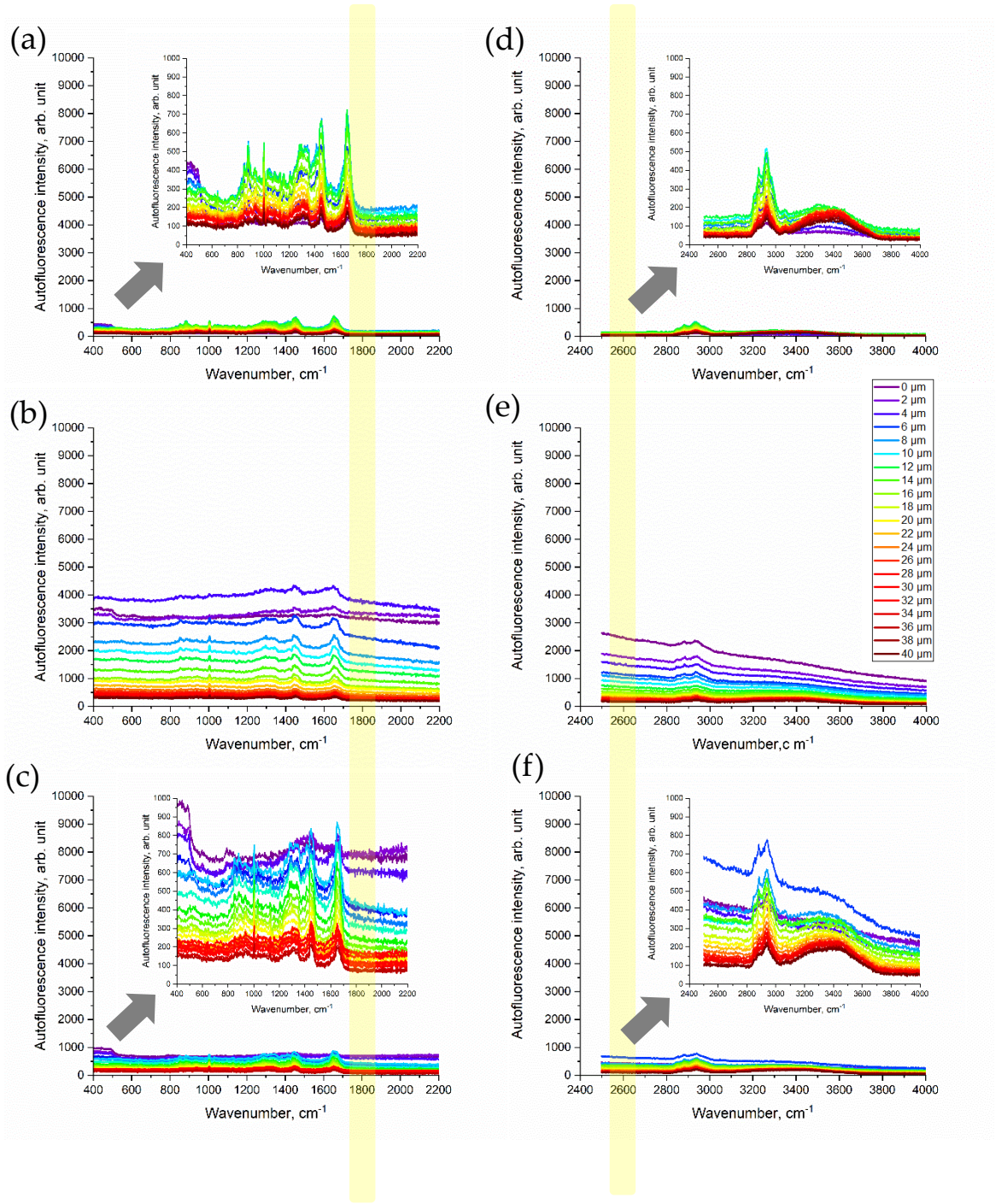


Figure S1: Representative Raman spectra of CS exposed (five cigarettes within five minutes) and non-exposed human forearm skin *in vivo* at different depths (0–40 µm) excited in NIR (785 nm) (a, b, c) and in red (d, e, f) spectral ranges. (a), (d) control skin before CS exposure; (b), (e) uncleaned skin after CS exposure; (c), and (f) cleaned skin after CS exposure. The arrows point to the inserts in (a), (c), (d) and (f) that show the zoomed spectra for clarity. The yellow color marks the area where AF intensity was analyzed where no Raman bands can interfere.

# Supplementary Figure S2

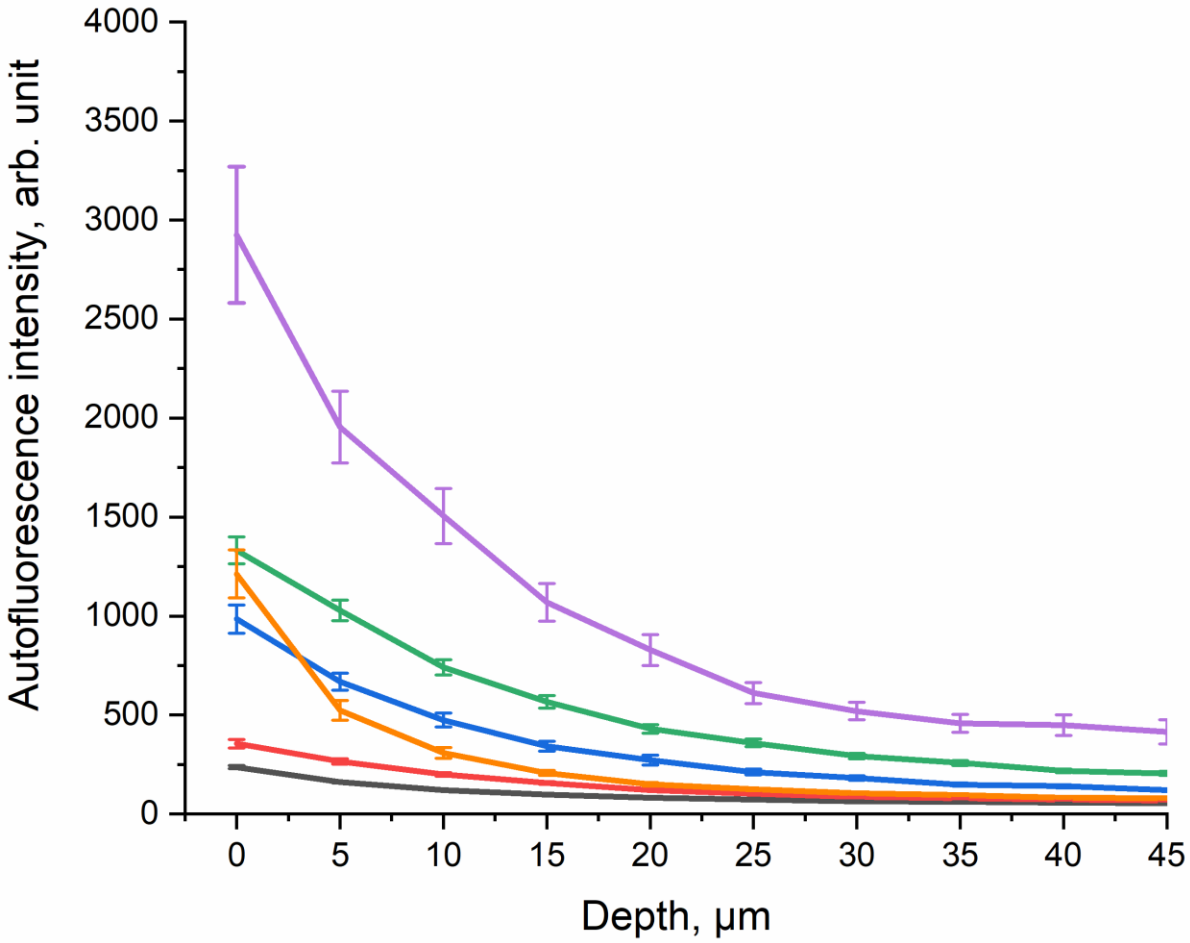


Figure S2: Depth profile of NIR (785 nm) excited AF intensity (mean ± SEM) of *ex vivo* porcine skin after dose-dependent exposure to CS (purple – five cigarettes, green – one cigarette, blue – ½ cigarette and red – ¼ cigarette, orange - 2 UVA-MED) immediately after CS exposure and after cleaning the skin probes

Figure S3

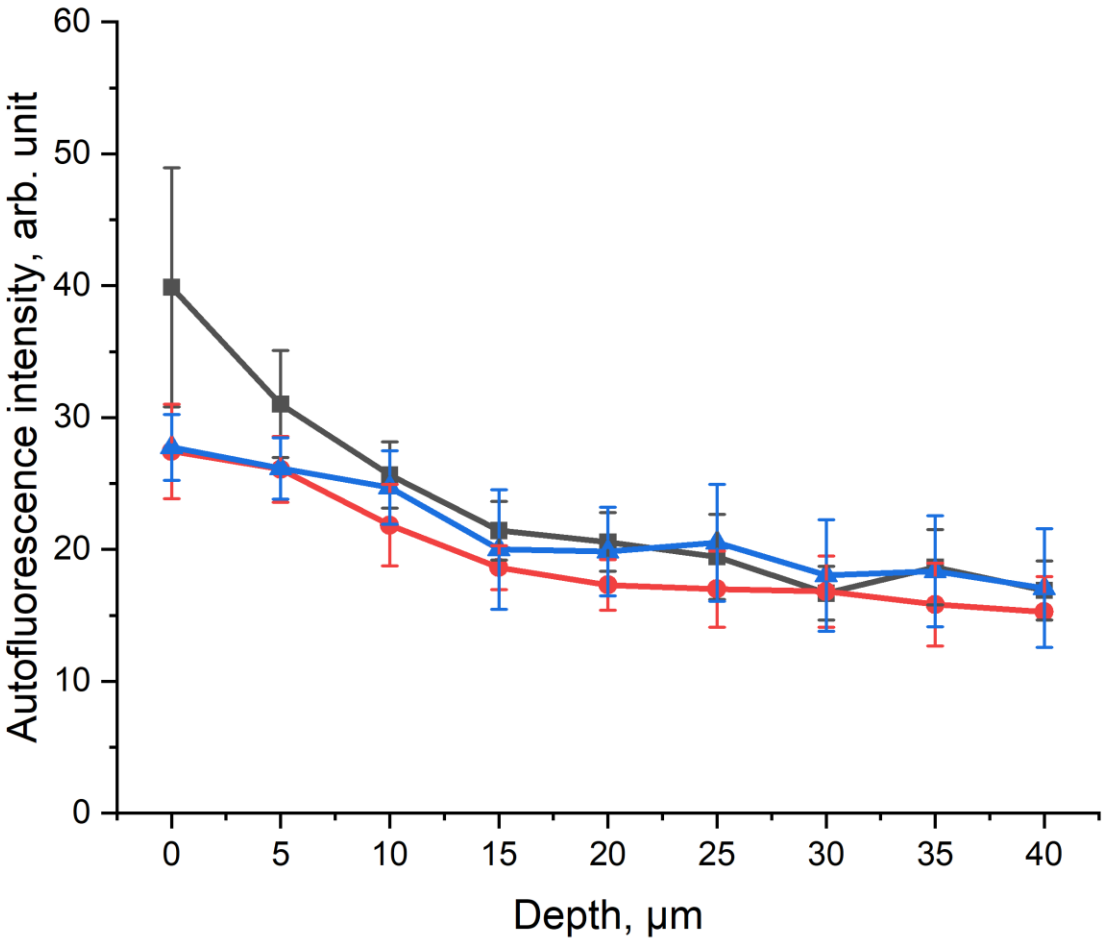


Figure S3: Depth profile of NIR (785 nm) excited AF intensity (mean ± SEM) of *ex vivo* porcine skin after 30 min $H_2O_2$ incubation (red circles – 2mM $H_2O_2$, blue triangles – 30% $H_2O_2$) compared to control excised porcine skin (black squares)

## 2.3 Evidence of the protective effect of anti-pollution products against oxidative stress in skin ex vivo using EPR spectroscopy and autofluorescence measurements

Authors: Phuong Thao Tran, Johannes Schleusener, Burkhard Kleuser, Katinka Jung, Martina C. Meinke, and Silke B. Lohan

Journal: European Journal of Pharmaceutics and Biopharmaceutics

Available online: https://doi.org/10.1016/j.ejpb.2024.114211



Amount performed by Phuong Thao Tran:

Design of experiments: 95%

Practical, experimental part: 95%

Data analysis: 95%

Interpretation of results: 100%

Writing: 95%

European Journal of Pharmaceutics and Biopharmaceutics 197 (2024) 114211

Contents lists available at ScienceDirect

European Journal of Pharmaceutics and Biopharmaceutics

journal homepage: www.elsevier.com/locate/ejpb

Research paper

# Evidence of the protective effect of anti-pollution products against oxidative stress in skin ex vivo using EPR spectroscopy and autofluorescence measurements

Phuong Thao Tran [a,b], Johannes Schleusener [a], Burkhard Kleuser [b], Katinka Jung [c], Martina C. Meinke [a,*], Silke B. Lohan [a]

[a] Charité – Universitätsmedizin Berlin, Corporate Member of Freie Universität Berlin and Humboldt-Universität zu Berlin, Department of Dermatology, Venereology and Allergology, Center of Experimental and Applied Cutaneous Physiology, Charitéplatz 1, 10117 Berlin, Germany
[b] Institute of Pharmacy, Department of Pharmacology, Freie Universität Berlin, Königin-Luise-Str. 2+4, 14195 Berlin, Germany
[c] Gematria TestLab GmbH, Parkstraße 23, 13187 Berlin, Germany

ARTICLE INFO

*Keywords:*
Anti-pollution products
Cigarette smoke
Electron paramagnetic resonance spectroscopy
Confocal Raman microspectroscopy
Oxidative stress
Radical formation

ABSTRACT

The concentration of air pollution is gradually increasing every year so that daily skin exposure is unavoidable. Dietary supplements and topical formulations currently represent the protective strategies to guard against the effects of air pollution on the body and the skin. Unfortunately, there are not yet enough methods available to measure the effectiveness of anti-pollution products on skin. Here, we present two *ex vivo* methods for measuring the protective effect against air pollution of different cream formulations on the skin: Electron paramagnetic resonance (EPR) spectroscopy and autofluorescence excited by 785 nm using a confocal Raman microspectrometer (CRM). Smoke from one cigarette was used as a model pollutant. EPR spectroscopy enables the direct measurement of free radicals in excised porcine skin after smoke exposure. The autofluorescence in the skin was measured *ex vivo*, which is an indicator of oxidative stress. Two antioxidants and a chelating agent in a base formulation and a commercial product containing an antioxidant mixture were investigated. The *ex vivo* studies show that the antioxidant epigallocatechin-3-gallate (EGCG) in the base cream formulation provided the best protection against oxidative stress from smoke exposure for both methods.

## 1. Introduction

Oxidative stress describes the imbalance between pro- and antioxidants and can lead to a wide range of inflammatory diseases, metabolic disorders, including cancer. Environmental toxins, like particulate matter, ozone, polycyclic aromatic hydrocarbons, cigarette smoke and UV radiation, can promote oxidative stress acutely, but also through long-term exposure. The skin acts as a protective barrier between our organs and the environment, protecting us from external influences. Our skin comes into contact with environmental toxins daily. Constant exposure to these toxins can cause oxidative stress in the skin by stimulating the production of reactive oxygen species (ROS). These can significantly affect the redox homeostasis of the skin by disturbing the balance between antioxidants and prooxidants. This leads to a chain reaction with far-reaching consequences for the body [1,2].

Leading manufacturers are taking advantage of growing consumer interest in protecting themselves from air pollution. Many products claim to have an anti-pollution effect. However, the test methods to verify this claim are still insufficient. To investigate the efficacy of anti-pollution products, this study compares two spectroscopic methods and examines two cream formulations, each containing a pure antioxidant, one containing a chelating agent, and a commercial product composed of three different antioxidants. Fig. 1 provides an overview of the experiments conducted in this research paper. Cigarette smoke was selected as a model pollutant that can be reproducibly applied [3].

Increasing outdoor and indoor air pollution is leading to more health risks for humans and animals. Cigarette smoke is often used as a model substance for air pollution, because it has a similar composition. It consists of particulate matter, nitrogen and sulphur dioxide and many other chemical substances [4]. In particular, the formation of radicals during the combustion of cigarettes can lead to increased oxidative stress. This is expressed through various reactions and chain reactions,

* Corresponding author.
*E-mail address:* martina.meinke@charite.de (M.C. Meinke).

https://doi.org/10.1016/j.ejpb.2024.114211
Received 15 November 2023; Received in revised form 29 January 2024; Accepted 5 February 2024
Available online 8 February 2024

such as the formation of hydrogen peroxide and hydroxyl radicals and the photo Fenton reactions. These can cause damage to the body, including the skin. Even the metal ions in cigarettes can cause additional damage by forming radicals and minimizing the levels of antioxidants already present in the body [5].

To counteract additional radical formation and the associated oxidative stress in skin, antioxidants are often used in protective products. They can be applied topically via skin care products. The aim of this work was therefore to investigate the protection properties of different skin care products.

For the formulation base, PHYSIOGEL® (PG) was used. The ingredients used in the commercial products are listed in the supplementary materials (S1). This formulation improved the epidermal permeability barrier and stratum corneum hydration [6], nevertheless, it can be used as a negative control for urban dust [7]. Epigallocatechin-3-gallate (EGCG), the main constituent of the catechins in green tea (*Camellia sinensis*), is known to have a high antioxidant capacity to scavenge free radicals [8,9]. Studies have also shown neuroprotective [10] and cardiovascular benefits [11]. The active ingredient is already widely used in the cosmetic industry. Vitamin E (Vit E) belongs to the group of fat-soluble vitamins, which are among the most important protective vitamins in the body and is to be ingested with food [12]. When applied topically, vitamin E can protect against oxidative skin damage caused by UV radiation [13]. The commercial product CE Ferulic ® consists of the vitamins C, E, and ferulic acid. Vitamin C is a water-soluble vitamin, exhibiting antioxidant properties [12]. When combined with vitamin E, there is a synergistic effect as vitamin E acts as a primary antioxidant and is regenerated by vitamin C [14]. The addition of ferulic acid further stabilizes this antioxidant system and also has an anti-inflammatory effect [15]. CE ferulic acid has also been shown to reduce the oxidative damage caused by ozone exposure. Here, the activation of the redox sensitive transcription factor was decreased in human keratinocytes [16].

For testing the protective effect of various anti-pollution products, an additional active ingredient was selected, that is not based on the antioxidant effect. Since pollution also involves reactions mediated by metal ions, a chelating agent that complexes these metal ions was selected. In this study, EDDS (ethylenediamine-N,N′-disuccinic acid) was used. EDDS occurs naturally in the *actinomycete Amycolatopsis orientalis* and is a sustainable alternative to EDTA, which is also widely used in the cosmetic industry. EDDS is more sustainable because it is biodegradable [17]. Its protective action is based on the complexation of metal ions to prevent the formation of free radicals [18,19].

In our study, *in tubo* models were used to predict the efficacy of the formulations used prior to animal and human testing. These are the measurement of the radical protection factor (RPF) for antioxidants and the chelating power for the chelating agent.

Two spectroscopic methods were applied to study the protective effect of antioxidant- and chelate-containing cream formulations on porcine skin *ex vivo*. With the EPR technology, free radicals generated by environmental factors, can be quantified using the spin probe PCA (3-(carboxyl) − 2, 2, 5, 5-tetramethyl-1-pyrrolidinyloxy). To obtain a more accurate result, UV-A irradiation was applied as an additional stressor *in situ*. For this purpose, the porcine ears were previously smoked with one cigarette in the small *ex vivo* smoke chamber (520 $cm^3$) according to a defined protocol [3]. The autofluorescence, which can be related to oxidative stress on porcine skin after cigarette smoke exposure, was determined using a confocal Raman spectrometer. The confocal Raman spectrometer functions as a sensitive fluorescence spectrometer in the infrared light spectrum. It was not used to investigate any Raman bands. This method does not require any additional stressor or marker [20].

## 2. Materials and methods

### 2.1. Research cigarettes

In this study, research cigarettes 1R6F were used. Ingredients per cigarette: tar 8.6 mg; nicotine 0.72 mg; carbon monoxide 10.1 mg [21].

### 2.2. Cigarette smoke exposure

For *ex vivo* measurements, a small chamber was used with one

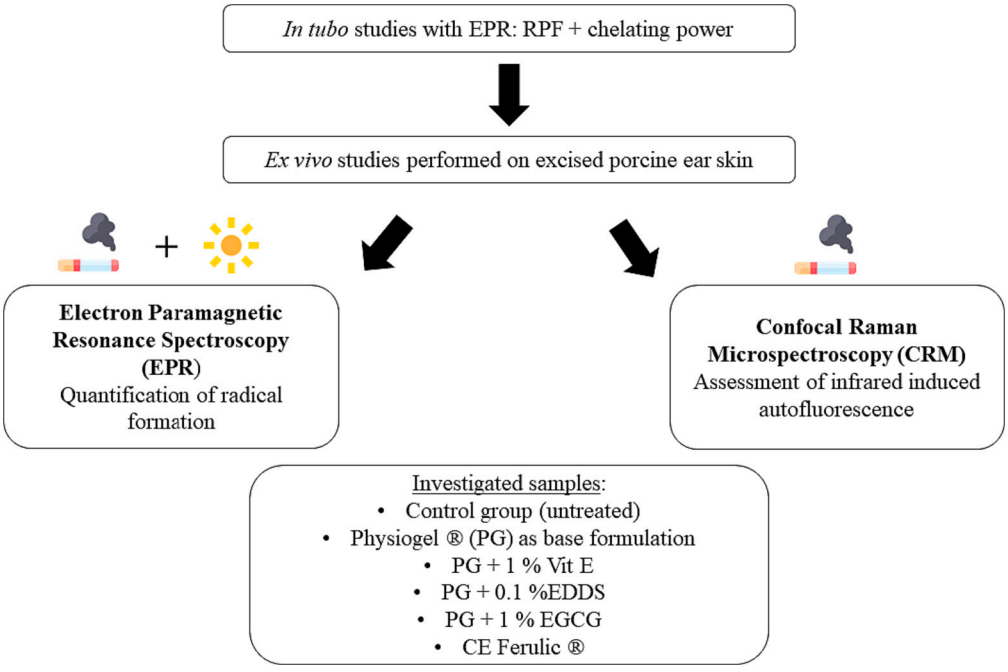


**Fig. 1.** Workflow of this research paper. Here, two *ex vivo* methods are utilized to measure the protective effect of five formulations against cigarette smoke exposure on excised porcine skin. First, the radical protection factor (RPF) and the chelating power were measured of the used formulations with EPR. In addition, EPR was used to quantify the radical formation in excised porcine skin after cigarette smoke exposure and UV-A irradiation (365 nm) at 18 $mW/cm^2$. With CRM, the autofluorescence was measured in excised porcine skin after cigarette smoke exposure alone.

cigarette without a filter. The skin samples were actively exposed to cigarette smoke for 5 min, according to Tran et. al [3]. For all investigations, the exposed smoke was tracked using a filter paper next to the skin areal [20].

### 2.3. Composition of anti-pollution formulations

Two antioxidants, vitamin E (α-tocopherol, Caesar & Loretz GmbH, Hilden, Germany) and EGCG (Teavigo®, Schwelm, Germany) and a chelate complex agent EDDS ((2S, 2′S)-2, 2′-(Ethane-1, 2-diylbis (azanediyl)) disuccinic acid, Sigma Aldrich, Switzerland) were separately incorporated into a placebo formulation (PHYSIOGEL®, Klinge Pharma, Holzkirchen, Germany). Concentrations are shown in Table 1.

In addition, one commercial product containing 15 % L-ascorbic acid, 1 % dl-α tocopherol, and 0.5 % trans ferulic acid (CE Ferulic®; SkinCeuticals Inc., Dallas, TX, USA) was investigated. The ingredients of all commercial products are listed in the supplementary materials (Fig. S1).

### 2.4. Electron paramagnetic resonance (EPR) spectroscopy

In this study the X-band EPR system MiniScope MS5000 (Magnettech, Freiberg Instruments GmbH, Freiberg, Germany) was used for determining the radical protection factor (RPF) of the studied formulation and for evaluating the radical formation in porcine skin.

For the RPF measurements, the following parameter settings were used: modulation amplitude 2 G, microwave (MW) attenuation 15 dB (MW power 3.16 mW), sweep time 20 s, sweep 95 G, $B_0$-field 3350 G, steps 1024 and number (pass) 1 [22].

For the radical formation investigations, the following parameter settings were used: microwave frequency 9.4 GHz, microwave power 10 dB (10 mW), modulation 0.20 mT, modulation frequency 100 kHz, sweep time (measuring time) 10 sec, coupling time 15 sec, magnetic field $B_0$ 337.16 mT, sweep 7.67 mT [3].

### 2.5. Irradiation unit

As an additional stressor, UV-A irradiation was used for evident measurement of free radicals by smoke exposure vs. untreated skin. An UV-A LED irradiation unit (Freiberg Instruments GmbH, Freiberg, Germany) with a wavelength of 365 ± 5 nm and a UV-A irradiance of 18 mW/cm$^2$ for 7 min was employed for the MS5000 EPR Magnettech system. The *in situ* irradiation is comparable to 1/3 minimal erythema dose for UV-A (MED, 9 J/cm$^2$) [23]. An 843-R power meter (Newport Corporation, CA, USA) was used to gauge the UV-A LED light source's intensity. As a result, the distance was determined using the skin sample that had been exposed to radiation inside the EPR device's resonator.

### 2.6. Radical protection factor (RPF)

To determine the radical protection factor of the used anti-pollution formulations, 2,2-Diphenyl-1- picrylhydrazyl (DPPH, Sigma-Aldrich, Steinheim, Germany) was used as a test radical for EPR spectroscopy investigations. Here, the antioxidant capacity was determined by measuring the radical scavenging activity of the samples as previously described [24,25]. For the formulations in PHYSIOGEL®, 150 mg were diluted in 10 mL of ethanol (Uvasol® Ethanol 99.9 %, Merck KGaA, Darmstadt, Germany). For CE Ferulic, 20 mg were diluted in 10 mL of ethanol. The samples were put into the ultrasonic bath (Banderlin Sonorex Super RK 102H, Berlin, Germany) for two hours at 35 kHz at constant 20 °C. Afterwards, 400 µL of the diluted formulations and 400 µL of a 1 mM DPPH solution were combined and were directly measured by EPR spectroscopy. The measurements were performed until the signal of DPPH in the EPR was stable. This could take up to 30 h. The samples were constantly swiveling in the dark at room temperature between the measurements.

**Table 1**
Test samples on skin.

| Tested formulations |
|---|
| PHYSIOGEL® (used as vehicle) |
| 1 % Vitamin E + PHYSIOGEL® |
| 1 % EGCG + PHYSIOGEL® |
| 0.1 % EDDS + PHYSIOGEL® |
| CE Ferulic ® |

### 2.7. Copper chelation

The chelating power was tested with the X-band EPR system MiniScope MS300 (Magnettech, Freiberg Instruments GmbH, Freiberg, Germany). The method was based on Bielfeldt et. al. [7].

Here, EDDS was tested against different concentrations of copper (Cu) (II) ions. Cu (II) is a paramagnetic ion showing a direct EPR absorbance. Dissolved in pure water, Cu (II) shows only one large EPR-absorption band. If the Cu (II) is correlated to other atoms, as it is the case when copper (II) is placed in solution containing amino acids or proteins, the Cu (II)-EPR-spectrum changes configuration into a 4-band absorption pattern. The position and intensities of these four absorption bands describe the Cu complexes, which are formed in the samples [26].

### 2.8. Radical formation on porcine skin

Porcine ears were obtained from a local butcher and were used until 2 days after slaughtering. The experiments were approved by the Veterinary Office Dahme-Spreewald according to Section 3, Article 17, Paragraph 1 of Regulation (EC) No 1069/2009 of the European Parliament and Council, dated October 21, 2009, laying down health regulations for animal products not intended for human consumption byproducts.

The hair on the porcine ears was carefully removed by shaving and cleaned under cold running water. Until use, the ears were stored at 4 °C. For the measurements with the MS5000 EPR spectrometer, 300 µm thick slices of split skin were cut using a dermatome (type GA 140, Aesculap-Werke AG, Melsungen, Germany). Up to 4 h after dermatomization, the split skin was stored in the refrigerator in moist towels until use.

In a tissue culture plate (24-well, Falcon, NC, USA) one filter disc (Filter Disks for Finn Chambers 8 mm (ø), Smart Practice, Denmark) was soaked with 38.4 µL, 1.5 mM PCA ((3-(carboxyl) − 2,2,5,5-tetramethyl-1-pyrrolidinyloxy) (Sigma-Aldrich, Steinheim, Germany). On top of the filter disc, an 8 mm (ø) punch biopsy from split skin was placed to be incubated with the spin probe PCA. For samples exposed for 5 min to cigarette smoke, the incubation time was 5 min at 32 °C; samples without smoke exposure were incubated for 5 min at 32 °C followed by 5 min at room temperature in a light-protected location. For smoke exposure, a small smoke chamber was used [3].

For EPR measurements, a 4 mm (ø) skin sample was taken from the center of the incubated biopsy. The skin sample was then measured in the EPR resonator using a tissue cell (Magnettech Freiberg Instruments GmbH, Freiberg, Germany).

With the aid of a temperature control unit (BTC01, Magnettech, Berlin, Germany), EPR measurements were carried out at 32 °C.

As control, the untreated excised porcine skin was analyzed without any application of formulations. Here, the metabolic activity of each excised porcine ear skin sample was measured. The anti-pollution formulations were tested according to ISO 24443. 2 mg/cm$^2$ of the tested formulation were evenly distributed for 2 min on the split skin using a massage device (Rehaforum Medical GmbH, Elmshorn, Germany). 30 min after application at room temperature, the EPR measurements were performed. Each skin measurement was performed in duplicate to demonstrate intra-individual differences [25].

#### 2.8.1. Radical formation measured ex vivo with EPR

Relative radical formation was calculated by analyzing the peak-to-peak intensity of the spin probe PCA. The supplementary materials show the native EPR spectra, which visualize the peak-to-peak intensity of PCA (Fig. S2). Calculation of the quantification was performed with the ESRstudio software (Magnettech Freiberg Instruments GmbH, Freiberg, Germany).

The cumulative radical formation was calculated by subtracting the radical formation due to UV-A irradiation alone from that due to cigarette smoke and UV-A irradiation to measure the impact of cigarette smoke on porcine skin alone.

### 2.9. Autofluorescence measured with CRM

#### 2.9.1. Setup

A CRM-based model 3510 skin composition analyzer (RiverD International B.V., Rotterdam, The Netherlands) was used as a sensitive spectrophotometer for measuring the autofluorescence. Here, following parameter settings were used: excitation wavelength 785 nm, exposure time 5 s, optical power on sample 20 mW [20]. The autofluorescence intensity at 1800 $cm^{-1}$ was analyzed. In the supplementary materials, native CRM spectra are shown (Fig. S3). The CRM device was operated from the skin surface down to 100 μm at 2 μm increments for *ex vivo* skin measurements. More details of the employed CRM system were described in [27]. It is utilized for the analysis of skin composition constituents [28] and drug delivery [29] in general.

#### 2.9.2. Preparation of excised porcine skin

3 × 4 $cm^2$ excised porcine ear skin were used for the CRM experiments. The hair was removed by trimming it with scissors. The anti-pollution formulations were tested according to the COLIPA standard (ISO 24443) procedure, comparable to the EPR method (Chapter 2.8). As control, the untreated skin was measured before and after cigarette smoke exposure.

#### 2.9.3. Investigation of depth-dependent autofluorescence intensity ex vivo

The analysis of the depth-dependent autofluorescence (AF) intensity was based on Tran et al. [20]. Here, the AF background at 1800 $cm^{-1}$ was used. The supplementary materials display full native CRM spectra to illustrate the AF background measured by CRM. To compare the AF values with each other, the AF value was normalized to the nicotine concentration of the respective sample. Here, per ear and per sample, five areas were analyzed at 1800 $cm^{-1}$.

### 2.10. Cigarette smoke exposure control

To control the amount of cigarette smoke exposure, a filter paper was placed next to the exposed skin area *ex vivo* for both methods. According to [3], the nicotine concentration was measured and used for further analysis.

### 2.11. Statistical analysis

The data are shown as mean ± standard error of the mean (SEM). IBM Statistical Package for the Social Sciences (SPSS) Statistics version 28 (IBM Corporation, Armonk, USA) was used for statistical analysis. For radical formation in porcine skin over time and depth-dependent autofluorescence in *ex vivo* skin, the statistical test of generalized estimating equation (GEE) was used. To identify outliers, the IQR method was used. Following the outlier test, data points identified as outliers were removed from the dataset to ensure the robustness of the analysis. The removal of outliers led to a slight decrease in the mean value of the data set. A *p*-value of less than 0.05 was considered as statistically significant.

## 3. Results

### 3.1. Radical scavenging activity of the formulations

The RPF values for the used cream formulations were analyzed with EPR spectroscopy (Table 2). The raw material EGCG exhibits the highest RPF of 139,000 ± 1,100 × $10^{14}$ radicals/mg compared to pure vitamin E which has an RPF of 18,000 ± 210 × $10^{14}$ radicals/mg. Both materials incorporated in PHYSIOGEL® at a concentration of 1 % exhibit 1 % of the actual RPF. The formulation CE Ferulic ® has the highest RPF value out of all formulations at 6,900 ± 220 $10^{14}$ radicals/mg, followed by 1 % green tea extract and 1 % vitamin E in PHYSIOGEL®. PHYSIOGEL® itself has no detectable radical protection factor and therefore was used as a placebo and vehicle for the active ingredients. EDDS dissolved in PHYSIOGEL® did not show any radical scavenging activity in this test method (Table 2). According to the RPF measurements, CE Ferulic shows a good radical protection.

### 3.2. Chelating power of EDDS

The copper-chelating power of EDTA, EDDS and EGCG is shown in Fig. 2a).

In comparison to EDTA, EDDS shows similar properties to quench the EPR signal. As expected, the antioxidant EGCG does not show a high chelating power, whereas EDTA and EDDS are known for its copper-chelating properties. To measure the chelating power of EDDS, copper was used in different concentrations (Fig. 2b). Here, the peak position and shape of the EPR spectra changes with the increasing number of ligands. A high chelating power refers to the ability of a ligand to bind metal ions.

### 3.3. Protection against radical formation after CS exposure + UV-A in porcine skin

To examine the efficacy of the used formulations against radical formation in porcine skin, we exposed these skin samples to cigarette smoke and UV-A irradiation and measured the radical formation with EPR spectroscopy. Fig. 3 shows the cumulative radical production in excised porcine skin after five minutes of exposure to the smoke induced by one cigarette. The cumulative radical concentrations in Table 3 were analyzed from the area under the curve in Fig. 3. The intensity of the PCA signal in excised porcine skin before exposure to CS + UV-A is shown in the supplementary material (Fig. S4). The cumulative radical production was not normalized to the nicotine concentration, because no correlation was found between nicotine concentration on skin after cigarette smoke exposure and the amount of induced radical production after cigarette smoke exposure and UV-A irradiation. However, a positive correlation was observed after exposure to cigarette smoke alone, indicating the sensitivity of the EPR method [3].

In this *ex vivo* EPR study, radical formation was the highest with the untreated skin (37.8 %) followed by PG, PG + EDDS and CE Ferulic. Only PG + vitamin E (22.0 %) and PG + EGCG (10.4 %) showed significant differences in radical formation compared to the untreated porcine skin. In addition, only PG + EGCG showed significant differences to the placebo formulation PG (Fig. 3).

**Table 2**
RPF values of used formulations.

| Formulation | RPF value [× $10^{14}$ radicals/mg] |
|---|---|
| Pure vitamin E | 18,000 ± 210 |
| Pure EGCG | 139,000 ± 1,100 |
| 1 % vitamin E in PHYSIOGEL® | 151 ± 4 |
| 1 % EGCG in PHYSIOGEL® | 1,360 ± 10 |
| 0.1 % EDDS in PHYSIOGEL® | < 20 |
| PHYSIOGEL® | < 20 |
| CE Ferulic ® | 6,900 ± 220 |

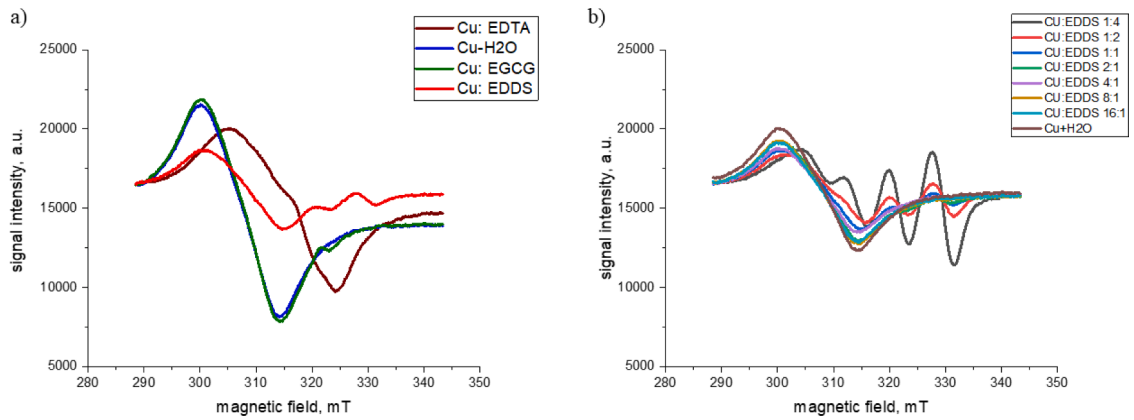


**Fig. 2.** (a) EPR spectra of different API with copper (1:1). (b) EPR spectra of EDDS with copper in different concentrations.

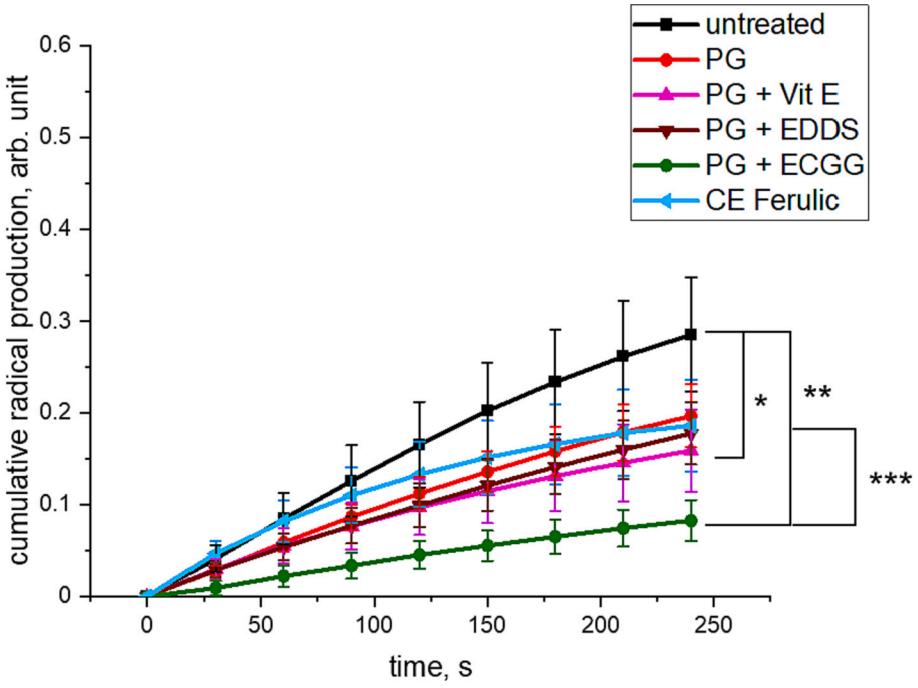


**Fig. 3.** Cumulative relative radical production (mean ± SEM) over time for untreated and treated excised porcine skin after cigarette smoke (CS) exposure in the smoking chamber for 5 min and UV-A irradiation *in situ* (9 J/cm$^2$), measured with EPR spectroscopy, n = 7 porcine ears, mean nicotine concentration: 160.1 ± 12.9 μg/cm$^2$, black squares – untreated; red circles – PHYSIOGEL ® (PG); pink triangles – PG + Vitamin E (Vit E); brown triangles – PG + EDDS; green circles – PG + EGCG, blue triangles – CE Ferulic; GEE was used for statistical analysis, *p ≤ 0.05, **p ≤ 0.01, ***p ≤ 0.001. (For interpretation of the references to colour in this figure legend, the reader is referred to the web version of this article.)

**Table 3**
Integral of cumulative radical formation until 240 s.

| Sample | Radical formation [a.u.] ± SEM |
|---|---|
| untreated | 38 ± 8 |
| 1 % vitamin E in PHYSIOGEL® | 22 ± 7 |
| 1 % EGCG in PHYSIOGEL® | 10 ± 3 |
| 0.1 % EDDS in PHYSIOGEL® | 23 ± 5 |
| PHYSIOGEL® | 26 ± 4 |
| CE Ferulic ® | 29 ± 8 |

### *3.4. Protection against overall oxidative stress ex vivo*

To validate the efficacy of the used formulation measured by EPR only against cigarette smoke of one cigarette and UV-A irradiation, the autofluorescence in excised porcine skin was investigated with the CRM after cigarette smoke exposure alone (Fig. 4). The AF intensity is the highest at the surface and decreases with increasing depth. All formulations, except 1 % vitamin E in PG, reduce the autofluorescence intensity compared to the untreated excised porcine skin.

In this study, 1 % EGCG in PG has performed best in reducing the effect of cigarette smoke in excised porcine skin. In addition, CE Ferulic did also decrease the autofluorescence by 50 % compared to the untreated skin on the surface.

After normalizing the AF intensity to the actual nicotine concentration on skin according to chapter 2.9 (Fig. 4b), both CE Ferulic and 1 % EGCG show the best result in protecting the porcine skin from additional oxidative stress due to CS exposure.

## 4. Discussion

In this study, we have investigated the efficacy of a number of anti-pollution products against cigarette smoke exposure.

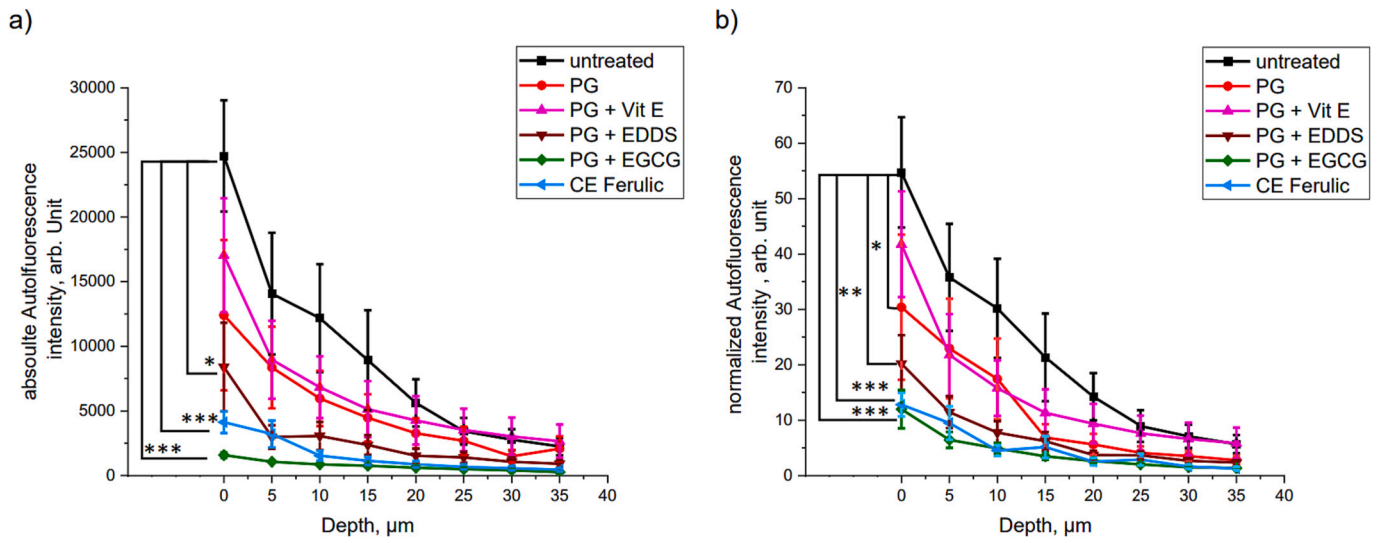


**Fig. 4.** Comparison of (a) absolute autofluorescence intensity and (b) autofluorescence intensity normalized to the nicotine concentration on porcine skin in untreated and treated excised porcine skin after 5 min CS exposure to five cigarettes, n = 7, mean nicotine concentration: 340 ± 26 µg/cm$^2$ measured with CRM; black squares – untreated, red circles – PG, pink triangles – PG + vitamin E, brown triangles – PG + EDDS, green circles – PG + EGCG, blue triangles – CE Ferulic, analyzed with GEE. (For interpretation of the references to colour in this figure legend, the reader is referred to the web version of this article.)

Cigarette smoke was chosen as a type of air pollutant due to its inclusion of all major air pollutants, such as particulate matter, polycyclic aromatic hydrocarbons, volatile organic compounds, and reactive oxygen species (ROS) [30].

In Europe, exposure to cigarette smoke in enclosed spaces is unavoidable. Indoor smoking is still permitted in some areas, resulting in daily exposure to smoke. In a previous study we found that the level of smoke exposure in the exposure chamber was equivalent to 8 h of exposure in a bar where indoor smoking is permitted, indicating that the experiment's exposure level reflects real-life conditions [3].

In this work, two different spectroscopic methods were used. EPR, which requires a marker substance and UV-A radiation as additional external stressor, for testing the efficacy of anti-pollution formulations *ex vivo*. CRM, which neither requires a marker substance, nor an additional stressor to measure autofluorescence after smoke exposure *ex vivo,* which correlates positively with the development of oxidative stress. RPF measurements and chelation performance were used to measure the efficacy of the formulations used *in tubo*.

The raw materials exhibit a high RPF alone, but require a vehicle to keep them in place on the skin. For instance, EGCG, a powder, presents challenges when applied topically. Therefore, it is important to use a vehicle for topical application and establish methods to measure the efficacy of the active ingredients in a formulation. Furthermore, it is crucial to test the various interactions between the vehicle and the active ingredient to evaluate the efficacy of the formulations [31]. Therefore, it is necessary to consider the concentrations of the active ingredient used in the formulations. The high RPF values were taken into account during the formulation process, and the concentrations of the raw materials were adjusted accordingly.

The commercial product CE Ferulic®, containing the vitamins C, E and ferulic acid, had the highest RPF value (6,900 ± 220 × $10^{14}$ radicals/mg) (Table 2). 1 % EGCG in PHYSIOGEL® showed a remarkably high value (1,360 ± 10 × $10^{14}$ radicals/mg) in the RPF measurements. Compared to the 1 % vitamin E formulation, the 1 % EGCG formulation has a tenfold higher RPF value. The RPF of the EDDS complex could not be measured, but the chelating power was measured. Compared to the well-known EDTA, EDDS showed a comparable and even better chelating power than EDTA. The antioxidant EGCG did not show a high chelating power (Fig. 2a).

Cigarette smoke induces free radicals in skin, which is enhanced by combination with UV-A irradiation, but this effect is not linear [3]. To counteract this effect, cream formulation which include antioxidants can be used. To date, there hasn't been enough research on the efficacy of these formulations. EPR spectroscopy and CRM represent methods that can close this gap. To counteract an imbalance in the redox homeostasis, antioxidants are often used in anti-pollution products. In this study, we compared three of them.

The 1 % EGCG formulation showed the best protection against oxidative stress induced by cigarette smoke and UV-A radiation (EPR) (Fig. 3) or cigarette smoke alone (CRM) (Fig. 4). As described in the literature, exposure to cigarette smoke leads to oxidative stress, which can also be induced by radical production [32].

EGCG is a catechin and the main component of the green tea plant, *Camellia sinensis*. It has the capacity to block redox-active transcription factors, chelate redox-active transition metal ions, and scavenge free radicals [33,34].

As mentioned above, the EGCG formulation performed best in both methods of investigating the efficacy of anti-pollution products. After application of the formulation and waiting for 30 min, this sample induced the lowest radical concentration in excised porcine skin (Fig. 3). In terms of AF, this was also reduced most by application of the cream (Fig. 4). EGCG is considered the most effective antioxidant for protecting excised skin from stressors such as exposure to cigarette smoke. This information is valuable for the development of skin care products, as some companies have previously used EGCG in their formulations. These methods can also be used to measure the effectiveness of EGCG in their products.

Vitamin E alone reduces radical formation in the skin (Fig. 3), but protection against AF by CRM has not been shown (Fig. 4). In the commercial product CE Ferulic®, vitamin E was combined with vitamin C and ferulic acid. CE Ferulic® performed very well in the CRM trials. Protection against oxidative stress induced AF caused by cigarette smoke was demonstrated. Surprisingly, it was not convincing in the EPR tests. With a high RPF of almost 7000 × $10^{14}$ radicals/mg, one would expect a high level of protection against radical formation in the skin. In comparison to untreated skin, no protective effect could be measured by EPR. PCA usually does not react with antioxidants, but in the case of high concentration, it does. The explanation is the scavenging of the marker directly by CE Ferulic. This can be demonstrated in the control measurements without smoke exposure and irradiation. The PCA decrease had been remarkable over time. For a linear progression to be measurable, the concentration would have to be increased accordingly.

Small antioxidant scavenging effects are corrected because all results are normalized to the control without induction of stress (Fig. S4).

The EPR method can be used to quantify the radicals generated. An additional stressor, in this case UV-A radiation, is required because the efficacy of the formulations cannot be compared precisely with cigarette smoke alone.

A disadvantage of the EPR method compared to CRM is that a spin probe is indispensable. As a result, the EPR method is limited when dealing with substances that have a high antioxidant capacity. The spin probe and its concentration must be adjusted according to the tested formulations. The nicotine concentration on the sample tested with the EPR method was smaller than on the sample subjected to the CRM method (Fig. S5). One of the reasons could be that two different batches of the same research cigarettes 1R6F was used. The study of Tran et al. showed that the same number of cigarettes lit does not equate to the same amount of nicotine in each sample [3]. As they are natural products, mainly tobacco plants, packed in cigarettes, they are difficult to standardize. Many factors including cigarette brand, size of smoking chamber and puff frequency can influence the amount of smoke exposure [35]. Therefore, it is very important to measure the exact cigarette smoke exposure for every sample.

In the CRM method, however, CE Ferulic® shows effective protection against oxidative stress caused by cigarette smoke. Vitamin E alone did not show a protective effect on porcine skin in the CRM method. A possible explanation for this may be that the pure vitamin E is rapidly depleted [36]. In combination with other antioxidants, the efficacy might still be guaranteed despite the stress induction [37].

Reactive oxygen species (ROS) induced by cigarette smoke can also be generated by metal ions, which are present in cigarette smoke [38]. To counteract ROS-induced oxidative stress, effective complexing and reducing agents can help to prevent this metal ion-induced peroxidation. In this study, EDDS was used. In contrast to the commonly used EDTA, it is biodegradable, which is very important today from a sustainability point of view. The experiments showed that the chelating power of EDDS is much higher than that of EDTA (Fig. 2a). Depending on the degree of complexation, the power is greater, see Fig. 2b. The protective effect of the EDDS formulation could only be demonstrated in the CRM. With EPR, induced radical production in EDDS-treated porcine skin was not significantly different from that in untreated skin. In CRM, the level of oxidative stress was significantly reduced compared to untreated skin. Although studies have shown that EDDS could prevent radical formation by complexing metal ions [19,39], this could not be demonstrated in the EPR experiments on skin. However, it is possible that it reduces the induction of oxidative stress through other pathways. In addition, UV-A radiation also induced more free radicals compared to cigarette smoke alone in skin [3] that EDDS could not scavenge. At the same time, it should be noted that the two methods deal with different aspects of stress induction assessment. The precise mechanisms underlying AF induction by oxidative stress remain elusive. It is possible that oxidation products within the stratum corneum will emit AF [40].

In the case of EDDS, this formulation cannot protect against the synergistic effect of UV-A radiation and cigarette smoke because UV-A radiation also induces radicals [41]. However, it is known that EDDS can only complex the metal ions, these ions usually can lead to further oxidative stress through radical formation [42]. The CRM method measures oxidative stress in a different way. The exact mechanisms are not clear yet. Here, it is measured selectively and in depth. In the case of EDDS, the metal ions present in cigarette smoke can be complexed by EDDS, thus reducing the induction of oxidative stress [43].

## 5. Conclusions

The aim of this study was to investigate the efficacy of formulations containing either antioxidants or a chelating agent and a commercial cream for the protective effect against the consequences of pollution in skin, here, using the example of cigarette smoke. Two different spectroscopic methods were used for this purpose: EPR spectroscopy was used to quantify radicals in skin, and CRM was used to investigate autofluorescence, which is related to oxidative stress in skin. In addition, CRM provides depth-dependent information. In both methods, the antioxidant EGCG was the most effective and forced the best protection against radicals or oxidative stress. The effect of the chelating agent EDDS should also not be neglected. Further experiments, especially *in vivo*, are needed to obtain a more precise picture of the protective effect of more products against environmental pollution and, in particular, cigarette smoke. Testing the effectiveness of formulations *in vivo* using autofluorescence is a major challenge due to the influence of various parameters, including the volunteers' antioxidant status, skin type, lifestyle, age, and gender. *In vivo* EPR is not sensitive enough for this purpose.

## CRediT authorship contribution statement

**Phuong Thao Tran:** . **Johannes Schleusener:** Validation, Writing – review & editing. **Burkhard Kleuser:** Methodology, Writing – review & editing. **Katinka Jung:** Data curation, Formal analysis, Writing – review & editing. **Martina C. Meinke:** Conceptualization, Funding acquisition, Project administration, Resources, Supervision, Writing – review & editing. **Silke B. Lohan:** Methodology, Project administration, Supervision, Writing – review & editing.

## Declaration of competing interest

The authors declare that they have no known competing financial interests or personal relationships that could have appeared to influence the work reported in this paper.

## Data availability

Data will be made available on request.

## Acknowledgments

This work was supported by the European Regional Development Fund within the program "Pro FIT—Programm zur Förderung von Forschung, Innovationen und Technologien", grant ID no: 10168708.

We like to thank Grit Sandig for technical support.

## Appendix A. Supplementary material

Supplementary data to this article can be found online at https://doi.org/10.1016/j.ejpb.2024.114211.

## References

[1] K.E. Kim, D. Cho, H.J. Park, Air pollution and skin diseases: Adverse effects of airborne particulate matter on various skin diseases, Life Sci. 152 (2016) 126–134.
[2] G. Bocheva, R.M. Slominski, A.T. Slominski, Environmental Air Pollutants Affecting Skin Functions with Systemic Implications, Int. J. Mol. Sci. 24 (2023) 10502.
[3] P.T. Tran, B. Beidoun, S.B. Lohan, R. Talbi, B. Kleuser, M. Seifert, et al., Establishment of a method to expose and measure pollution in excised porcine skin with electron paramagnetic resonance spectroscopy, Ecotoxicol. Environ. Saf. 247 (2022) 114258.
[4] F. Soleimani, S. Dobaradaran, G.E. De-la-Torre, T.C. Schmidt, R. Saeedi, Content of toxic components of cigarette, cigarette smoke vs cigarette butts: A comprehensive systematic review, Sci. Total Environ. 813 (2022) 152667.
[5] W.A. Pryor, Cigarette smoke radicals and the role of free radicals in chemical carcinogenicity, Environ. Health Perspect. 105 (1997) 875–882.
[6] S. Jeong, S.H. Lee, B.D. Park, Y. Wu, G. Man, M.-Q. Man, Comparison of the Efficacy of Atopalm® Multi-Lamellar Emulsion Cream and Physiogel® Intensive Cream in Improving Epidermal Permeability Barrier in Sensitive Skin, Dermatol. Ther. 6 (2016) 47–56.
[7] S. Bielfeldt, K. Jung, S. Laing, A. Moga, K.P. Wilhelm, Anti-pollution effects of two antioxidants and a chelator-Ex vivo electron spin resonance and in vivo cigarette smoke model assessments in human skin, Skin Res Technol. 27 (2021) 1092–1099.

[8] L. Wang, W. Lee, Y.R. Cui, G. Ahn, Y.-J. Jeon, Protective effect of green tea catechin against urban fine dust particle-induced skin aging by regulation of NF-κB, AP-1, and MAPKs signaling pathways, Environ. Pollut. 252 (2019) 1318–1324.
[9] Y.C. Boo, Can plant phenolic compounds protect the skin from airborne particulate matter? Antioxidants. 8 (2019) 379.
[10] A.R. Khalatbary, E. Khademi, The green tea polyphenolic catechin epigallocatechin gallate and neuroprotection, Nutr. Neurosci. 23 (2020) 281–294.
[11] R.J. Moore, K.G. Jackson, A.M. Minihane, Green tea (Camellia sinensis) catechins and vascular function, Br. J. Nutr. 102 (2009) 1790–1802.
[12] T. Doba, G.W. Burton, K.U. Ingold, Antioxidant and co-antioxidant activity of vitamin C. The effect of vitamin C, either alone or in the presence of vitamin E or a water-soluble vitamin E analogue, upon the peroxidation of aqueous multilamellar phospholipid liposomes. Biochimica et Biophysica Acta (BBA)-Lipids and Lipid, Metabolism 835 (1985) 298–303.
[13] M. Lopez-Torres, J.J. Thiele, Y. Shindo, D. Han, L. Packer, Topical application of α-tocopherol modulates the antioxidant network and diminishes ultraviolet-induced oxidative damage in murine skin, Br. J. Dermatol. 138 (1998) 207–215.
[14] J.E. Packer, T.F. Slater, R.L. Willson, Direct observation of a free radical interaction between vitamin E and vitamin C, Nature 278 (1979) 737–738.
[15] K. Zduńska, A. Dana, A. Kolodziejczak, H. Rotsztejn, Antioxidant Properties of Ferulic Acid and Its Possible Application, Skin Pharmacol. Physiol. 31 (2018) 332–336.
[16] G. Valacchi, C. Sticozzi, G. Belmonte, F. Cervellati, J. Demaude, N. Chen, et al., Vitamin C Compound Mixtures Prevent Ozone-Induced Oxidative Damage in Human Keratinocytes as Initial Assessment of Pollution Protection, PLoS One 10 (2015) e0131097.
[17] P.H.M. Wang, M. Agach, M. Libii, S. Chonez, S. Gregoire, B. Lee, J.T. Simonnet, An eco-friendly system for stabilization of retinol: a step towards attending performance with improved environmental respect, Int. J. Cosmet. Sci. (2023).
[18] K.R. Naqvi, J.M. Marsh, S. Godfrey, M.G. Davis, M.J. Flagler, J. Hao, V. Chechik, The role of chelants in controlling Cu(II)-induced radical chemistry in oxidative hair colouring products, Int. J. Cosmet. Sci. 35 (2013) 41–49.
[19] E.H. Fowles, B.C. Gilbert, M.R. Giles, A.C. Whitwood, The effects of chelating agents on radical generation in alkaline peroxide systems, and the relevance to substrate damage, Free Radic. Res. 41 (2007) 515–522.
[20] P.T. Tran, P. Tawornchat, B. Kleuser, S.B. Lohan, J. Schleusener, M.C. Meinke, M. E. Darvin, Red- and Near-Infrared-Excited Autofluorescence as a Marker for Acute Oxidative Stress in Skin Exposed to Cigarette Smoke Ex Vivo and In Vivo, Antioxidants. (2023) 12.
[21] Y. Sakai, S. Mori, M. Yanagimachi, T. Takahashi, K. Shibuya, A. Kumagai, et al., Inter-laboratory reproducibility and interchangeability of 3R4F and 1R6F reference cigarettes in mainstream smoke chemical analysis and toxicity assays, Contributions to Tobacco & Nicotine Research. 29 (2020) 119–135.
[22] Y. Zhang, N. Heinemann, F. Rademacher, M.E. Darvin, C. Raab, C.M. Keck, et al., Skin care product rich in antioxidants and anti-inflammatory natural compounds reduces itching and inflammation in the skin of atopic dermatitis patients, Antioxidants (basel) (2022) 11.
[23] B.L. Diffey, P.M. Farr, The normal range in diagnostic phototesting, Br. J. Dermatol. 120 (1989) 517–524.
[24] M.C. Meinke, S.F. Haag, S. Schanzer, N. Groth, I. Gersonde, J. Lademann, Radical protection by sunscreens in the infrared spectral range, Photochem. Photobiol. 87 (2011) 452–456.
[25] V.H.P. Infante, S.B. Lohan, S. Schanzer, P. Campos, J. Lademann, M.C. Meinke, Eco-friendly sunscreen formulation based on starches and PEG-75 lanolin increases the antioxidant capacity and the light scattering activity in the visible light, J Photochem Photobiol b. 222 (2021) 112264.
[26] P. Comba, T.W. Hambley, M.A. Hitchman, H. Stratemeier, Interpretation of electronic and EPR spectra of copper (II) amine complexes: a test of the MM-AOM method, Inorg. Chem. 34 (1995) 3903–3911.
[27] M. Darvin, M. Meinke, W. Sterry, J. Lademann, Optical methods for noninvasive determination of carotenoids in human and animal skin, J. Biomed. Opt. 18 (2013) 061230.
[28] C. Choe, J. Schleusener, J. Lademann, M.E. Darvin, Keratin-water-NMF interaction as a three layer model in the human stratum corneum using in vivo confocal Raman microscopy, Sci Rep. 7 (2017) 15900.
[29] G. Kourbaj, A. Gaiser, S. Bielfeldt, D. Lunter, Assessment of penetration and permeation of caffeine by confocal Raman spectroscopy in vivo and ex vivo by tape stripping, Int. J. Cosmet. Sci. 45 (2023) 14–28.
[30] F. Xu, S. Yan, M. Wu, F. Li, X. Xu, W. Song, et al., Ambient ozone pollution as a risk factor for skin disorders, Br. J. Dermatol. 165 (2011) 224–225.
[31] A. Lan, Y. Lui, J. Zuo, S.B. Lohan, S. Schanzer, S. Wiemann, et al., Methodology to reach full spectral photo-protection by selecting the best combination of physical filters and antioxidants, Cosmetics 10 (2023) 1.
[32] G. Percoco, A. Patatian, F. Eudier, M. Grisel, T. Bader, E. Lati, et al., Impact of cigarette smoke on physical-chemical and molecular proprieties of human skin in an ex vivo model, Exp. Dermatol. 30 (2021) 1610–1618.
[33] M.I. Prasanth, B.S. Sivamaruthi, C. Chaiyasut, T. Tencomnao, A review of the role of green tea (camellia sinensis) in antiphotoaging, stress resistance, neuroprotection, and autophagy, Nutrients 11 (2019) 474.
[34] J. Ye, Q. Li, Y. Zhang, Q. Su, Z. Feng, P. Huang, et al., ROS scavenging and immunoregulative EGCG@Cerium complex loaded in antibacterial polyethylene glycol-chitosan hydrogel dressing for skin wound healing, Acta Biomater. (2023).
[35] R. Goel, Z.T. Bitzer, S.M. Reilly, J. Foulds, J. Muscat, R.J. Elias, J.P. Richie Jr, Influence of smoking puff parameters and tobacco varieties on free radicals yields in cigarette mainstream smoke, Chem. Res. Toxicol. 31 (2018) 325–331.
[36] L. Packer, G. Valacchi, Antioxidants and the response of skin to oxidative stress: vitamin e as a key indicator, Skin Pharmacol. Appl. Skin Physiol. 15 (2002) 282–290.
[37] J.-Y. Lin, M.A. Selim, C.R. Shea, J.M. Grichnik, M.M. Omar, N.A. Monteiro-Riviere, S.R. Pinnell, UV photoprotection by combination topical antioxidants vitamin C and vitamin E, J. Am. Acad. Dermatol. 48 (2003) 866–874.
[38] R. Wolf, D. Wolf, V. Ruocco, Smoking and the skin, radically speaking 1, Clin. Dermatol. 16 (1998) 633–639.
[39] A. Rastogi, S.R. Al-Abed, D.D. Dionysiou, Effect of inorganic, synthetic and naturally occurring chelating agents on Fe (II) mediated advanced oxidation of chlorophenols, Water Res. 43 (2009) 684–694.
[40] A.N. Semenov, B.P. Yakimov, A.A. Rubekina, D.A. Gorin, V.P. Drachev, M. P. Zarubin, et al., The oxidation-induced autofluorescence hypothesis: Red edge excitation and implications for metabolic imaging, Molecules 25 (2020) 1863.
[41] K. Burke, H. Wei, Synergistic damage by UVA radiation and pollutants, Toxicol. Ind. Health 25 (2009) 219–224.
[42] R. Kohen, Skin antioxidants: their role in aging and in oxidative stress—new approaches for their evaluation, Biomed. Pharmacother. 53 (1999) 181–192.
[43] L. Chen, T. Liu, M.a. Ca, Metal complexation and biodegradation of EDTA and S, S-EDDS: a density functional theory study, Chem. A Eur. J. 114 (2010) 443–454.

Table S1 Ingredients list of investigated formulations

| Physiogel ® | CE Ferulic ® |
|---|---|
| Aqua, Butyrospermum Parkii Butter, Pentylene Glycol, Glycerin, Behenyl Alcohol, Niacinamide, Caprylic/Capric Triglyceride, Panthenol, Hydrogenated Phosphatidylcholine, Behenic Acid, Isostearyl Isostearate, Hydroxyacetophenone, Polyacrylate Crosspolymer-6, T-Butyl Alcohol. | Aqua, ethoxydiglycol, glycerin, propylene glycol, laureth-23, phenoxyethanol, triethanolamine, panthenol, sodium hyaluronate, main ingredients: L Ascorbic Acid 15.0 %, Alpha Tocopherol 1.0 %, Ferulic Acid 0.5 %. |

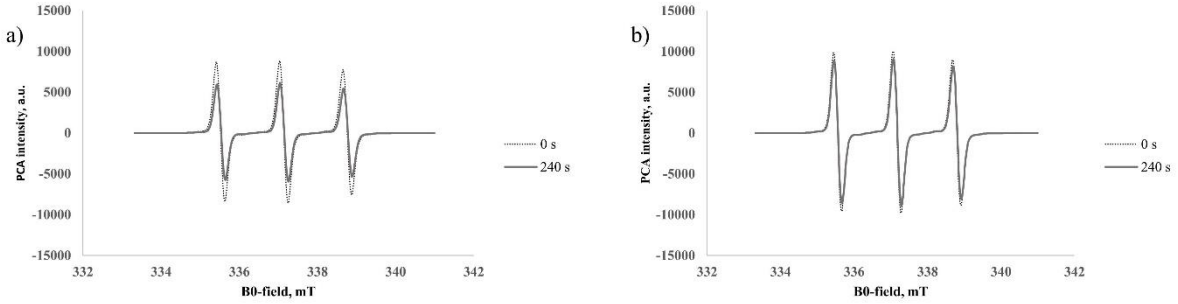


Figure S2 Exemplary native EPR spectra of the spin probe PCA. a) 1.5 mM PCA in untreated excised porcine skin after Cigarette smoke (CS) exposure and UV-A irradiation at 365 nm (18 mW/cm$^2$). The dotted spectrum shows the PCA intensity at 0 s. The grey spectrum shows the PCA intensity at 240 s. b) 1.5 mM PCA in pre-treated excised porcine skin with PG + 1 % EGCG formulation after CS exposure + UV-A irradiation. The dotted spectrum shows the PCA intensity at 0 s. The grey spectrum shows the PCA intensity at 240 s.
PCA reacts with radicals and becomes less EPR active as the number of radicals increases, resulting in a decrease in PCA intensity. The decrease in PCA intensity was greater in the untreated skin compared to the pretreated skin, indicating that the cream protected against radical formation in the skin.

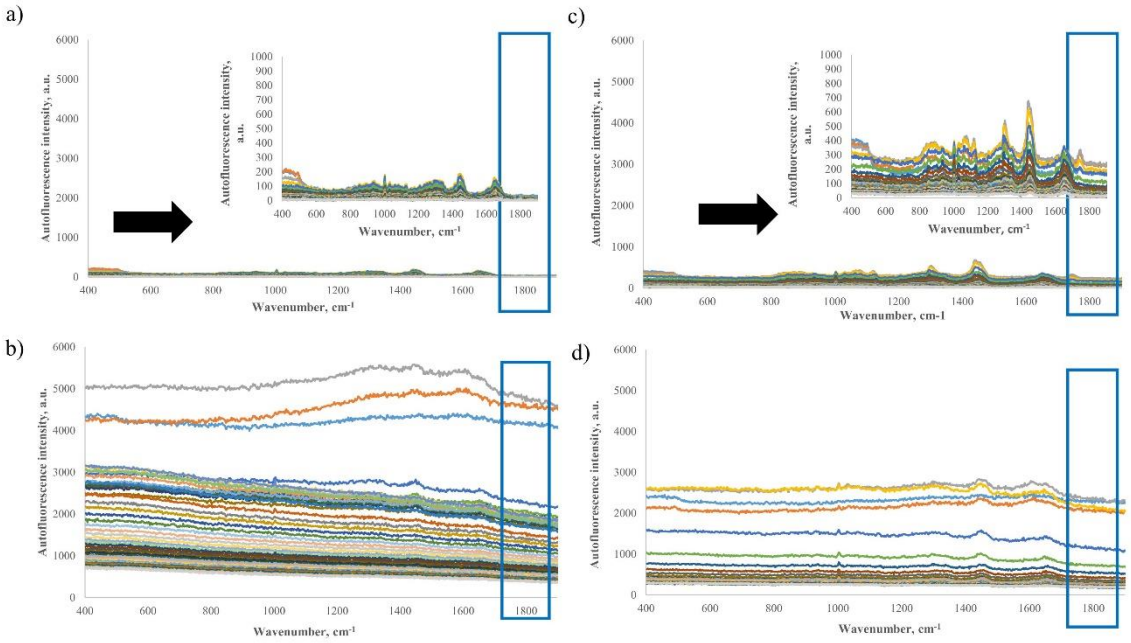


Figure S3 Exemplary native CRM spectra of a) untreated excised porcine skin before cigarette smoke exposure (control) b) untreated excised porcine skin after cigarette smoke exposure c) pretreated excised porcine skin with PG + 1 % EGCG before cigarette smoke exposure (control) d) pretreated excised porcine skin with PG + 1 % EGCG after cigarette smoke exposure

The blue box indicates the analyzed autofluorescence at 1800 $cm^{-1}$. The black arrows lead to the zoomed in spectrum of each sample. An increase in autofluorescence intensity indicates that the skin was subjected to oxidative stress. The increase in autofluorescence was lower in the pretreated skin compared to the untreated skin, meaning that the treatment protected the skin from oxidative stress induced by cigarette smoke exposure.

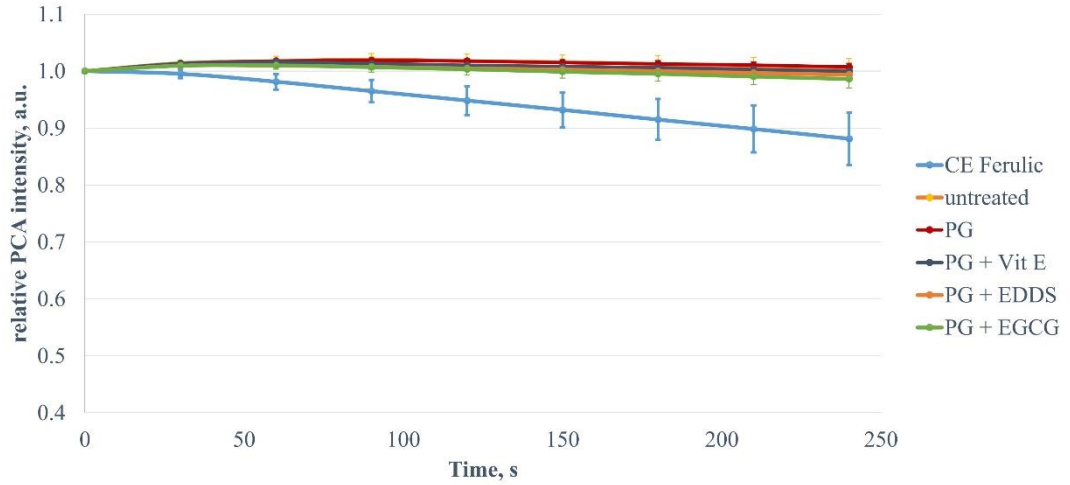


Figure S4 Relative signal intensity of PCA(1.5 mM) in excised porcine skin without smoke exposure over time (n=7). The relative PCA intensity in excised porcine skin pretreated with CE Ferulic ® decreases over time without induction of an external stressor, indicating that the formulation itself reacts with spin probe alone. Hence, the EPR measurement of the protective effect of CE Ferulic has been influenced by its high content in antioxidants.

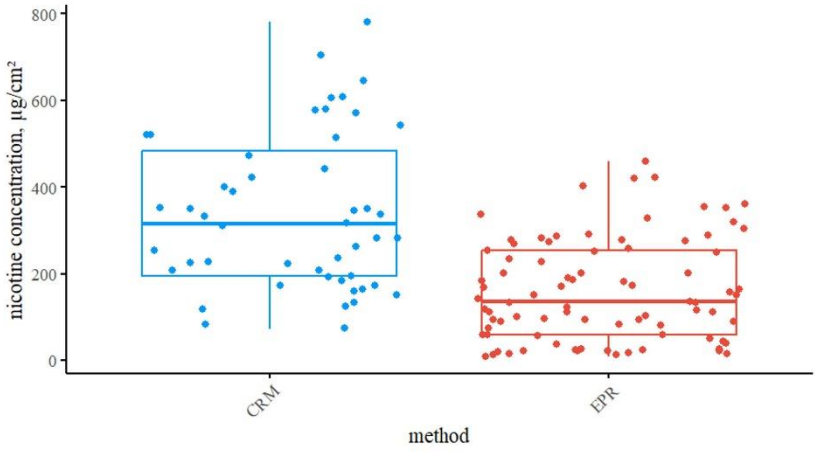


Figure S5 Nicotine concentration per µg/cm² extracted from the filter paper placed next to each sample for each method. The blue box plot resemble all measured nicotine concentrations of all CRM samples obtained from seven ears and six groups (n= 42). The red box plot resemblance all measured nicotine concentrations of all EPR samples obtained from seven ears and six groups and its duplicates (n=84).

# 3. Discussion

## 3.1 Methods to expose and measure the effect of cigarette smoke on skin

Air pollution leads to diseases and stress, not only in our lungs but also in our skin [68, 69]. In vitro models have been used to measure the cellular and molecular mechanisms behind air pollution and cigarette smoke exposure [115, 116]. The impact of air pollution on skin was measured by considering the alteration and modulation of the amount of melanin [20, 154]. Furthermore, EPR was used to investigate the free radicals of mainstream and sidestream smoke. Previous studies have demonstrated the induction of free radicals by cigarette smoke [155, 156]. However, this effect measured in skin has not been correlated to the amount of exposure so far. Furthermore, an additional stressor like UV irradiation was required to measure the free radicals in the skin following exposure to cigarette smoke [73].

The aim of this thesis was to establish an EPR method for measuring free radicals in excised skin after cigarette smoke exposure. Therefore, in this work an additional ex vivo method (CRM) was used to measure the effect of oxidative stress following exposure to cigarette smoke that could be transferred to an in vivo setting.

To measure the effect of cigarette smoke exposure on the skin, it was necessary to establish the method of exposure. Several questions need to be answered: How should the exposure to cigarette smoke be carried out? Should real-life conditions be simulated? How can the actual amount of exposure on the skin be measured?

The following chapter will discuss the method of exposure and the comparison of two different chambers.

In the first study, the bigger chamber with a volume of 3800 $cm^3$ was built to fit a participant's forearm to perform in vivo investigations. The smaller chamber with a volume of 520 $cm^3$ was built for ex vivo measurements of excised skin (Figure 8). The chambers were originally equipped with various vents to investigate the effects of different air pollutants, including cigarette smoke and ozone. However, the initial experiments on controlling cigarette smoke showed that establishing a new setup for exposing skin explants to air pollution was more time-consuming than expected. The impact of the parameter of burning cigarettes inside the exposure chamber will be discussed in chapter 3.1.2. Therefore, the main focus of this thesis was cigarette smoke as a model for air pollution [3].

Both chambers were used effectively to expose skin to cigarette smoke in a reproducible manner. Here, the results of two laboratories using different chambers are comparable. Our working group used both the big and small chamber for EPR studies. The cooperation partner GematriaTestLab used the small chamber for their EPR studies. Both EPR studies were executed with two different EPR machines. This was made possible due to the quantification of the amount of smoke on the skin directly. Quantifying the amount of exposure is crucial as it directly affects the skin's reaction. It also helps to compare and discuss the results [3].

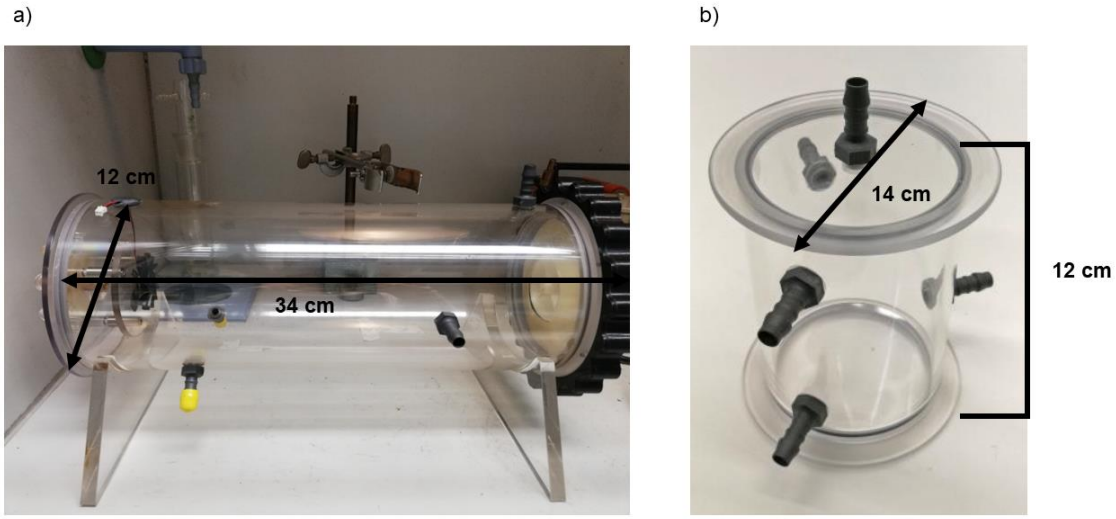


**Figure 8a) big exposure chamber for ex and in vivo studies b) small exposure chamber for ex vivo studies.**

One caveat was that the bigger chamber requires the burning of more cigarettes to exceed the threshold for measuring induced radicals. Specifically, five cigarettes must be burnt in the bigger chamber compared to one cigarette in the smaller chamber to achieve high levels of cigarette smoke. In the future, smaller chambers can be used to expose cigarette smoke directly on skin that are easier to handle. It is important to note that actual measurement of the amount of exposure is necessary as well.

Different chambers have been tested in the past to measure the effect of cigarettes on the skin. The study by Pelle et al. used a cylindrical chamber that was connected to a rubber sleeve where the arm of the participant was put through [157]. The chamber used in this study is comparable with the big chamber used in this work, as the size of chamber in Pelle et. al's work has a length of 41 cm and a diameter of 11cm. Here, one cigarette was burnt for five minutes twice. For the analysis, lipid peroxidation was measured in the forearm. Exact levels of exposure were not defined [157]. Another study was carried out

by Bielfeldt et al., where a small chamber of 200 mL volume was placed on the volar forearm or the back of the participant. In that study, one cigarette was burnt for five minutes. No exact levels of exposure were defined in that study as well. The samples were also analyzed for traces of lipid peroxidation. Here, MDA and squalene monohydroperoxide were used as markers for oxidative stress [73]. In both studies, a vacuum pump was used to draw the cigarette smoke over the sample area to mimic real-life conditions, but exact amounts of cigarette smoke exposure were not determined. However, it is important to determine the precise amount of cigarette smoke exposure, as the components of the smoke in the main and side streams have the potential to form radicals. The dose dependency of the effect of cigarette smoke should not be neglected either.

The following section discusses the properties of cigarette smoke and what impact it has on different exposure and measurement methods and their effect on skin.

### 3.1.1 Cigarette smoke as model for air pollution

Cigarette smoke was chosen as a model pollutant in this work. Everyone encounters cigarette smoke in their daily lives, and it is everywhere, even on indoor surfaces [71, 158]. It is difficult to totally protect ourselves from smoke exposure. Studies have shown that even in neonatal intensive care units, traces of nicotine from thirdhand smoke can be found and that even infants in intensive care metabolize this component of thirdhand smoke [159].

The chemical profile of cigarette smoke resembles different components such as PAHs that are also found in diesel exhaust for example [71, 81]. Compared to diesel exhaust, cigarette smoke has a similar PM 2.5 concentration as well [160]. Cigarette smoke was used a model for air pollution because it was easier to handle and easier to obtain and, initially, easier to dose.

Cigarette smoke extract (CSE) has been widely used in studies in the past, especially in in vitro models [115, 116]. As mentioned in section (1.3.1), it does not mimic real-life conditions very well. Its advantage is that it is easier to dose and handle than exposure to cigarette smoke in a chamber. Prieux et al. described its main disadvantage as being that the CSE mainly contains the particulate phase of the cigarette and excludes the main constituents of cigarette smoke. In addition, there is a difference between fresh and aged CSE, as the presence of short-lived radicals decreases [24].

To obtain an objective evaluation of the direct impact of cigarette smoke on the skin, it is advantageous to use a smoke chamber where the supply of cigarette smoke can be regulated and measured.

### 3.1.2 The impact of the parameters in the exposure chamber on the effect on skin

The choice of cigarette brand affects the concentration of pollutants in the chamber. Different brands use different blends of tobacco leaves in their cigarettes [76]. As tobacco leaves are a natural product, it is difficult to standardize each individual cigarette, even if it contains the same blend. The variation of different brands is caused by different filter systems, changing ventilation systems, and the design of the cigarette itself [76, 78, 113].

Another parameter, that could influence the concentration of cigarette smoke, is the puff frequency and volume. Studies have shown that these parameters influence the concentration of alkaloids, such as nicotine [78, 161].

The size of the exposure chamber is also important. In the presented studies, two chambers of different sizes were compared. In the smaller chamber, only one cigarette burn was enough to induce radical production in excised skin. In the bigger chamber, five cigarettes were needed to see comparable results. In this study, the filter of a cigarette was cut off to allow more mainstream smoke to enter the exposure chamber, resulting in higher radical production in excised porcine skin. Zhao et al. described that the filter eliminated 52.0 % of the PM mass, 17.1 % of the particle-phase ROS, and a small reduction in gas-phase ROS was also determined which is in alignment with this work's findings [162].

Comparable results were obtained using both big and small chambers with the EPR method. To measure significant differences between untreated skin and skin after CS exposure, a threshold of 140 µg nicotine per cm² was needed to be exceeded. This amount is equivalent to smoking five cigarettes in total in this setup. To observe an increase in autofluorescence in excised skin, only 0.25 cigarettes inside the big chamber were required when measuring the AF intensities. The threshold of 33 µg nicotine per cm² was lower compared to the exceeding threshold needed to measure free radicals [3, 9].

To expose skin samples to cigarette smoke in a reproducible way, a new method had to be developed using the new exposure chambers. A vacuum pump was connected to the chamber to allow the cigarette smoke to flow throughout the chamber in a reproducible manner. To monitor the level of exposure, a particle-measuring device was connected to

the chamber through one of the vents. Unfortunately, one burning cigarette maxed out the particle monitor at 400 mg/m³.

Therefore, different valves were installed in this experimental setup to regulate the amount of smoke inside the exposure chamber, so that the particle monitor would not max out. In addition, a wash bottle was installed between the exposure chamber and the pump in order for the smoke to pass through the bottle. The water-soluble or ethanol-soluble constituents of the CS would remain inside the solution of the wash bottle after passing it. The particle concentration inside the chamber after CS exposure was correlated to the amount of nicotine that remained inside the wash bottle.

In this study, nicotine was used as a surrogate parameter. It has been already described as a potential marker for environmental tobacco smoke (ETS) in literature because it is unique to cigarette smoke. In addition, nicotine is one of the major constituents of cigarette smoke. Furthermore, nicotine can be found in both particulate and gaseous phases and on top, is soluble in aqueous and ethanolic solutions. Therefore, it is easy detectable inside the wash bottle containing either water or ethanol. Most importantly, the sensitivity of the analysis of pure nicotine is high, even at low concentrations [78].

The study of Wang et al. has shown a positive correlation between the amount of PM2.5 with the amounts of tar and nicotine found in cigarettes [163]. Therefore, nicotine was an ideal surrogate parameter for this study.

Another study has confirmed this works findings by showing a dose-dependent relationship between the number of smoked cigarettes and inflammatory responses in human participants. Kuschner et al. was able to show that concentrations of neutrophils, macrophages, IL-1 beta, and IL-8 that are responsible for inflammatory responses inside the body increased with the number of cigarettes smoked [164].

This shows that it is important to take the concentration of exposure, smoking intensity and frequency for every investigation into account because these factors have an influence on the effect of cigarette smoke on skin. In this work, a filter paper was positioned next to each skin sample at exposure to analyze the actual amount of exposure by quantifying the nicotine concentration on the skin. Here, a dose-depended relationship was established between the actual concentration of nicotine on the skin and the radical production that was measured in skin after exposure [3]. Compared to other studies, this method allows for a precise measurement and correlation of cigarette smoke exposure and the effect of it with each sample. The quantification of cigarette smoke in addition to the measurements sets it apart from other methods and accurately correlates the impact on the skin.

## 3.2 Methods to measure the effect of cigarette smoke in skin

### 3.2.1 Electron Paramagnetic Resonance (EPR) Spectroscopy

Previous pre-clinical and clinical studies have shown that air pollution and cigarette smoke, for example, can induce reactive oxygen species (ROS) or inflammation, which can directly or indirectly cause skin hyperpigmentation [165]. The EPR technique is appropriate for identifying radical formation in skin. Initially, radical generation was examined and measured in excised porcine skin, followed by an analysis of the oxidative status after smoke exposure. The decay of the spin probe PCA was utilized for indication. Owing to its five-membered ring structure, PCA is largely unaffected to get reduced by antioxidants [130]. This fact is important for further research relating to the effectiveness of anti-pollution products. In addition, TEMPO was employed to gauge antioxidative status. As illustrated in the in vivo study by Lohan et al., TEMPO was used to analyze the antioxidative status of active smokers. In this instance, the decay of TEMPO was indicative of the endogenous antioxidant status of the skin area under investigation [166].

By using two different X-band EPR spectroscopy devices, the effect of two stressors cigarette smoke and UVA irradiation on excised porcine skin was analyzed in this work. The main stressor used in these investigations was cigarette smoke. Cigarette smoke is known to generate free radicals in its particulate and gas phase [85]. In excised porcine skin, cigarette smoke alone was able to induce radicals. However, when combined with UVA irradiation in situ at 18 mW/cm², more radicals are induced in the skin than after cigarette smoke exposure alone. This is due to the synergistic effect when UVA irradiation and cigarette smoke are combined. UVA irradiation at 18 mW/cm² alone induces more radicals than cigarette smoke alone, but the amount was not higher than the combination of both stressors. With both EPR devices MS 5000 and MS 300, it was possible to measure the effect of cigarette smoke exposure in excised porcine skin. For the MS 5000, the spin probe PCA was used and for the MS 300; both the spin probes PCA and TEMPO were used as spin probe. Both methods could show that first; the induced radical production in the skin was significantly higher after cigarette smoke exposure than before cigarette smoke exposure. The antioxidative status of the porcine skin described by the TEMPO levels was reduced by cigarette smoke exposure alone, indicating that endogenous antioxidants in the skin were depleted due to the stress [3].

The use of spin probe TEMPO was not pursued in further investigations due to its potential to react with the antioxidants present in the anti-pollution formulation.

It has already been mentioned that the EPR method with PCA has already been established with UV radiation as a stressor [167-169]. To have a positive control for the EPR measurements, UV irradiation was also used in this work. Compared to cigarette smoke alone, UVA irradiation induced more radicals in excised porcine skin (Figure 9) [3].

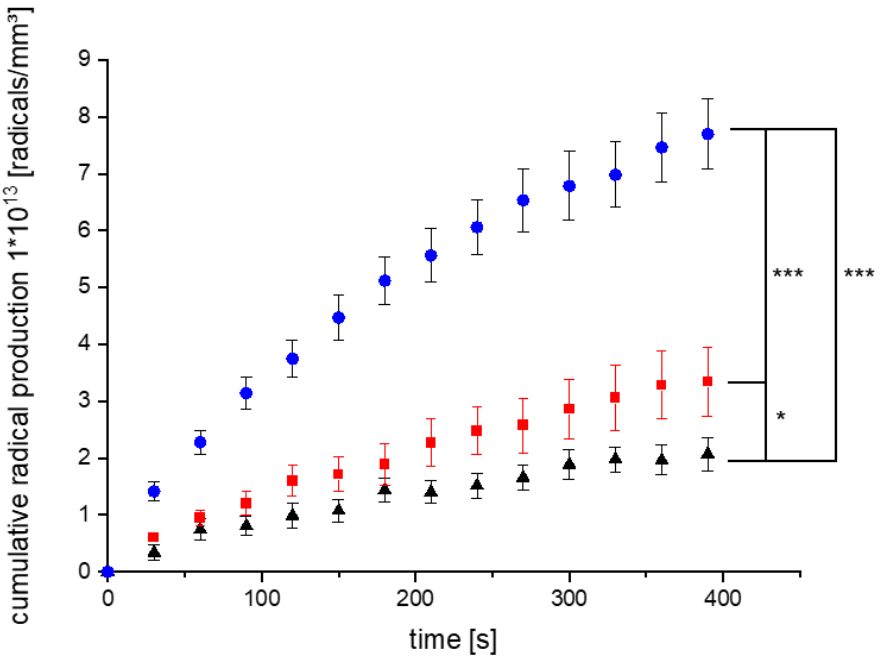


**Figure 9 cumulative radical production in excised porcine skin after induction of different stressors.** Black triangles: cigarette smoke exposure, red squares: UVA irradiation at 18 mW/cm² (365 nm), blue circles: cigarette smoke exposure and UVA irradiation, ***p ≤ 0.001, *p ≤ 0.05 [3]

UVA radiation is known to be one of the main initiators of ROS generation in the skin [49]. On a molecular level, Photons must be absorbed by endogenous photosensitizers such as porphyrin and cytochromes for ROS to be generated. ROS are produced as a result of the excited photosensitizer's reaction with oxygen (see chapter 1.2.4.3).

Pollution, especially cigarette smoke consists of thousands of different components that can cause oxidative stress through radical induction. Important components are particulate matter, PAHs, nitrogen oxides, and radicals in gas and particulate phase as well. Gas-phase radicals have a short half-life; therefore, they barely pass through the cigarette to be exposed to the environment. Radicals from the particulate phase are long-lived but therefore more stable (see chapter 1.2.4.2). Consequently, free radicals with long half-lives and promising diffusion times have the potential to propagate their damaging effects. Numerous redox-sensitive signaling pathways that regulate physiological responses, such as inflammation, are triggered by ROS and RNS. On the other side, inflammation can lead to the generation of endogenous oxidative species. Thus, the oxidative damage caused

by exposure to cigarette smoke is likely to be multifaceted, involving both the oxidative potential of cigarette smoke and unintended biological responses [170].

When combined, the radical production exceeded the production after UVA irradiation and CS exposure alone. In the study by Ibuki et al., 8-OHdG was used as a marker for DNA damage caused by oxidative stress. The effect of UVA irradiation and Benz[a]pyrene (B[a]P), one of the components of cigarette smoke, on human skin fibroblasts were investigated [171]. The level of 8-OHdG was higher after UVA irradiation than after B[a]P exposure. The combination resulted in a higher level of 8-OHdG than either stressor alone, confirming our findings that this is based on synergistic effects. Synergistic effects have been shown not only in this work but also in several other studies. Pavlou et al. showed that the combination of both cigarette smoke and UV irradiation had an effect on murine skin. The in vivo data showed that it increased levels of erythema values, squamous cell carcinoma, and TEWL [172]. Grenier et al. have investigated the synergistic effects of UV irradiation and cigarette smoke on primary human keratinocytes. Cell viability decreased more drastically when both stressors were combined [173].

Comparing different results remains challenging due to the use of different techniques. Additionally, the mentioned experiments did not always measure exposure accurately, as cigarette smoke concentrations can vary between brands, puff protocols, and exposure chamber sizes. Nonetheless, most previous studies have detected a correlation between exposure to cigarette smoke and an increase in oxidative stress in skin. Our study not only correlated the nicotine concentration inside the chamber with the actual particle concentration per $m^3$, but also linked the amount of cigarette smoke exposure to the actual radical production in excised porcine skin. Our method is more accurate as it allows for quantification of exposure on each sample and is a useful tool for checking the reproducibility of the method.

### 3.2.2 Autofluorescence measurements using CRM

The present study investigates the impact of cigarette smoke on the skin, using EPR as the analytical method. This approach enables the analysis and quantification of radical production in the skin. Nevertheless, other methods are also available to explore the effects of cigarette smoke on the skin. The transfer of the ex vivo EPR method to in vivo conditions was considered, but an alternative approach had to be sought due to the EPR method's failure to produce reliable results under in vivo conditions.

The transition from ex vivo to in vivo was successful under varying conditions such as the investigation of radical formation in human skin after UV irradiation [174], where radical production was studied following exposure to sunlight. The light had to be exposed in situ

to obtain reliable results. However, replicating the same experimental setup for cigarette smoke exposure was challenging. The need for an exposure chamber made in situ smoke exposure unsuitable, thereby making it impossible to precisely measure radical production on the same skin area. In addition, the low sensitivity of the L-band EPR made it difficult to transfer this method to in vivo conditions.

Furthermore, cigarette smoke alone did not indicate an increase in radical production measured by the L-band EPR machine. Additional UVA irradiation was necessary for that effect to occur. As presented in this thesis, the combination of cigarette smoke exposure and UVA irradiation resulted in a synergistic increase in radical production in the skin. However, this combination was still insufficient to observe an increase in radical production in vivo by EPR. In summary, the in vivo EPR approach exhibited low sensitivity in monitoring cigarette smoke's impact on the skin. Therefore, it was imperative to develop a novel technique applicable to in vivo conditions. Previously, Confocal Raman Microspectroscopy (CRM) was employed to assess the oxidative state of skin. Here, the Raman bands of carotenoids were investigated [175].

In previous research, CRM has been utilized to quantify naturally occurring and topically administered carotenoids within the stratum corneum in vivo in a depth-dependent manner. As stated in section (1.2.2), carotenoid levels have the potential to reflect an individual's antioxidative status [174, 176].

Our study used a novel evaluation that focused on the analysis of autofluorescence in the background rather than Raman bands. Autofluorescence (AF) of the skin has previously been documented at an excitation wavelength of 785 nm, with minimal levels attributed to melanin. In addition, the oxidation of SC components was described [177, 178].

Exposure to cigarette smoke resulted in an elevation of AF in excised porcine skin. Our findings demonstrate that the AF increase is dependent on depth. It should be noted that cigarette smoke alone was adequate to increase the AF value of excised porcine skin. It has been confirmed that the constituents of cigarette smoke are not the cause of increased AF, but rather the induction of skin oxidation resulting from exposure to CS. Neither nicotine alone nor cigarette smoke captured on a glass slide resulted in increased AF [9]. With the EPR method comparable results were shown as CS exposure led to induction of radicals in excised porcine skin [3]. No extra stressor was necessary. Furthermore, this AF measurement technique eliminates the necessity for a marker substance, enabling direct measurement of the impact of cigarette smoke exposure on the skin.

According to recent studies, the skin may contain fluorophores, which are primarily proteins such as keratin, collagen, and elastin, as well as other substances such as

melanin and porphyrins. These fluorophores can be used for a variety of diagnostic purposes, such as skin aging [177, 179]. At 785 nm, it has been demonstrated that porphyrins are capable of emitting AF. Their role in metabolic processes is significant. Exposure to cigarette smoke that induces oxidative stress may result in an elevation of AF [177, 180, 181].

Another marker of oxidative stress in skin is advanced glycation end products (AGE) that are responsible for metabolic by-products associated with oxidative stress. Studies have attempted to measure the AF spectra of skin to estimate AGE levels [182, 183]. For example, they analyzed the correlation between Raman bands and AF in human skin in the NIR range. They were able to detect changes in the Raman spectrum. Although this work focused on AF at 1800 $cm^{-1}$, a change was also detected at other wave numbers (see Figure 10). This could be related to AGE.

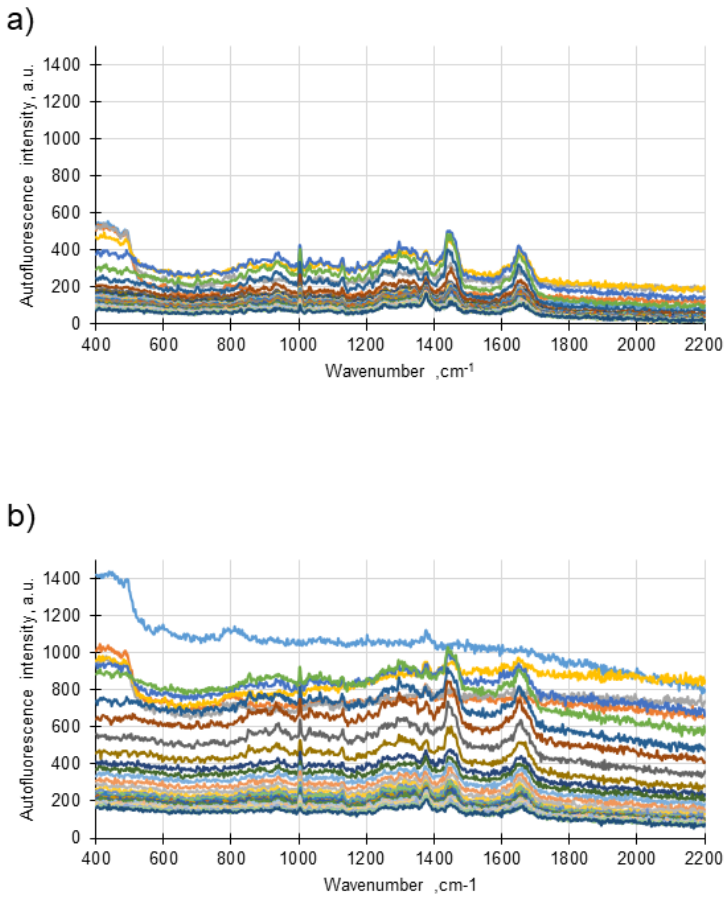


**Figure 10 Exemplary Raman spectra at different depths with its autofluorescence background of a)** of non-exposed excised porcine skin **b)** of excised porcine skin after exposure to one cigarette.

It is important to note that there is a limited number of skin fluorophores capable of absorbing light in the red and near-infrared spectrums. This results in minimal reabsorption

and lead to a high degree of accuracy in the detection of red and near-infrared quanta at different depths [184].

Interestingly, the AF intensities after cigarette smoke exposure were higher in excised porcine skin compared to the AF intensities after UVA irradiation (Figure 11). In contrast, the EPR method shows the opposite trend (Figure 9).

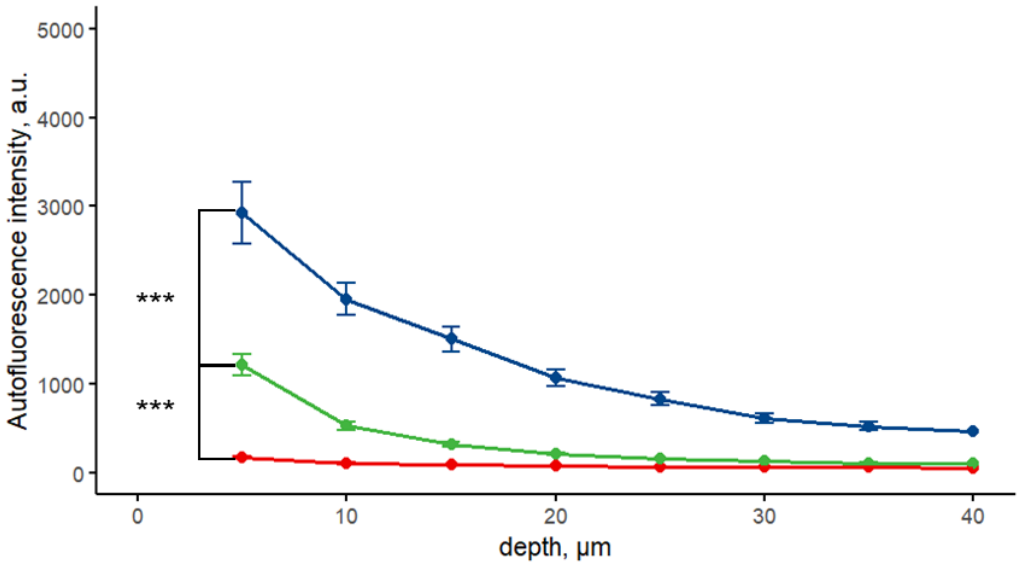


**Figure 11 depth-dependent AF intensities after CS exposure compared to after UVA irradiation at 2 MED.** Control (red), UVA irradiation at 2 MED (green), 5 cigarettes after cleaning process (blue), ***p ≤ 0.001.

A possible explanation for this effect could be that the increase of AF includes oxidated substances which are not only radical species or caused by radical species. UVA is known to produce high amounts of radicals in skin, whereas cigarette smoke can cause damage through different pathways and not only radicals (Figure 3). The EPR device is only able to quantify radicals which explains a higher radical production in excised skin after UVA irradiation than after cigarette smoke exposure alone.

With the CRM technique, the effect of cigarette smoke exposure on excised porcine skin has been investigated using 0.25, 0.5, 1, and 5 cigarettes. Here, no significant ($p \leq 0.1$) dose-response relationship between nicotine concentration and the measured AF in excised skin could be shown [9]. In comparison, the EPR method revealed a dose-dependency correlation ($p \leq 0.05$) between the nicotine concentration and the induced radicals in excised porcine skin [3].

Nevertheless, the CRM method was able to measure oxidative stress-induced AF that not only included the induction of radicals in excised porcine skin. It therefore provides an alternative method for measuring the effect of cigarette smoke ex and in vivo, whereas the transfer from ex vivo to in vivo failed with the EPR technique.

### 3.2.3 Ex vivo vs in vivo

This study has established two methods for assessing the impact of cigarette smoke on excised porcine skin. Porcine skin is a suitable skin model for analyzing these effects. However, conducting research on human skin in vivo is considered the most reliable approach. Therefore, the AF method using the CRM as an in vivo method was developed to assess the effects of cigarette smoke exposure on human skin.

Here, the big exposure chamber was used to conduct in vivo experiments. The forearms of ten participants were measured before and after being exposed to cigarette smoke. The degree of exposure had to be adjusted to ensure that the concentration of smoke was sufficient to increase the level of AF. In this in vivo study, the smoke of five cigarettes was necessary to elevate AF levels, whereas only 0.25 cigarettes were required in the ex vivo study on porcine skin to increase AF levels compared to non-exposed skin. The outcomes suggest that cigarette smoke can trigger oxidative stress by elevating AF levels in human skin in vivo. Despite the removal of cigarette smoke debris from the skin, increased AF levels were detected, indicating that the impact of cigarette smoke could be measured in deeper SC layers (Figure 12).

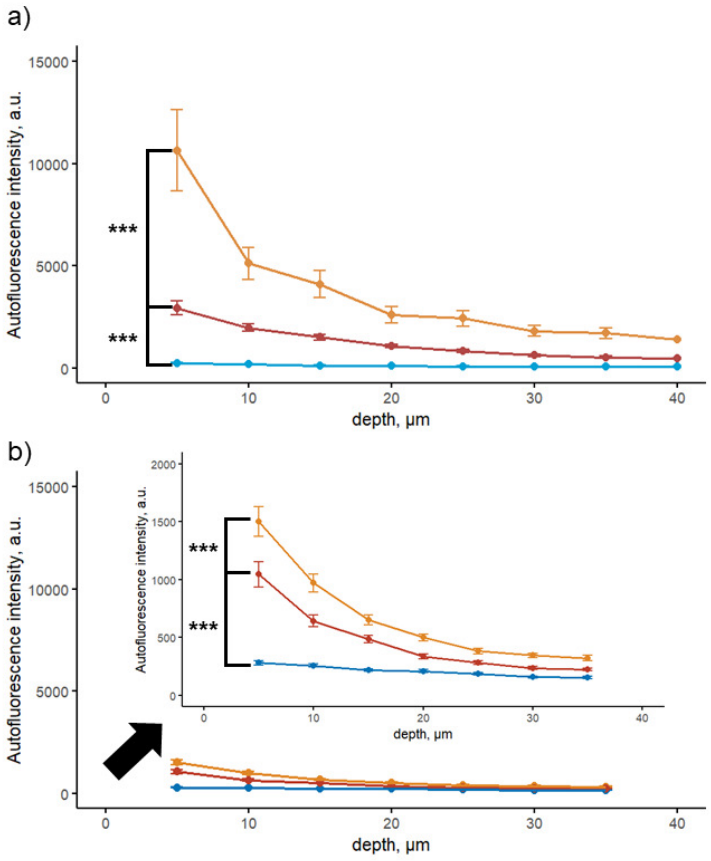


**Figure 12 a) depth-dependent AF intensities of in vivo human skin after five cigarettes** at 45.5 ± 9.3 µg/cm² and **b) depth-dependent AF intensities of ex vivo porcine skin after five cigarettes** at 180 ± 29.8 µg/cm², yellow = smoked, red = cleaned, blue = control, ***p ≤ 0.001

The concentration of nicotine on the filter paper after five cigarettes was lower in the in vivo studies than in the ex vivo studies because the chamber system was not completely closed with the arm inside. The pressure generated was not similar to that of a chamber system with a lid. There was a tendency indicating that increased cigarette consumption could lead to higher AF values ex vivo, although no correlation was established with increased dosage. Nevertheless, even exposure to a small amount of cigarette smoke resulted in increased AF levels in the skin when compared with non-exposed skin. Furthermore, by imitating real-life circumstances, the obtained results are considered more dependable than those acquired through in vitro and ex vivo studies. Interestingly, the AF values of the in vivo human skin study is lower (1500 a.u.) compared to the ex vivo porcine skin studies (3000 a.u.) even though the nicotine concentrations (45 - 49 µg/cm²) are comparable [9].

The lower increase of AF could fall back to the higher antioxidative status in living human skin, hence showing better protection. Meinke et al. showed a difference in antioxidant status between ex vivo and in vivo skin. One likely reason for the disparity could be the insufficient oxygen supply to the excised skin samples during the measurements. Additionally, the level of oxidative stress induction can be affected by endogenous antioxidants [174]. When comparing the antioxidative statuses of porcine and human skin, it is important to note that they are not identical. Chapter 1.1.2 highlights that pigs have the ability to synthesize their own vitamin C. Therefore, they have a different antioxidative system [34]. Haag et. al also could show that oxidative stress induced by UV irradiation was higher in excised porcine skin compared to excised human skin [185].

Another aspect to consider is the concentration of melanin in the skin under investigation. Melanin emits autofluorescence in the near-infrared (NIR) regions. Consequently, the in vivo AF study exclusively included participants with skin types I-III, as higher skin types exhibit high levels of melanin, interfering with the AF measurements [178]. Therefore, this method has limitations when measuring skin types IV-VI.

To ensure precision, the individual typology angle (°ITA) values of every participant must be measured to form a focused group for analyzing the increase in AF following exposure to cigarette smoke. °ITA classifies the degree of constitutive pigmentation of skin [186].

To gain a more comprehensive understanding, the participant's antioxidant status could be monitored pre- and post-cigarette smoke exposure. The AF levels induced by oxidative stress could be correlated with the antioxidative status of the participant. This is why it could be important to analyze carotenoid levels. Carotenoid levels indicate a person's antioxidant status. This was already done by Lademann et al. in the past [55].

Nevertheless, the transition from ex vivo to in vivo was positive, as the CRM technique successfully measured cigarette smoke effects on skin without requiring markers or additional stressors.

### 3.2.4 Evaluation of methods to measure the effect of cigarette smoke in skin

The effects of cigarette smoke and air pollution on the skin can be quantified using various techniques. ROS are closely associated with oxidative stress and can therefore be used as a marker of oxidative stress. These methods for ROS detection can be categorized into fluorescence-dependent and spectrophotometry techniques, for instance [187]. The measurement of intracellular ROS can be accomplished by utilizing DCFH assays. This technique is categorized as a micro-fluorometric assay, in which the non-fluorescent dichlorodihydrofluorescein diacetate (DCFH-DA) is transformed into the fluorescent 2',7'-dichlorofluorescein (DCF) upon oxidation [188]. Hergesell et al.'s study demonstrated that exposure to cigarette smoke resulted in elevated ROS levels in excised porcine skin using the DCFH method [74].

However, the numerous reaction steps required to produce these results may be a disadvantage and could lead to potential false leads. Additionally, sunlight exposure may significantly impact the evaluation of ROS levels, particularly at lower concentrations, making the method non-specific [189, 190].

One spectrophotometry technique presented in this study is EPR. This technique enables the quantification and characterization of radical production ex vivo. One advantage of this technique is its ability to directly identify and quantify free radicals without the need for intermediate reactions [191]. The L-band for in vivo EPR investigations is seldom used due to high acquisition and maintenance costs, such as those for spin probes, and because only a few working groups have the expertise to handle the device. The in vivo EPR method was previously extended to in vivo conditions successfully in our working group [174]. However, it was not feasible when cigarette smoke was used as a stressor. It is also expensive compared to the DCFH assay. Purchasing a new EPR machine is not a budget-friendly option. The DCFH assay, on the other hand, only requires a plate reader, which is already available in most laboratories. In summary, both techniques can measure ROS in vitro [192]. EPR has the advantage of measuring ROS ex vivo and in vivo, but it is very expensive. On the contrary, the DCFH assay is a cost-effective and accessible option.

There are alternative techniques for measuring the effects of air pollution, especially cigarette smoke, such as gene expression analysis. The measurement of gene expression serves as an indicator of pathological conditions or inflammatory reactions. Regarding cigarette smoke, a review by Prieux et al. reported that cigarette smoke exposure induces

inflammatory responses through certain interleukins. Excessive production of pro-inflammatory cytokines, such as IL-1α, IL-6, and IL-18 in the skin was observed [24].

In our study, additional methods could have been incorporated to provide a more comprehensive understanding of the impact of cigarette smoke exposure. The next step would be to investigate the signaling pathways as cigarette smoke exposure significantly affects the skin and leads to inflammation, skin aging, and potentially, the development of cancer [67, 71].

The technique of gene expression was utilized in Grether-Beck et al.'s research to evaluate melanin and pigmentation-associated gene expression following diesel exhaust particle (DEP) exposure. The results demonstrated that DEP exposure caused tanning both ex and in vivo in human skin [20]. However, the drawback is that tanning results took 3 to 9 days to develop, given that human skin tanning may require several days to develop according to Miller et al. [193].

Retrieving these results is comparatively quicker than conducting epidemiological studies, which may take years to decades to see the results. In this study, traffic-related air pollution exposure was found to be associated with clinical indicators of skin pigmentation. However, the pathways and the evidence that are needed to clarify the relationship between air pollution and skin pigmentation were still not clear after epidemiological studies [83, 84]. Epidemiological studies remain relevant as they assist in generalizing outcomes from cell cultures to real-world scenarios [24].

As tanning results take a few days to manifest, this research employed a different approach to assess the impact of air pollution, specifically exposure to cigarette smoke. Employing the AF measuring method, the findings manifested instantly. This is because the autofluorescence triggered by oxidative stress was immediately visible in the CRM. This instant manifestation offers an advantage when examining the efficacy of anti-pollution products. However, the study encountered a challenge: melanin impeded the measurements as high melanin content generates autofluorescence in the CRM. Hence, there are limitations in conducting human studies as individuals with a skin type categorized as IV or higher by the Fitzpatrick scale [194]. The CRM method cannot distinguish between AF triggered by oxidative stress from cigarette smoke and that caused by the participant's melanin content.

Despite its limitations in darker skin types, the CRM method appears to be more responsive to the impact of cigarette smoke exposure than UVA radiation. Consequently, it demonstrates the outcomes of oxidative stress from diverse pathways, not just radical production in the skin. Regrettably, the precise mechanism remains insufficiently elucidated, but it will be clarified in the future.

The impact of seasonal changes should not be disregarded. During summer, test subjects are exposed to increased sunlight, which can stimulate melanin production and result in a higher measured AF value. Additionally, the presence of carotenoids may vary due to individual lifestyle factors such as stress and alcohol consumption, which can also affect antioxidant status. Further research could explore the effects of prolonged exposure to cigarette smoke.

## 3.3 Efficacy of antipollution products

Air pollution can lead to oxidative stress, premature aging, inflammation, and the aggravation of diseases, and in extreme cases, even cancer. Given that individuals are constantly exposed to air pollution, adopting effective protective measures is critical. Possible ways to protect yourself include consuming appropriate foods and supplements or using skin products [25].

Over time, there has been a growing demand for anti-pollution products. These products claim to protect the skin from the harmful effects of air pollution. In the past, several companies have made claims about their products without having done sufficient testing to prove this. In addition, there are insufficient methods to assess the effectiveness against the impacts of air pollution, and there is no regulatory body that verifies cosmetic claims before the product's release onto the market. This can lead to a misconception regarding the safety of the product against air pollution [195].

Therefore, the aim of this work was to establish methods that not only measure the effect of air pollution on the skin but also to evaluate the efficacy of anti-pollution products, which should protect the skin against an increased radical formation or other oxidative stress processes induced by cigarette smoke exposure.

### 3.3.1 Comparison of two methods to measure the efficacy of anti-pollution products

Two approaches were developed in this research to determine the impact of cigarette smoke exposure on ex vivo and in vivo skin. The EPR technique quantified radical formation in excised porcine skin, whereas the CRM demonstrated oxidative stress-induced autofluorescence in excised porcine skin and in vivo human skin [3, 9].

Physiogel ® was chosen as the base formulation because it has a clean and simple formulation that does not contain emulsifiers.

When evaluating the effectiveness of anti-pollution formulations, two methods revealed a marked discrepancy between untreated excised porcine skin and skin with various

treatments such as vitamin E, EDDS and EGCG. Notably, one formulation, EGCG in Physiogel® performed optimally in both methods, successfully shielding the underlying skin from the harmful impacts of cigarette smoke exposure [10].

The EPR technique is a non-invasive method for detecting radical formation in tissues ex vivo, in vivo, and in cell cultures [167]. For the investigation of the protective effect of various cream formulations the spin probe PCA was used. The measurements offer the potential to record radical production throughout the entire skin punch surface. However, the effect decreases at deeper depths due to limitations in spin probe penetration and microwave frequency settings [196]. PCA shows a slow rate of cell penetration, indicating that metabolic radicals have only little impact on the amount of radicals measured in the skin [197].

In this particular case, the PCA responded to the commercial product CE Ferulic® due to the elevated level of antioxidants [10]. Such a reaction is inevitable, particularly with high concentrations. Therefore, in future studies, it is recommended to increase the spin probe concentration as the higher concentration can maintain the linear range when the PCA signal decreases. Alternatively, using different spin probes that are more stable against highly concentrated antioxidants are also an option. Important is the control if a direct interaction takes place.

Unfortunately, cigarette smoke exposure alone did not induce sufficient radical formation that the EPR method could measure. Furthermore, no difference was observed between the group treated with anti-pollution formulations and the untreated group. Therefore, additional UVA irradiation was used to provoke more radical formation, so that the difference between both groups could be observed [10]. This work's findings suggest that the combined effect of cigarette smoke and UVA irradiation was able to promote radical formation in pretreated skin, an effect that is consistent with previous literature [3]. This study investigated the protective effect of individual creams using the synergistic effect of UVA irradiation combined with cigarette smoke. The disadvantage is that formulations containing UV filters need special attention because they would show a decrease in radical formation due to UVA absorption. A control with UVA irradiation alone could solve this problem in the future.

Furthermore, the transfer to in vivo conditions was not successful, meaning that the efficacy of anti-pollution products could not be measured in participants. The in vivo L-band EPR device was unable to measure the effect of cigarette smoke alone or in combination with UVA irradiation due to its lack of sensitivity. Additionally, the marker TEMPO could potentially interfere with the individual products, resulting in non-

reproducible results. Therefore, an alternative and preferred non-invasive method had to be developed. The AF method was adapted to in vivo conditions so the efficacy of each cream could be investigated.

The EPR technique is a reliable method when it comes to measuring and identifying radicals in tissue samples. In contrast, the AF method evaluates the oxidative stress-induced autofluorescence in excised skin. However, there is still a lack of clear explanations for this phenomenon shown in the CRM. It remains a good method to evaluate the effectiveness of anti-pollution products as it considers all pathways that may contribute to oxidative stress responses, beyond just the induction of radicals. The AF method demonstrates a depth-dependent effect of cigarette smoke exposure on excised porcine skin. Additionally, it is possible to identify the penetration depth of the used formulations with the CRM, indicating continued protection against the harmful effects of cigarette smoke exposure.

The CRM technique's biggest advantage is that is does not need an extra marker or an additional stressor like UVA irradiation to not only measure the effect of cigarette smoke exposure but also evaluate different anti-pollution formulations on skin. Cigarette smoke exposure was strong enough to measure the damage with the CRM technique. However, with the EPR technique, there is a need for a marker and an additional stressor. This technique was only able to measure a difference between the various formulations when cigarette smoke was combined with UVA irradiation. The results showed that cigarette smoke exposure alone was not potent enough to see a difference and measure the efficacy of different formulations with the EPR technique.

In addition, the preparation time for the CRM technique is lower. With the CRM technique, 3x4 cm skin areas were removed from the cartilage. Before cream application, the only time-consuming step was to trim each hair from the skin because shaving could damage the SC and falsify the results. With the EPR, the potential damage of the SC can be neglected. In comparison, the preparation of the excised porcine skin for EPR measurements takes longer. This method requires very thin split skin, which needs to be freshly cut as it dries out quickly. Furthermore, the application of the spin probe and the incubation time of the spin probe are adding more time to the process.

The current AF method was not proven successful in in vivo measurements. A slightly significant difference was found between untreated and treated skin after exposure to cigarette smoke. When normalized to the actual nicotine concentration, no significant difference could be found (Figure 13).

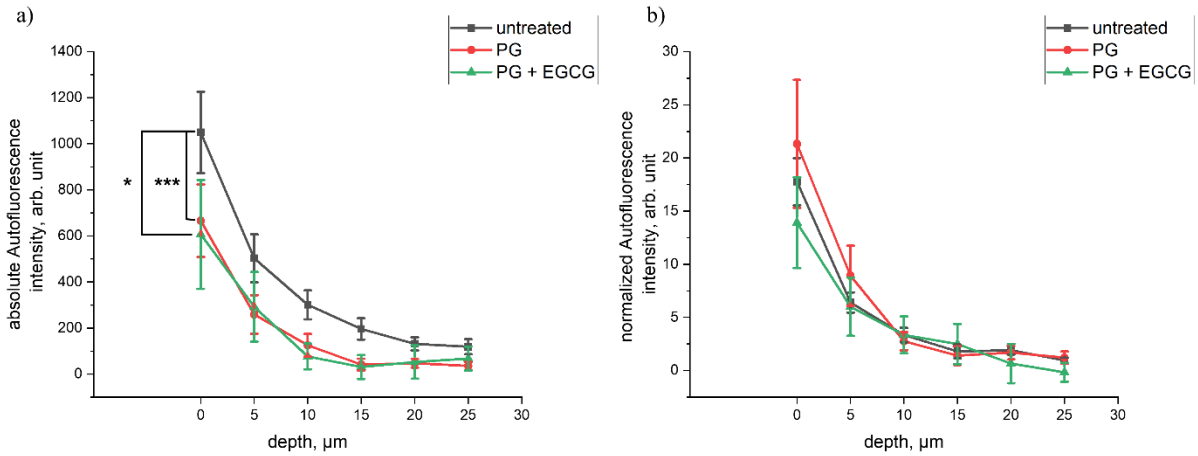


**Figure 13 Comparison of a) absolute autofluorescence intensity and b) autofluorescence intensity normalized to the nicotine concentration on human skin in vivo after 10 min CS exposure with five cigarettes,** mean nicotine concentration 41.8 ± 5.6 µg/cm², n= 11, measured with CRM

The in vivo human study conducted on untreated skin tested using Physiogel® and EGCG integrated in Physiogel® revealed both formulations to be inefficient in reducing oxidative stress-induced autofluorescence after cigarette smoke exposure. Possible reasons may include that the cigarette smoke exposure was not high enough to see a difference. Compared to the ex vivo studies, the nicotine concentration in vivo was more than eight times lower. Another issue is the varying nicotine concentration, which is challenging to achieve in vivo due to differences in the volunteers' arms. It is not always possible to ensure that the arm is perfectly aligned with the chamber opening. A smaller chamber design, like the one used by Bielefeldt et al., would be beneficial and easily applicable to the area under investigation. In addition, which would possibly lead to higher nicotine levels as well.

### 3.3.2 Antioxidants and chelators for anti-pollution products

Air pollution has various pathways that have not yet been fully elucidated. Cigarette smoke exposure, for example, can cause skin damage through multiple pathways [170]. One of the methods presented can measure and quantify radicals in the skin, focusing on ROS-mediated oxidative stress. To counteract the action of ROS, endogenous and exogenous antioxidants can help. The cream formulations' effectiveness was tested using EPR and CRM. To highlight the effect, UVA irradiation was also used in the EPR measurements.

This work compared the base formulation Physiogel® with the commercial product CE Ferulic® using two antioxidants and a chelating agent. Results showed that the formulation containing 1% EGCG was the most effective in both methods. Research shows that EGCG

has anti-inflammatory and antioxidant properties. These protect against UV damage and skin aging [52, 198, 199]. However, the light sensitivity of EGCG and its low permeability make it challenging to use in cosmetics [200].

Studies indicate that applying an EGCG concentration of over 5 % topically can sensitize the skin of guinea pigs. However, this concentration only caused minor dermal irritation in rats and none in rabbits [201]. Therefore, a concentration of 1 % was incorporated in Physiogel ®.

Vitamin E was used at equivalent concentrations but showed inferior EPR results compared to EGCG. Vitamin E possesses both antioxidant and anti-inflammatory properties, as well as photoprotection properties against UV radiation [54]. The induction power increased significantly due to synergistic effects and pathways, which could lead to stress. This was revealed by the EPR measurements, which included both cigarette smoke and UVA irradiation. The EPR measurements were focused on the formation of radicals due to cigarette smoke exposure and UVA irradiation together, and therefore, vitamin E alone could not deplete the formed radicals. It is possible that the antioxidant capacity of vitamin E may not match that of EGCG. The hypothesis that vitamin E has a lower antioxidant capacity than EGCG was supported by measuring the radical protection factor (RPF) [10]. Previous studies have implemented the RPF to evaluate the effectiveness of radical protection against UV irradiation in sunscreens, in which antioxidants were additionally included [202, 203].

Vitamin E exhibited protection against cigarette smoke on the skin in CRM measurements. Only one stressor was responsible for inducing oxidative stress, and the quantity was reduced as no additional UVA irradiation was required to observe a distinction between untreated and treated skin [10].

A high RPF was achieved using CE Ferulic®, a commercial product containing a combination of vitamin C, vitamin E, and ferulic Acid. It was found to be efficient in protecting excised porcine skin against oxidative stress caused by cigarette smoke. The formulation has also been tested against other stressors, such as DEP and ozone, and found to provide protection in those cases as well [20, 204, 205]. However, the formulation reacted with the spin probe used in the EPR measurements. Therefore, it was not possible to conduct a thorough evaluation of the protective effects against both cigarette smoke and UVA irradiation. However, previous studies have demonstrated the protective properties against combined pollutants, including UV irradiation, ozone, and diesel exhaust particles [204].

As outlined previously, both the ex vivo methods of measuring efficacy have their advantages and disadvantages. Given the time consumption required for testing numerous formulations, it is recommended to initially employ the radical protection factor (RPF) method to assess the level of protection. This method provides a dependable indication of which formulations provide exceptional safeguards against an increased radical formation in vitro.

When measuring chelating power, a comparable method involves assessing the ability to chelate copper using EPR. Metal chelators can impact protective efficacy in formulations designed to protect skin from pollution. As mentioned earlier, iron present in pollution and cigarette smoke can catalyze the Fenton reaction, generating more ROS and leading to oxidative stress. Studies have found that the use of both antioxidant and chelator agents could have an additive impact on protecting the skin against air pollution exposure [206].

In this study, EDDS demonstrated a protective effect in the CRM method, although no such effect was observed in the EPR method. This discrepancy may be because EPR measures radical formation, whereas EDDS chelates metals that may generate ROS indirectly. Furthermore, this protective effect did not manifest itself under additional UVA irradiation, which generated more ROS than cigarette smoke alone. Due to the variety of pathways used by cigarette smoke exposure to harm the skin, EPR cannot accurately reflect the impact of all pathways but the source of further pathways. CRM, however, can measure the overall oxidative stress-induced AF.

### 3.3.3 Guideline for formulating and testing anti-pollution products

Various products are available on the market that claim to offer protection against pollution. However, the validity of such claims needs to be established through proper efficacy testing [25].

In the European Union, the European Cosmetics Regulation No. 1223/2009 imposes strict regulations to ensure that claims made on cosmetic products do not mislead consumers. Claims must be supported by evidence in the product information file to prove their efficacy. So far, there are no mandatory anti-pollution tests that are reproducible, standardized and regulated [207]. Therefore, the objective of this work was to establish methods that can be used for proper anti-pollution testing.

In this study, the EPR and CRM approaches were used to evaluate the effectiveness of the protection of the skin from exposure to cigarette smoke. In developing anti-pollution products, the method's applicability should be clear beforehand. Notably, the protective properties of EDDS were only observed in the CRM approach as it considers overall

oxidative stress-induced AF. Furthermore, when developing formulations, it is imperative to ensure that the product does not react with the marker. Concerning CE Ferulic®, there was a reaction with the spin probe PCA using the EPR method. This implies that the EPR method cannot measure high concentrations of antioxidants. However, the EPR method can evaluate radical formation caused by exposure to cigarette smoke.

Consider the concentration of the formulations and products used, as dose-dependency has not yet been established. This is particularly relevant for products containing antioxidants, as high concentrations can lead to a pro-oxidative effect. For instance, research has shown that vitamin C can be pro-oxidative at higher concentrations [208]. High concentrations of EGCG can also be skin irritating [201]. Consequently, when testing anti-pollution efficacy, it is necessary to test different concentrations.

Another aspect to consider is the need to adapt testing to real-life conditions. In reality, multiple pollutants can harm us. The world is a dynamic system in which many factors can contribute to inducing stress on our bodies. Therefore, these formulations need to be tested against a variety of pollutants and combinations of stressors, as their combined effects can intensify the impact of air pollution.

# 4. Conclusion and Outlook

## 4.1 Conclusion

This thesis elucidates the impact of the pollutant cigarette smoke on the skin. A reproducible exposure method was established to expose skin explants to cigarette smoke. Two exposure chambers were constructed and employed based on the research's objectives. The smaller chamber was utilized for ex vivo trials while the bigger chamber was utilized for both ex vivo and in vivo experiments. The impact of cigarette smoke exposure and the effectiveness of anti-pollution products can be assessed using two methods, namely EPR and CRM. It is evident that each method has its own advantages and disadvantages. EPR showed better sensitivity to UVA irradiation, while the CRM method performed better against smoke exposure. Only CRM was appropriate for in vivo measurements at present, but adjustments will be necessary in the future when testing formulations in vivo. Nevertheless, both approaches are highly potent and could supplement the existing techniques in the times ahead. These methods can contribute to the necessary overhaul of cosmetic product regulations because anti-pollution products lack regulations regarding uncontrolled claims.

## 4.2 Outlook

In the future, the following step ought to be to elucidate the effect of AF after cigarette smoke exposure. In this regard, multiphoton tomography can be a viable alternative for the study of anti-pollution products since it presents an essential non-invasive diagnostic tool for dermatology by accurately measuring the composition of the dermal matrix. Depth and epidermal thickness considerably affect the assessment process [209]. Furthermore, this technique uncovers distinct patterns in autofluorescence levels of human skin fluorophores such as keratin, NAD(P)H, melanin, and elastin and collagen networks in relation to the wavelength of excitation [210].

Further research is needed to assess the effectiveness of anti-pollution products in real-life conditions through in vivo studies. Appropriate adaptations of current methods would be necessary to achieve this aim. The redox status of participants should also be monitored given the significance of the body's defensive system. Additionally, investigating the impact of these products on individuals with irritated skin or diseases could provide valuable insights. As a lot of people are suffering from their symptoms and air pollution is only worsening their condition, testing the claims is even more important.

In addition to assessing the redox status of participants, measuring ITA values can be employed for prior close monitoring. As the CRM technique is not appropriate for individuals with high levels of melanin in their skin, participants with very light skin are

required. Importantly, the ITA value facilitates the measurement of skin reflectance, including the absorption and scattering of light by melanin in the skin [211].

It would be intriguing to investigate melanin's role in general. Notably, while melanin interferes with measurements in the CRM method, it can also be a consequence of exposure to diesel exhaust [20].

It is advisable to use the established method and materials used in this study. Different pollutants should be used to verify the efficacy of the method.

Combining different stressors is also advisable to mimic real-life conditions, as our bodies are exposed to different pollutants at the same time. Strategies should therefore be adapted to the same conditions in which we live. As the existing chambers have different ventilation systems, it would be possible to combine them.

In terms of active ingredients in anti-pollution formulations, the focus has been on antioxidants as they can counteract the formation of radicals in the skin due to exposure to air pollution. Different active ingredients can be used depending on the mechanism. Products can reduce particle exposure by cleansing the skin. They can prevent the deposition and penetration of pollutants on the skin and restore and strengthen the skin barrier. Cleaning products should be tested with this method to measure their protection efficacy [149].

There is a wide range of choices, and more research is needed to test their effectiveness in protecting the skin from pollution [149]. To begin, our working group collaborated with DGK (Cosmetic Science e.V.) to develop a matrix aimed at introducing the topic to a wider audience and providing useful information on anti-pollution methods [212].

# 5. List of publications

**Tran, P. T.**; Beidoun, B.; Lohan, S. B.; Talbi, R.; Kleuser, B.; Seifert, M.; Jung, K.; Sandig, G.; Meinke, M. C. Establishment of a method to expose and measure pollution in excised porcine skin with electron paramagnetic resonance spectroscopy. Ecotoxicology and Environmental Safety 2022, 247, 114258. DOI: https://doi.org/10.1016/j.ecoenv.2022.114258.

**Tran, P. T.**; Tawornchat, P.; Kleuser, B.; Lohan, S. B.; Schleusener, J.; Meinke, M. C.; Darvin, M. E. Red- and Near-Infrared-Excited Autofluorescence as a Marker for Acute Oxidative Stress in Skin Exposed to Cigarette Smoke Ex Vivo and In Vivo. Antioxidants 2023, 12 (5). DOI: 10.3390/antiox12051011.

**Tran, P. T.;** Schleusener, J.; Kleuser, B.; Jung K.; Meinke, M. C.; Lohan, S. B. Evidence of the protective effect of anti-pollution products against oxidative stress in skin ex vivo using EPR spectroscopy and autofluorescence measurements. European Journal of Pharmaceutics and Biopharmaceutics 197: 114211. DOI: https://doi.org/10.1016/j.ejpb.2024.114211

## Oral presentations

### Conference

The International Society for Biophysics and Imaging of the Skin, Berlin, Germany, June 2022

### In house

Research Seminar at the Department of Dermatology, Venerology and Allergology, Charité – Universitätsmedizin Berlin, October 2021

### Poster presentation

Redox Biology, Ghent, Belgium, August 2022

9$^{th}$ International Conference in Oxidative Stress in Skin Medicine and Biology, online, September 2021

### Scholarships and awards

Doctoral scholarship II by Charité Universitaetsmedizin Berlin, October 2020 – February 2023

Young Investigator Award at 9$^{th}$ International Conference in Oxidative Stress in Skin Medicine and Biology, online, September 2021

Elsevier Young Investigator Award at Redox Biology in Ghent, Belgium, August 2022

# 6. References

[1] Morita A, Torii K, Maeda A, Yamaguchi Y. Molecular Basis of Tobacco Smoke-Induced Premature Skin Aging. Journal of Investigative Dermatology Symposium Proceedings. 2009;14:53-5.
[2] Kim KE, Cho D, Park HJ. Air pollution and skin diseases: Adverse effects of airborne particulate matter on various skin diseases. Life Sciences. 2016;152:126-34.
[3] Tran PT, Beidoun B, Lohan SB, Talbi R, Kleuser B, Seifert M, et al. Establishment of a method to expose and measure pollution in excised porcine skin with electron paramagnetic resonance spectroscopy. Ecotoxicology and Environmental Safety. 2022;247:114258.
[4] Rentschler J, Leonova N. Global air pollution exposure and poverty. Nature Communications. 2023;14:4432.
[5] Organization WH. WHO global air quality guidelines: particulate matter (PM2. 5 and PM10), ozone, nitrogen dioxide, sulfur dioxide and carbon monoxide: World Health Organization; 2021.
[6] Fenner J, Clark RA. Anatomy, physiology, histology, and immunohistochemistry of human skin. Skin tissue engineering and regenerative medicine. 2016;1.
[7] Gilaberte Y, Prieto-Torres L, Pastushenko I, Juarranz Á. Chapter 1 - Anatomy and Function of the Skin. In: Hamblin MR, Avci P, Prow TW, editors. Nanoscience in Dermatology. Boston: Academic Press; 2016. p. 1-14.
[8] Hoffmann D, Hoffmann I, El-Bayoumy K. The less harmful cigarette: a controversial issue. A tribute to Ernst L. Wynder. Chemical research in toxicology. 2001;14:767-90.
[9] Tran PT, Tawornchat P, Kleuser B, Lohan SB, Schleusener J, Meinke MC, Darvin ME. Red- and Near-Infrared-Excited Autofluorescence as a Marker for Acute Oxidative Stress in Skin Exposed to Cigarette Smoke Ex Vivo and In Vivo. Antioxidants. 2023;12:1011.
[10] Tran PT, Schleusener J, Kleuser B, Jung K, Meinke MC, Lohan SB. Evidence of the protective effect of anti-pollution products against oxidative stress in skin ex vivo using EPR spectroscopy and autofluorescence measurements. European Journal of Pharmaceutics and Biopharmaceutics. 2024;197:114211.
[11] Venus M, Waterman J, McNab I. Basic physiology of the skin. Surgery (Oxford). 2010;28:469-72.
[12] Kolarsick PA, Kolarsick MA, Goodwin C. Anatomy and physiology of the skin. Journal of the Dermatology Nurses' Association. 2011;3:203-13.
[13] Proksch E. pH in nature, humans and skin. The Journal of dermatology. 2018;45:1044-52.
[14] Eckert RL. Structure, function, and differentiation of the keratinocyte. Physiological reviews. 1989;69:1316-46.
[15] Valacchi G, Sticozzi C, Pecorelli A, Cervellati F, Cervellati C, Maioli E. Cutaneous responses to environmental stressors. Annals of the New York Academy of Sciences. 2012;1271:75-81.
[16] Reichrath J, Reichrath, Albright. Sunlight, vitamin D and skin cancer: Springer; 2008.
[17] Plikus MV, Wang X, Sinha S, Forte E, Thompson SM, Herzog EL, et al. Fibroblasts: Origins, definitions, and functions in health and disease. Cell. 2021;184:3852-72.
[18] Choi I, Lee S, Hong YK. The new era of the lymphatic system: no longer secondary to the blood vascular system. Cold Spring Harb Perspect Med. 2012;2:a006445.
[19] Harper RA, Grove G. Human skin fibroblasts derived from papillary and reticular dermis: differences in growth potential in vitro. Science. 1979;204:526-7.
[20] Grether-Beck S, Felsner I, Brenden H, Marini A, Jaenicke T, Aue N, et al. Air pollution-induced tanning of human skin*. British Journal of Dermatology. 2021;185:1026-34.
[21] Riley PA. Melanin. The international journal of biochemistry & cell biology. 1997;29:1235-9.

[22] Teunissen M. Dynamic nature and function of epidermal Langerhans cells in vivo and in vitro: a review, with emphasis on human Langerhans cells. The Histochemical journal. 1992;24:697-716.
[23] Boulais N, Misery L. Merkel cells. Journal of the American Academy of Dermatology. 2007;57:147-65.
[24] Prieux R, Eeman M, Rothen-Rutishauser B, Valacchi G. Mimicking cigarette smoke exposure to assess cutaneous toxicity. Toxicology in Vitro. 2020;62:104664.
[25] Rembiesa J, Ruzgas T, Engblom J, Holefors A. The impact of pollution on skin and proper efficacy testing for anti-pollution claims. Cosmetics. 2018;5:4.
[26] Williams FM. In vitro studies—how good are they at replacing in vivo studies for measurement of skin absorption? Environmental Toxicology and Pharmacology. 2006;21:199-203.
[27] Tfayli A, Piot O, Draux F, Pitre F, Manfait M. Molecular characterization of reconstructed skin model by Raman microspectroscopy: comparison with excised human skin. Biopolymers: Original Research on Biomolecules. 2007;87:261-74.
[28] Franz TJ, Lehman PA, Raney SG. Use of Excised Human Skin to Assess the Bioequivalence of Topical Products. Skin Pharmacology and Physiology. 2009;22:276-86.
[29] Hwang J-h, Jeong H, Lee N, Hur S, Lee N, Han JJ, et al. Ex Vivo Live Full-Thickness Porcine Skin Model as a Versatile In Vitro Testing Method for Skin Barrier Research. International Journal of Molecular Sciences. 2021;22:657.
[30] Debeer S, Le Luduec JB, Kaiserlian D, Laurent P, Nicolas JF, Dubois B, Kanitakis J. Comparative histology and immunohistochemistry of porcine versus human skin. Eur J Dermatol. 2013;23:456-66.
[31] Kong R, Bhargava R. Characterization of porcine skin as a model for human skin studies using infrared spectroscopic imaging. Analyst. 2011;136:2359-66.
[32] Darvin ME, Richter H, Zhu YJ, Meinke MC, Knorr F, Gonchukov SA, et al. Comparison of in vivo and ex vivo laser scanning microscopy and multiphoton tomography application for human and porcine skin imaging. Quantum Electronics. 2014;44:646.
[33] Choe C, Schleusener J, Lademann J, Darvin ME. Human skin in vivo has a higher skin barrier function than porcine skin ex vivo—comprehensive Raman microscopic study of the stratum corneum. Journal of Biophotonics. 2018;11:e201700355.
[34] Fernández-Dueñas D, Mariscal G, Ramírez E, Cuarón J. Vitamin C and β-carotene in diets for pigs at weaning. Animal feed science and technology. 2008;146:313-26.
[35] Sullivan TP, Eaglstein WH, Davis SC, Mertz P. THE PIG AS A MODEL FOR HUMAN WOUND HEALING. Wound Repair and Regeneration. 2001;9:66-76.
[36] Nakai K, Tsuruta D. What Are Reactive Oxygen Species, Free Radicals, and Oxidative Stress in Skin Diseases? International Journal of Molecular Sciences. 2021;22:10799.
[37] Preiser J-C. Oxidative Stress. Journal of Parenteral and Enteral Nutrition. 2012;36:147-54.
[38] Percoco G, Patatian A, Eudier F, Grisel M, Bader T, Lati E, et al. Impact of cigarette smoke on physical-chemical and molecular proprieties of human skin in an ex vivo model. Experimental Dermatology. 2021;30:1610-8.
[39] Dupont E, Gomez J, Bilodeau D. Beyond UV radiation: a skin under challenge. International journal of cosmetic science. 2013;35:224-32.
[40] Turrens JF. Mitochondrial formation of reactive oxygen species. J Physiol. 2003;552:335-44.
[41] Bouayed J, Bohn T. Exogenous antioxidants--Double-edged swords in cellular redox state: Health beneficial effects at physiologic doses versus deleterious effects at high doses. Oxid Med Cell Longev. 2010;3:228-37.
[42] Dontha S. A review on antioxidant methods. Asian J Pharm Clin Res. 2016;9:14-32.
[43] Abreu IA, Cabelli DE. Superoxide dismutases—a review of the metal-associated mechanistic variations. Biochimica et Biophysica Acta (BBA) - Proteins and Proteomics. 2010;1804:263-74.

[44] Steenvoorden DPT, Beijersbergen van Henegouwen GMJ. The use of endogenous antioxidants to improve photoprotection. Journal of Photochemistry and Photobiology B: Biology. 1997;41:1-10.
[45] Biliński T, Krawiec Z, Liczmański A, Litwińska J. Is hydroxyl radical generated by the Fenton reaction in vivo? Biochemical and biophysical research communications. 1985;130:533-9.
[46] Gaweł S, Wardas M, Niedworok E, Wardas P. Malondialdehyde (MDA) as a lipid peroxidation marker. Wiadomosci lekarskie (Warsaw, Poland: 1960). 2004;57:453-5.
[47] Pilger A, Rüdiger H. 8-Hydroxy-2′-deoxyguanosine as a marker of oxidative DNA damage related to occupational and environmental exposures. International archives of occupational and environmental health. 2006;80:1-15.
[48] Ottum MS, Mistry AM. Advanced glycation end-products: modifiable environmental factors profoundly mediate insulin resistance. Journal of Clinical Biochemistry and Nutrition. 2015;57:1-12.
[49] Chen J, Liu Y, Zhao Z, Qiu J. Oxidative stress in the skin: Impact and related protection. International Journal of Cosmetic Science. 2021;43:495-509.
[50] BOYERA N, GALEY I, BERNARD BA. Effect of vitamin C and its derivatives on collagen synthesis and cross-linking by normal human fibroblasts. International Journal of Cosmetic Science. 1998;20:151-8.
[51] Pinnell SR, Yang H, Omar M, Riviere NM, DeBuys HV, Walker LC, et al. Topical L-Ascorbic Acid: Percutaneous Absorption Studies. Dermatologic Surgery. 2001;27:137-42.
[52] Masaki H. Role of antioxidants in the skin: anti-aging effects. Journal of dermatological science. 2010;58:85-90.
[53] Azzi A, Gysin R, Kempná P, Munteanu A, Villacorta L, Visarius T, Zingg J-M. Regulation of gene expression by α-tocopherol. Biological Chemistry. 2004;385:585-91.
[54] Trevithick JR, Xiong H, Lee S, Shum DT, Sanford SE, Karlik SJ, et al. Topical tocopherol acetate reduces post-UVB, sunburn-associated erythema, edema, and skin sensitivity in hairless mice. Archives of Biochemistry and Biophysics. 1992;296:575-82.
[55] Lademann J, Köcher W, Yu R, Meinke MC, Na Lee B, Jung S, et al. Cutaneous Carotenoids: The Mirror of Lifestyle? Skin Pharmacology and Physiology. 2014;27:201-.
[56] Katiyar SK. Skin photoprotection by green tea: antioxidant and immunomodulatory effects. Current Drug Targets-Immune, Endocrine & Metabolic Disorders. 2003;3:234-42.
[57] Murphy G, Nagase H. Progress in matrix metalloproteinase research. Molecular Aspects of Medicine. 2008;29:290-308.
[58] Dunaway S, Odin R, Zhou L, Ji L, Zhang Y, Kadekaro AL. Natural Antioxidants: Multiple Mechanisms to Protect Skin From Solar Radiation. Front Pharmacol. 2018;9:392.
[59] Burke KE. Photodamage of the skin: protection and reversal with topical antioxidants. Journal of Cosmetic Dermatology. 2004;3:149-55.
[60] Wölfle U, Seelinger G, Bauer G, Meinke MC, Lademann J, Schempp CM. Reactive molecule species and antioxidative mechanisms in normal skin and skin aging. Skin Pharmacol Physiol. 2014;27:316-32.
[61] Korkina L, Pastore S. The role of redox regulation in the normal physiology and inflammatory diseases of skin. FBE. 2009;1:123-41.
[62] Raad H, Serrano-Sanchez M, Harfouche G, Mahfouf W, Bortolotto D, Bergeron V, et al. NADPH oxidase-1 plays a key role in keratinocyte responses to UV radiation and UVB-induced skin carcinogenesis. Journal of investigative Dermatology. 2017;137:1311-21.
[63] Kampa M, Castanas E. Human health effects of air pollution. Environmental Pollution. 2008;151:362-7.
[64] Qian Z, Chapman RS, Hu W, Wei F, Korn LR, Zhang J. Using air pollution based community clusters to explore air pollution health effects in children. Environment International. 2004;30:611-20.
[65] Mannucci PM, Franchini M. Health Effects of Ambient Air Pollution in Developing Countries. International Journal of Environmental Research and Public Health. 2017;14:1048.

[66] Krutmann J, Liu W, Li L, Pan X, Crawford M, Sore G, Seite S. Pollution and skin: from epidemiological and mechanistic studies to clinical implications. J Dermatol Sci. 2014;76:163-8.
[67] Damevska K, Boev B, Mirakovski D, Petrov A, Darlenski R, Simeonovski V. How to prevent skin damage from air pollution. Part 1: Exposure assessment. Dermatologic Therapy. 2020;33:e13171.
[68] Perez-Padilla R, Schilmann A, Riojas-Rodriguez H. Respiratory health effects of indoor air pollution [Review article]. The International Journal of Tuberculosis and Lung Disease. 2010;14:1079-86.
[69] Fussell JC, Kelly FJ. Oxidative contribution of air pollution to extrinsic skin ageing. Free Radical Biology and Medicine. 2020;151:111-22.
[70] Makino ET, Jain A, Tan P, Nguyen A, Moga A, Charmel C, et al. Clinical Efficacy of a Novel Two-Part Skincare System on Pollution-Induced Skin Damage. J Drugs Dermatol. 2018;17:975-81.
[71] Araviiskaia E, Berardesca E, Bieber T, Gontijo G, Sanchez Viera M, Marrot L, et al. The impact of airborne pollution on skin. J Eur Acad Dermatol Venereol. 2019;33:1496-505.
[72] Borgerding M, Klus H. Analysis of complex mixtures–cigarette smoke. Experimental and Toxicologic Pathology. 2005;57:43-73.
[73] Bielfeldt S, Jung K, Laing S, Moga A, Wilhelm KP. Anti-pollution effects of two antioxidants and a chelator—Ex vivo electron spin resonance and in vivo cigarette smoke model assessments in human skin. Skin Research and Technology. 2021;27:1092-9.
[74] Hergesell K, Valentová K, Velebný V, Vávrová K, Dolečková I. Common cosmetic compounds can reduce air pollution-induced oxidative stress and pro-inflammatory response in the skin. Skin Pharmacology and Physiology. 2022;35:156-65.
[75] Vu AT, Taylor KM, Holman MR, Ding YS, Hearn B, Watson CH. Polycyclic aromatic hydrocarbons in the mainstream smoke of popular US cigarettes. Chemical research in toxicology. 2015;28:1616-26.
[76] Stedman RL. Chemical composition of tobacco and tobacco smoke. Chemical reviews. 1968;68:153-207.
[77] Geiss O, Kotzias D. Tobacco, Cigarettes and Cigarette Smoke-An Overview. 2007.
[78] Lei X, Goel R, Sun D, Bhangu G, Bitzer ZT, Trushin N, et al. Free Radical and Nicotine Yields in Mainstream Smoke of Chinese Marketed Cigarettes: Variation with Smoking Regimens and Cigarette Brands. Chemical Research in Toxicology. 2020;33:1791-7.
[79] Jaccard G, Djoko DT, Korneliou A, Stabbert R, Belushkin M, Esposito M. Mainstream smoke constituents and in vitro toxicity comparative analysis of 3R4F and 1R6F reference cigarettes. Toxicology Reports. 2019;6:222-31.
[80] Slone S, McNees CR, Craft M, Ji H, Shearer A, Shelton B, et al. Evaluation of the 1R6F certified reference cigarette for proficiency testing of mainstream smoke parameters. Accreditation and Quality Assurance. 2023;28:69-76.
[81] Löfroth G. Environmental tobacco smoke: overview of chemical composition and genotoxic components. Mutation Research/Genetic Toxicology. 1989;222:73-80.
[82] Borchardt B, Kastaun S, Pashutina Y, Viechtbauer W, Kotz D. Motivation to stop smoking in the German population between 2016 - 2021 and associated factors: results from a repeated cross-sectional representative population survey (German Study on Tobacco Use, DEBRA study). BMJ Open. 2023;13:e068198.
[83] Hüls A, Vierkötter A, Gao W, Krämer U, Yang Y, Ding A, et al. Traffic-related air pollution contributes to development of facial lentigines: further epidemiological evidence from Caucasians and Asians. The Journal of investigative dermatology. 2016;136:1053-6.
[84] Li M, Vierkötter A, Schikowski T, Hüls A, Ding A, Matsui MS, et al. Epidemiological evidence that indoor air pollution from cooking with solid fuels accelerates skin aging in Chinese women. Journal of dermatological science. 2015;79:148-54.
[85] Pryor WA. Cigarette smoke radicals and the role of free radicals in chemical carcinogenicity. Environmental health perspectives. 1997;105:875-82.

[86] Church DF, Pryor WA. Free-radical chemistry of cigarette smoke and its toxicological implications. Environmental health perspectives. 1985;64:111-26.
[87] St. Helen G, Goniewicz ML, Dempsey D, Wilson M, Jacob III P, Benowitz NL. Exposure and kinetics of polycyclic aromatic hydrocarbons (PAHs) in cigarette smokers. Chemical research in toxicology. 2012;25:952-64.
[88] Jenkins RA, Tomkins B, Guerin MR. The chemistry of environmental tobacco smoke: composition and measurement: CRC Press; 2000.
[89] Cross C, Halliwell B, Allen A. Antioxidant protection: a function of tracheobronchial and gastrointestinal mucus. The Lancet. 1984;323:1328-30.
[90] Dellinger B, Khachatryan L, Masko S, Lomnicki S. Free radicals in tobacco smoke. Mini-Reviews in Organic Chemistry. 2011;8:427-33.
[91] Puri P, Nandar SK, Kathuria S, Ramesh V. Effects of air pollution on the skin: A review. Indian J Dermatol Venereol Leprol. 2017;83:415-23.
[92] McCarty KM, Santella RM, Steck SE, Cleveland RJ, Ahn J, Ambrosone CB, et al. PAH–DNA adducts, cigarette smoking, GST polymorphisms, and breast cancer risk. National Institute of Environmental Health Sciences; 2009.
[93] de Gruijl FR. Photocarcinogenesis: UVA vs. UVB Radiation. Skin Pharmacology and Applied Skin Physiology. 2002;15:316-20.
[94] Soter N. Acute effects of ultraviolet radiation on the skin. Seminars in dermatology1990. p. 11-5.
[95] D'Orazio J, Jarrett S, Amaro-Ortiz A, Scott T. UV radiation and the skin. International journal of molecular sciences. 2013;14:12222-48.
[96] Sklar LR, Almutawa F, Lim HW, Hamzavi I. Effects of ultraviolet radiation, visible light, and infrared radiation on erythema and pigmentation: a review. Photochemical & Photobiological Sciences. 2013;12:54-64.
[97] Nichols JA, Katiyar SK. Skin photoprotection by natural polyphenols: anti-inflammatory, antioxidant and DNA repair mechanisms. Archives of Dermatological Research. 2010;302:71-83.
[98] Casetti F, Miese A, Mueller M, Simon J, Schempp C. Double trouble from sunburn: UVB-induced erythema is associated with a transient decrease in skin pigmentation. Skin Pharmacology and Physiology. 2011;24:160-5.
[99] Holick MF. Sunlight, UV-radiation, vitamin D and skin cancer: how much sunlight do we need? Sunlight, vitamin D and skin cancer. 2008:1-15.
[100] Wicks NL, Chan JW, Najera JA, Ciriello JM, Oancea E. UVA phototransduction drives early melanin synthesis in human melanocytes. Current Biology. 2011;21:1906-11.
[101] Rigel DS, Rigel EG, Rigel AC. Effects of altitude and latitude on ambient UVB radiation. Journal of the American Academy of Dermatology. 1999;40:114-6.
[102] Mustafa F, Jaafar M. Comparison of wavelength-dependent penetration depths of lasers in different types of skin in photodynamic therapy. Indian Journal of Physics. 2013;87:203-9.
[103] BRENNEISEN P, SIES H, SCHARFFETTER-KOCHANEK K. Ultraviolet-B Irradiation and Matrix Metalloproteinases. Annals of the New York Academy of Sciences. 2002;973:31-43.
[104] Wondrak GT, Jacobson MK, Jacobson EL. Endogenous UVA-photosensitizers: mediators of skin photodamage and novel targets for skin photoprotection. Photochemical & photobiological sciences. 2006;5:215-37.
[105] Dalle Carbonare M, Pathak MA. Skin photosensitizing agents and the role of reactive oxygen species in photoaging. Journal of Photochemistry and Photobiology B: Biology. 1992;14:105-24.
[106] Karran P, Brem R. Protein oxidation, UVA and human DNA repair. DNA Repair. 2016;44:178-85.
[107] Borska L, Andrys C, Krejsek J, Palicka V, Vorisek V, Hamakova K, et al. Influence of dermal exposure to ultraviolet radiation and coal tar (polycyclic aromatic hydrocarbons) on the skin aging process. Journal of Dermatological Science. 2016;81:192-202.

[108] Bourgart E, Persoons R, Marques M, Rivier A, Balducci F, von Koschembahr A, et al. Influence of exposure dose, complex mixture, and ultraviolet radiation on skin absorption and bioactivation of polycyclic aromatic hydrocarbons ex vivo. Archives of Toxicology. 2019;93:2165-84.
[109] Saladi R, Austin L, Gao D, Lu Y, Phelps R, Lebwohl M, Wei H. The Combination of Benzo[a]pyrene and Ultraviolet A Causes an In Vivo Time-related Accumulation of DNA Damage in Mouse Skin ¶. Photochemistry and Photobiology. 2003;77:413-9.
[110] Hopf NB, Spring P, Hirt-Burri N, Jimenez S, Sutter B, Vernez D, Berthet A. Polycyclic aromatic hydrocarbons (PAHs) skin permeation rates change with simultaneous exposures to solar ultraviolet radiation (UV-S). Toxicology Letters. 2018;287:122-30.
[111] Djordjevic MV, Doran KA. Nicotine Content and Delivery Across Tobacco Products. In: Henningfield JE, London ED, Pogun S, editors. Nicotine Psychopharmacology. Berlin, Heidelberg: Springer Berlin Heidelberg; 2009. p. 61-82.
[112] Ziarati P, Mousavi Z, Pashapour S. Analysis of heavy metals in cigarette tobacco. Journal of Medical Discovery. 2017;2:1-6.
[113] Hammond D, Wiebel F, Kozlowski LT, Borland R, Cummings KM, O'Connor RJ, et al. Revising the machine smoking regime for cigarette emissions: implications for tobacco control policy. Tobacco Control. 2007;16:8-14.
[114] Piao MJ, Ahn MJ, Kang KA, Ryu YS, Hyun YJ, Shilnikova K, et al. Particulate matter 2.5 damages skin cells by inducing oxidative stress, subcellular organelle dysfunction, and apoptosis. Archives of Toxicology. 2018;92:2077-91.
[115] Ono Y, Torii K, Fritsche E, Shintani Y, Nishida E, Nakamura M, et al. Role of the aryl hydrocarbon receptor in tobacco smoke extract–induced matrix metalloproteinase-1 expression. Experimental dermatology. 2013;22:349-53.
[116] Jeong SH, Park JH, Kim JN, Park YH, Shin SY, Lee YH, et al. Up-regulation of TNF-alpha secretion by cigarette smoke is mediated by Egr-1 in HaCaT human keratinocytes. Experimental dermatology. 2010;19:e206-e12.
[117] Tanaka H, Ono Y, Nakata S, Shintani Y, Sakakibara N, Morita A. Tobacco smoke extract induces premature skin aging in mouse. Journal of dermatological science. 2007;46:69-71.
[118] Patatian A, Delestre-Delacour C, Percoco G, Ramdani Y, Di Giovanni M, Peno-Mazzarino L, et al. Skin biological responses to urban pollution in an ex vivo model. Toxicology Letters. 2021;348:85-96.
[119] Costa A, Facchini G, Pinheiro ALTA, da Silva MS, Bonner MY, Arbiser J, Eberlin S. Honokiol protects skin cells against inflammation, collagenolysis, apoptosis, and senescence caused by cigarette smoke damage. International Journal of Dermatology. 2017;56:754-61.
[120] Dalrymple A, McEwan M, Brandt M, Bielfeldt S, Bean E-J, Moga A, et al. A novel clinical method to measure skin staining reveals activation of skin damage pathways by cigarette smoke. Skin Research and Technology. 2022;28:162-70.
[121] Vierkötter A, Schikowski T, Ranft U, Sugiri D, Matsui M, Krämer U, Krutmann J. Airborne particle exposure and extrinsic skin aging. Journal of investigative dermatology. 2010;130:2719-26.
[122] Ácsová A, Hojerová J, Hergesell K, Hideg É, Csepregi K, Bauerová K, et al. Antioxidant and Anti-Pollution Effect of Naturally Occurring Carotenoids Astaxanthin and Crocin for Human Skin Protection. ChemistrySelect. 2022;7:e202201595.
[123] Yang YS, Lim HK, Hong KK, Shin MK, Lee JW, Lee SW, Kim N-I. Cigarette smoke-induced interleukin-1 alpha may be involved in the pathogenesis of adult acne. Annals of dermatology. 2014;26:11-6.
[124] Bakker MG, Fowler B, Bowman MK, Patience GS. Experimental methods in chemical engineering: electron paramagnetic resonance spectroscopy-EPR/ESR. The Canadian Journal of Chemical Engineering. 2020;98:1668-81.
[125] Kleschyov AL, Wenzel P, Munzel T. Electron paramagnetic resonance (EPR) spin trapping of biological nitric oxide. Journal of Chromatography B. 2007;851:12-20.

[126] Eaton GR, Eaton SS, Barr DP, Weber RT. Basics of Continuous Wave EPR. Quantitative EPR: A Practitioners Guide. Vienna: Springer Vienna; 2010. p. 1-14.
[127] Roessler MM, Salvadori E. Principles and applications of EPR spectroscopy in the chemical sciences. Chemical Society Reviews. 2018;47:2534-53.
[128] Kempe S, Metz H, Mäder K. Application of Electron Paramagnetic Resonance (EPR) spectroscopy and imaging in drug delivery research – Chances and challenges. European Journal of Pharmaceutics and Biopharmaceutics. 2010;74:55-66.
[129] Rohn S, Kroh LW. Electron spin resonance – A spectroscopic method for determining the antioxidative activity. Molecular Nutrition & Food Research. 2005;49:898-907.
[130] Haag SF, Lademann J, Meinke MC. Application of EPR-spin Probes to Evaluate Penetration Efficiency, Storage Capacity of Nanotransporters, and Drug Release. Percutaneous Penetration Enhancers Drug Penetration Into/Through the Skin: Methodology and General Considerations. 2017:215-28.
[131] Meinke MC, Busch L, Lohan SB. Wavelength, dose, skin type and skin model related radical formation in skin. Biophysical Reviews. 2021;13:1091-100.
[132] Herrling T, Fuchs J, Rehberg J, Groth N. UV-induced free radicals in the skin detected by ESR spectroscopy and imaging using nitroxides. Free Radical Biology and Medicine. 2003;35:59-67.
[133] Plonka PM. Electron paramagnetic resonance as a unique tool for skin and hair research. Experimental Dermatology. 2009;18:472-84.
[134] Halliwell B, Whiteman M. Measuring reactive species and oxidative damage in vivo and in cell culture: how should you do it and what do the results mean? British Journal of Pharmacology. 2004;142:231-55.
[135] Klare JP, Steinhoff H-J. Spin labeling EPR. Photosynthesis research. 2009;102:377-90.
[136] Dong P, Teutloff C, Lademann J, Patzelt A, Schäfer-Korting M, Meinke MC. Solvent effects on skin penetration and spatial distribution of the hydrophilic nitroxide spin probe pca investigated by epr. Cell Biochemistry and Biophysics. 2020;78:127-37.
[137] Shames AI, Zegrya GG, Samosvat DM, Osipov VY, Vul AY. Size effect in electron paramagnetic resonance spectra of impurity centers in diamond particles. Physica E: Low-dimensional Systems and Nanostructures. 2023;146:115523.
[138] Elpelt A, Ivanov D, Nováčková A, Kováčik A, Sochorová M, Saeidpour S, et al. Investigation of TEMPO partitioning in different skin models as measured by EPR spectroscopy – Insight into the stratum corneum. Journal of Magnetic Resonance. 2020;310:106637.
[139] Brand-Williams W, Cuvelier M-E, Berset C. Use of a free radical method to evaluate antioxidant activity. LWT-Food science and Technology. 1995;28:25-30.
[140] Hugo Infante V, Maria Maia Campos P, Darvin M, Lohan S, Schleusener J, Schanzer S, et al. Cosmetic Formulations with Melaleuca alternifolia Essential Oil for the Improvement of Photoaged Skin: A Double-Blind, Randomized, Placebo-Controlled Clinical Study. Photochemistry and Photobiology. 2023;99:176-83.
[141] Nardi G, Manet I, Monti S, Miranda MA, Lhiaubet-Vallet V. Scope and limitations of the TEMPO/EPR method for singlet oxygen detection: the misleading role of electron transfer. Free Radical Biology and Medicine. 2014;77:64-70.
[142] Gulcin İ, Alwasel SH. DPPH Radical Scavenging Assay. Processes. 2023;11:2248.
[143] Duraipandian S, Zheng W, Ng J, Low J, Ilancheran A, Huang Z. Near-infrared-excited confocal Raman spectroscopy advances in vivo diagnosis of cervical precancer. Journal of Biomedical Optics. 2013;18:067007.
[144] Giridhar G, Manepalli RRKN, Apparao G. Chapter 7 - Confocal Raman Spectroscopy. In: Thomas S, Thomas R, Zachariah AK, Mishra RK, editors. Spectroscopic Methods for Nanomaterials Characterization: Elsevier; 2017. p. 141-61.
[145] Ariese F, Davies GR, Hooijschuur JH, Verkaaik MFC. Will Raman meet bacteria on Mars? An overview of the optimal Raman spectroscopic techniques for carotenoid

biomarkers detection on mineral backgrounds. Netherlands Journal of Geosciences - Geologie en Mijnbouw. 2016;95:141-51.
[146] Llères D, Swift S, Lamond AI. Detecting Protein-Protein Interactions In Vivo with FRET using Multiphoton Fluorescence Lifetime Imaging Microscopy (FLIM). Current Protocols in Cytometry. 2007;42:12.0.1-.0.9.
[147] Monici M. Cell and tissue autofluorescence research and diagnostic applications. Biotechnology Annual Review: Elsevier; 2005. p. 227-56.
[148] Darvin ME. Optical Methods for Non-Invasive Determination of Skin Penetration: Current Trends, Advances, Possibilities, Prospects, and Translation into In Vivo Human Studies. Pharmaceutics. 2023;15:2272.
[149] Mistry N. Guidelines for Formulating Anti-Pollution Products. Cosmetics. 2017;4:57.
[150] Vávrová K, Kováčik A, Opálka L. Ceramides in the skin barrier. European Pharmaceutical Journal. 2017;64:28-35.
[151] Liu H, Cao J, Jiang W. Evaluation and comparison of vitamin C, phenolic compounds, antioxidant properties and metal chelating activity of pulp and peel from selected peach cultivars. LWT - Food Science and Technology. 2015;63:1042-8.
[152] Galaris D, Barbouti A, Korantzopoulos P. Oxidative stress in hepatic ischemia-reperfusion injury: the role of antioxidants and iron chelating compounds. Current Pharmaceutical Design. 2006;12:2875-90.
[153] Almeida IF, Amaral MH, Costa PC, Bahia MF, Valentão P, Andrade PB, et al. Oak leaf extract as topical antioxidant: Free radical scavenging and iron chelating activities and in vivo skin irritation potential. Biofactors. 2008;33:267-79.
[154] Abbas S, Alam S, Singh KP, Kumar M, Gupta SK, Ansari KM. Aryl hydrocarbon receptor activation contributes to benzanthrone-induced hyperpigmentation via modulation of melanogenic signaling pathways. Chemical Research in Toxicology. 2017;30:625-34.
[155] Valavanidis A, Haralambous E. A comparative study by electron paramagnetic resonance of free radical species in the mainstream and sidestream smoke of cigarettes with conventional acetate filters and 'bio-filters'. Redox Report. 2001;6:161-71.
[156] Baum SL, Anderson IG, Baker RR, Murphy DM, Rowlands CC. Electron spin resonance and spin trap investigation of free radicals in cigarette smoke: development of a quantification procedure. Analytica chimica acta. 2003;481:1-13.
[157] Pelle E, Miranda EP, Fthenakis C, Mammone T, Marenus K, Maes D. Cigarette Smoke-Induced Lipid Peroxidation in Human Skin and Its Inhibition by Topically Applied Antioxidants. Skin Pharmacology and Applied Skin Physiology. 2001;15:63-8.
[158] Lopez MJ, Nebot M, Albertini M, Birkui P, Centrich F, Chudzikova M, et al. Secondhand smoke exposure in hospitality venues in Europe. Environmental Health Perspectives. 2008;116:1469-72.
[159] Northrup TF, Stotts AL, Suchting R, Khan AM, Green C, Klawans MR, et al. Thirdhand Smoke Contamination and Infant Nicotine Exposure in a Neonatal Intensive Care Unit: An Observational Study. Nicotine & Tobacco Research. 2020;23:373-82.
[160] Invernizzi G, Ruprecht A, Mazza R, Rossetti E, Sasco A, Nardini S, Boffi R. Particulate matter from tobacco versus diesel car exhaust: an educational perspective. Tobacco control. 2004;13:219-21.
[161] Bush LP, Grunwald C, Davis DL. Influence of puff frequency and puff volume on the alkaloid content of smoke. Journal of Agricultural and Food Chemistry. 1972;20:676-8.
[162] Zhao J, Hopke PK. Concentration of reactive oxygen species (ROS) in mainstream and sidestream cigarette smoke. Aerosol Science and Technology. 2012;46:191-7.
[163] Wang B, Ho SSH, Ho KF, Huang Y, Chan CS, Feng NSY, Ip SHS. An environmental chamber study of the characteristics of air pollutants released from environmental tobacco smoke. Aerosol and Air Quality Research. 2012;12:1269-81.
[164] Kuschner W, D'Alessandro A, Wong H, Blanc P. Dose-dependent cigarette smoking-related inflammatory responses in healthy adults. European Respiratory Journal. 1996;9:1989-94.

[165] Bouchard KV, Costin GE. Promoting New Approach Methodologies (NAMs) for research on skin color changes in response to environmental stress factors: tobacco and air pollution. Front Toxicol. 2023;5:1256399.
[166] Lohan SB, Bühring K, Lauer A-C, Friedrich A, Lademann J, Buss A, et al. Analysis of the Status of the Cutaneous Endogenous and Exogenous Antioxidative System of Smokers and the Short-Term Effect of Defined Smoking Thereon. Antioxidants. 2020;9:537.
[167] Lohan SB, Ivanov D, Schüler N, Berger B, Albrecht S, Meinke MC. EPR Spectroscopy as a Method for ROS Quantification in the Skin. In: Espada J, editor. Reactive Oxygen Species: Methods and Protocols. New York, NY: Springer US; 2021. p. 137-48.
[168] Lohan SB, Müller R, Albrecht S, Mink K, Tscherch K, Ismaeel F, et al. Free radicals induced by sunlight in different spectral regions – in vivo versus ex vivo study. Experimental Dermatology. 2016;25:380-5.
[169] Lohan S, Ivanov D, Schüler N, Berger B, Zastrow L, Lademann J, Meinke M. Switching from healthy to unhealthy oxidative stress–does the radical type can be used as an indicator? Free Radical Biology and Medicine. 2021;162:401-11.
[170] Halliwell BB, Poulsen HE. Cigarette smoke and oxidative stress: Springer; 2006.
[171] Ibuki Y, Warashina T, Noro T, Goto R. Coexposure to benzo[a]pyrene plus ultraviolet A induces 8-oxo-7,8-dihydro-2′-deoxyguanosine formation in human skin fibroblasts: preventive effects of anti-oxidant agents. Environmental Toxicology and Pharmacology. 2002;12:37-42.
[172] Pavlou P, Rallis M, Deliconstantinos G, Papaioannou G, Grando S. In-vivo data on the influence of tobacco smoke and UV light on murine skin. Toxicology and Industrial Health. 2009;25:231-9.
[173] Grenier A, Morissette MC, Rochette PJ, Pouliot R. Toxic Interaction Between Solar Radiation and Cigarette Smoke on Primary Human Keratinocytes. Photochemistry and Photobiology. 2023;99:1258-68.
[174] Meinke MC, Müller R, Bechtel A, Haag SF, Darvin ME, Lohan SB, et al. Evaluation of carotenoids and reactive oxygen species in human skin after UV irradiation: a critical comparison between in vivo and ex vivo investigations. Experimental Dermatology. 2015;24:194-7.
[175] Darvin ME, Lademann J, von Hagen J, Lohan SB, Kolmar H, Meinke MC, Jung S. Carotenoids in Human Skin In Vivo: Antioxidant and Photo-Protectant Role against External and Internal Stressors. Antioxidants. 2022;11:1451.
[176] Lademann J, Caspers PJ, van der Pol A, Richter H, Patzelt A, Zastrow L, et al. In vivo Raman spectroscopy detects increased epidermal antioxidative potential with topically applied carotenoids. Laser Physics Letters. 2009;6:76-9.
[177] Semenov AN, Yakimov BP, Rubekina AA, Gorin DA, Drachev VP, Zarubin MP, et al. The Oxidation-Induced Autofluorescence Hypothesis: Red Edge Excitation and Implications for Metabolic Imaging. Molecules. 2020;25:1863.
[178] Yakimov BP, Shirshin EA, Schleusener J, Allenova AS, Fadeev VV, Darvin ME. Melanin distribution from the dermal–epidermal junction to the stratum corneum: non-invasive in vivo assessment by fluorescence and Raman microspectroscopy. Scientific reports. 2020;10:14374.
[179] Giovannacci I, Magnoni C, Vescovi P, Painelli A, Tarentini E, Meleti M. Which are the main fluorophores in skin and oral mucosa? A review with emphasis on clinical applications of tissue autofluorescence. Archives of Oral Biology. 2019;105:89-98.
[180] Schleusener J, Lademann J, Darvin ME. Depth-dependent autofluorescence photobleaching using 325, 473, 633, and 785 nm of porcine ear skin ex vivo. Journal of biomedical optics. 2017;22:091503-.
[181] Gabarra Almeida Leite M, Maia Campos PM. Correlations between sebaceous glands activity and porphyrins in the oily skin and hair and immediate effects of dermocosmetic formulations. Journal of cosmetic dermatology. 2020;19:3100-6.

[182] Uk K, Berezin VB, Papayan GV, Petrishchev NN, Galagudza MM. Spectrometer for fluorescence–reflection biomedical research. J Opt Technol. 2013;80:40-8.
[183] Meerwaldt R, Links T, Graaff R, Thorpe SR, Baynes JW, Hartog J, et al. Simple noninvasive measurement of skin autofluorescence. Annals of the New York Academy of Sciences. 2005;1043:290-8.
[184] Chen Y, Wang S, Zhang F. Near-infrared luminescence high-contrast in vivo biomedical imaging. Nature Reviews Bioengineering. 2023;1:60-78.
[185] Haag S, Bechtel A, Darvin M, Klein F, Groth N, Schäfer-Korting M, et al. Comparative study of carotenoids, catalase and radical formation in human and animal skin. Skin pharmacology and physiology. 2010;23:306-12.
[186] Del Bino S, Bernerd F. Variations in skin colour and the biological consequences of ultraviolet radiation exposure. British Journal of Dermatology. 2013;169:33-40.
[187] Zhang Y, Dai M, Yuan Z. Methods for the detection of reactive oxygen species. Analytical Methods. 2018;10:4625-38.
[188] Rosenkranz AR, Schmaldienst S, Stuhlmeier KM, Chen W, Knapp W, Zlabinger GJ. A microplate assay for the detection of oxidative products using 2′,7′-dichlorofluorescin-diacetate. Journal of Immunological Methods. 1992;156:39-45.
[189] Yu D, Zha Y, Zhong Z, Ruan Y, Li Z, Sun L, Hou S. Improved detection of reactive oxygen species by DCFH-DA: New insight into self-amplification of fluorescence signal by light irradiation. Sensors and Actuators B: Chemical. 2021;339:129878.
[190] Chen X, Zhong Z, Xu Z, Chen L, Wang Y. 2′,7′-Dichlorodihydrofluorescein as a fluorescent probe for reactive oxygen species measurement: Forty years of application and controversy. Free Radical Research. 2010;44:587-604.
[191] Peijnenburg WJ, Ruggiero E, Boyles M, Murphy F, Stone V, Elam DA, et al. A method to assess the relevance of nanomaterial dissolution during reactivity testing. Materials. 2020;13:2235.
[192] Ahlberg S, Rancan F, Epple M, Loza K, Höppe D, Lademann J, et al. Comparison of different methods to study effects of silver nanoparticles on the pro- and antioxidant status of human keratinocytes and fibroblasts. Methods. 2016;109:55-63.
[193] Miller SA, Coelho SG, Zmudzka BZ, Beer JZ. Reduction of the UV burden to indoor tanners through new exposure schedules: a pilot study. Photodermatology, Photoimmunology & Photomedicine. 2006;22:59-66.
[194] Alexis AF. Lasers and light-based therapies in ethnic skin: treatment options and recommendations for Fitzpatrick skin types V and VI. British Journal of Dermatology. 2013;169:91-7.
[195] Ferreira M, Matos A, Couras A, Marto J, Ribeiro H. Overview of Cosmetic Regulatory Frameworks around the World. Cosmetics. 2022;9:72.
[196] Krzykawska-Serda M, Michalczyk-Wetula D, Płonka PM. Dermatological Applications of EPR: Skin-Deep or In-Depth? In: Shukla AK, editor. Electron Spin Resonance Spectroscopy in Medicine. Singapore: Springer Singapore; 2019. p. 153-87.
[197] Swartz HM, Sentjurc M, Morse II PD. Cellular metabolism of water-soluble nitroxides: effect on rate of reduction of cell/nitroxide ratio, oxygen concentrations and permeability of nitroxides. Biochimica et Biophysica Acta (BBA)-Molecular Cell Research. 1986;888:82-90.
[198] Bae J-Y, Choi J-S, Choi Y-J, Shin S-Y, Kang S-W, Han SJ, Kang Y-H. (−)Epigallocatechin gallate hampers collagen destruction and collagenase activation in ultraviolet-B-irradiated human dermal fibroblasts: Involvement of mitogen-activated protein kinase. Food and Chemical Toxicology. 2008;46:1298-307.
[199] Kim J, Hwang J-S, Cho Y-K, Han Y, Jeon Y-J, Yang K-H. Protective Effects of (–)-Epigallocatechin-3-Gallate on UVA- and UVB-Induced Skin Damage. Skin Pharmacology and Applied Skin Physiology. 2001;14:11-9.
[200] Puri A, Nguyen HX, Banga AK. Microneedle-mediated intradermal delivery of epigallocatechin-3-gallate. International Journal of Cosmetic Science. 2016;38:512-23.

[201] Isbrucker RA, Edwards JA, Wolz E, Davidovich A, Bausch J. Safety studies on epigallocatechin gallate (EGCG) preparations. Part 2: Dermal, acute and short-term toxicity studies. Food and Chemical Toxicology. 2006;44:636-50.
[202] Meinke MC, Syring F, Schanzer S, Haag SF, Graf R, Loch M, et al. Radical Protection by Differently Composed Creams in the UV/VIS and IR Spectral Ranges. Photochemistry and Photobiology. 2013;89:1079-84.
[203] Infante VHP, Lohan SB, Schanzer S, Campos PMBGM, Lademann J, Meinke MC. Eco-friendly sunscreen formulation based on starches and PEG-75 lanolin increases the antioxidant capacity and the light scattering activity in the visible light. Journal of Photochemistry and Photobiology B: Biology. 2021;222:112264.
[204] Ferrara F, Woodby B, Pecorelli A, Schiavone ML, Pambianchi E, Messano N, et al. Additive effect of combined pollutants to UV induced skin OxInflammation damage. Evaluating the protective topical application of a cosmeceutical mixture formulation. Redox Biology. 2020;34:101481.
[205] Valacchi G, Sticozzi C, Belmonte G, Cervellati F, Demaude J, Chen N, et al. Vitamin C Compound Mixtures Prevent Ozone-Induced Oxidative Damage in Human Keratinocytes as Initial Assessment of Pollution Protection. PLOS ONE. 2015;10:e0131097.
[206] Pambianchi E, Ferrara F, Pecorelli A, Benedusi M, Choudhary H, Therrien J-P, Valacchi G. Deferoxamine Treatment Improves Antioxidant Cosmeceutical Formulation Protection against Cutaneous Diesel Engine Exhaust Exposure. Antioxidants. 2021;10:1928.
[207] Pinto M. “ANTI-POLLUTION” CLAIMS IN COSMETIC PRODUCTS. Critical Analyst2020.
[208] Podmore ID, Griffiths HR, Herbert KE, Mistry N, Mistry P, Lunec J. Vitamin C exhibits pro-oxidant properties. Nature. 1998;392:559-.
[209] Kaatz M, Sturm A, Elsner P, König K, Bückle R, Koehler MJ. Depth-resolved measurement of the dermal matrix composition by multiphoton laser tomography. Skin Research and Technology. 2010;16:131-6.
[210] Breunig HG, Studier H, König K. Multiphoton excitation characteristics of cellular fluorophores of human skin in vivo. Opt Express. 2010;18:7857-71.
[211] Wu Y, Tanaka T, Akimoto M. Utilization of individual typology angle (ITA) and hue angle in the measurement of skin color on images. bioimages. 2020;28:1-8.
[212] e.V. DCS. Anti-Pollution Matrix.